Supporting Information for

The Influence of Carbonate Ligands on the Hydrolytic Stability and Reduction of Platinum(IV) Prodrugs

Shu Chen,[ab] Ka-Yan Ng,[a] Qiyuan Zhou,[ab] Houzong Yao,[ab] Zhiqin Deng,[ab] Man-Kit Tse,[a] and Guangyu Zhu*[ab]

[a]Department of Chemistry, City University of Hong Kong, 83 Tat Chee Avenue, Hong Kong SAR 999077, People's Republic of China

[b]City University of Hong Kong Shenzhen Research Institute, Shenzhen 5108057, People's Republic of China

*Email: guangzhu@cityu.edu.hk

Contents

Figures S49–S51. HPLC chromatograms for the purity test of the Pt(IV) complexes of **1a-1b**, **1a′-1b′**, **2a-2b**, **2a′-2b′**, **3a-3b**, and **3a′-3b′**.

Figures S52–S54. HPLC chromatograms for the stability test of the Pt(IV) complexes of **1a-1b**, **1a′-1b′**, **2a-2b**, **2a′-2b′**, **3a-3b**, and **3a′-3b′**.

Figures S55-S57. The decay profiles of the Pt(IV) complexes **1a-1b**, **1a′-1b′**, **2a-2b**, **2a′-2b′**, **3a-3b**, and **3a′-3b′** in a PBS buffer (pH 7.4) at 37 °C within 24 hours.

Figure S58. HPLC chromatograms of Pt(IV) complexes **1a'**, **1b'**, **2a'**, and **2b'** in medium and PBS, respectively.

Figure S59. HPLC chromatograms of Pt(IV) complexes **1a'**, **1b'**, **2a'**, and **2b'** in medium at 37 °C from 0 to 24 h.

Figure S60. ESI-HRMS spectrum and proposed hydrolytic pathway of *c,t,c*-$[Pt(NH_3)_2(OCOOPhCF_3)(OCOCH_3)(Cl)_2]$ **3a'** in PBS-buffered $H_2{}^{18}O$ after 24 h.

Figure S61. ESI-HRMS spectrum and proposed hydrolytic pathway of *c,t,c*-$[Pt(NH_3)_2$-$(OCOCH_3)Cl(Cl)_2]$ in PBS-buffered $H_2{}^{18}O$ after 24 h.

Figure S62–S64. HPLC chromatograms for the reduction test of the Pt(IV) complexes of **1a-1b**, **1a′-1b′**, **2a-2b**, **2a′-2b′**, **3a-3b**, and **3a′-3b′**.

Figure S65-S67. The decay profiles of the Pt(IV) complexes **1a-1b**, **1a′-1b′**, **2a-2b**, **2a′-2b′**, **3a-3b**, and **3a′-3b′** in a PBS buffer (pH 7.4) at 37 °C with excess amount of sodium ascorbate.

Figures S68-S70. Cyclic voltammograms for Pt(IV) complexes of **1a-1b**, **1a′-1b′**, **2a-2b**, **2a′-2b′**, **3a-3b**, and **3a′-3b′**.

Figures S71-S74. The investigation of reduction products of **2b′**.

Table S1. ^{195}Pt, and selected ^{1}H, ^{13}C NMR chemical shifts of the carbonate and carboxylate Pt(IV) complexes in DMSO-d_6.

Table S2. The equation for pseudo first order reaction and half-life of cisplatin-based Pt(IV) complexes.

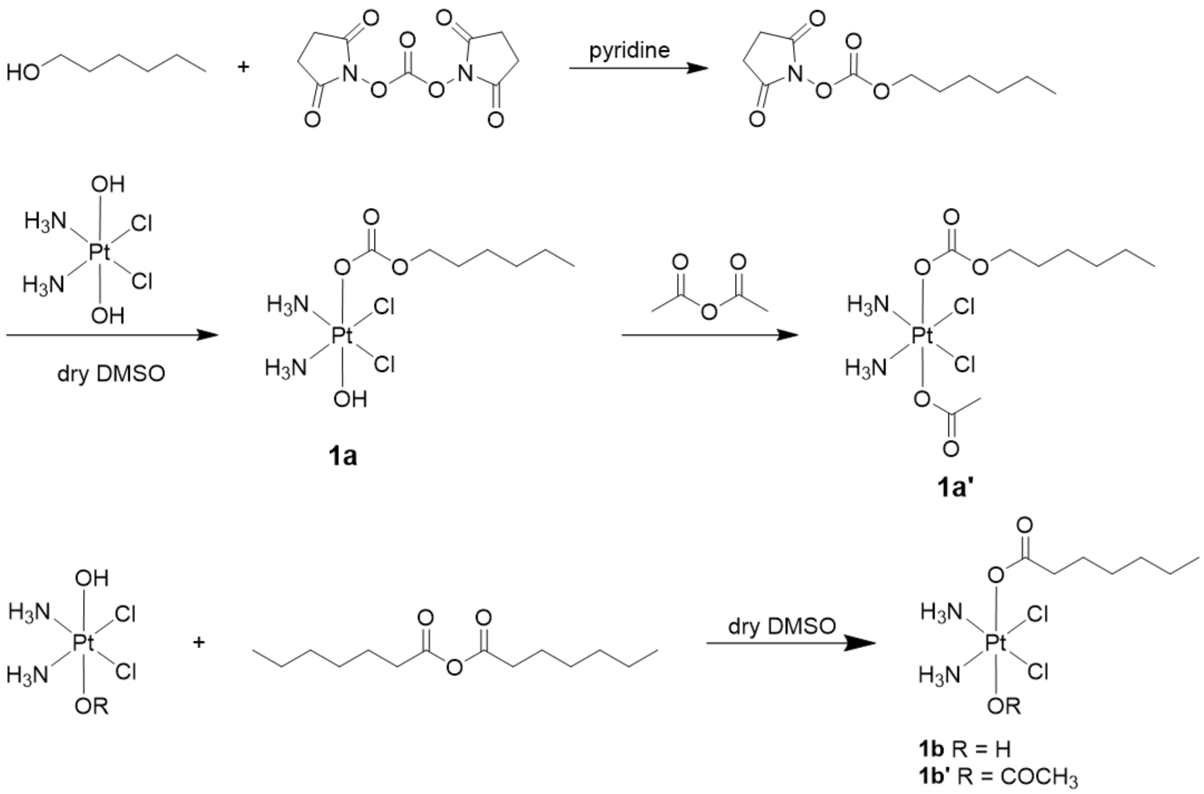

Scheme S1. Synthetic pathway of complexes **1a**, **1a′**, **1b**, and **1b′** bearing carboxylate or carbonate axial ligands.

I

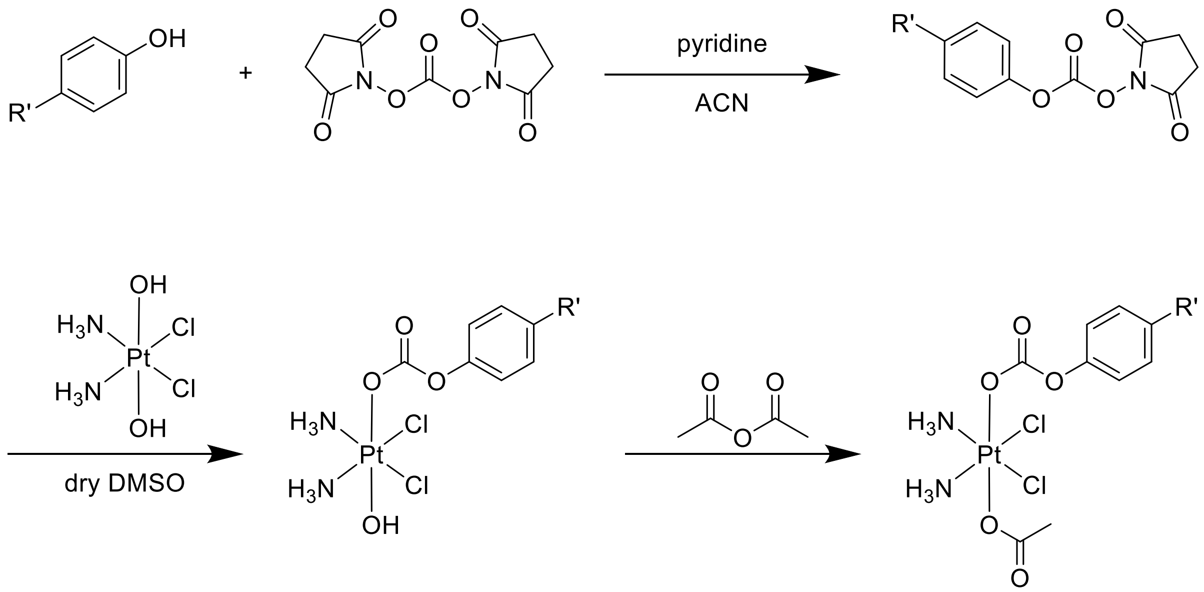

2a R' = H
3a R' = CF_3

2a' R' = H
3a' R' = CF_3

Scheme S2. Synthetic pathway of complexes **2a**, **2a'**, **3a**, and **3a'** bearing an axial carbonate ligand.

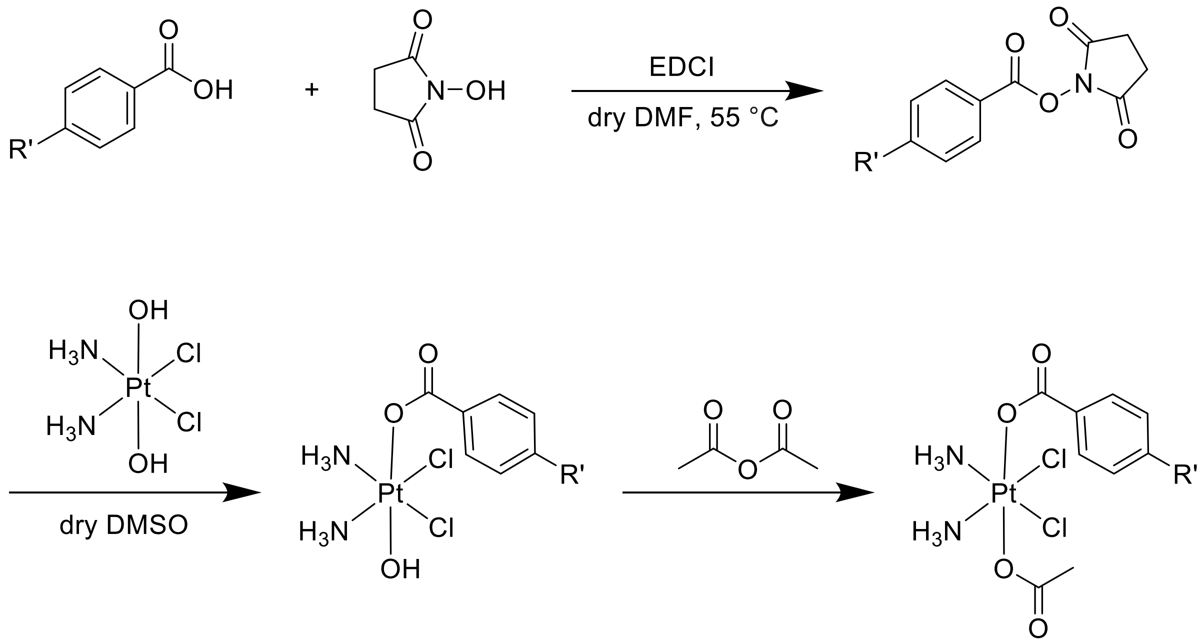

2b R' = H
3b R' = CF_3

2b' R' = H
3b' R' = CF_3

Scheme S3. Synthetic pathway of complexes **2b**, **2b'**, **3b**, and **3b'** bearing an axial carboxylate ligand.

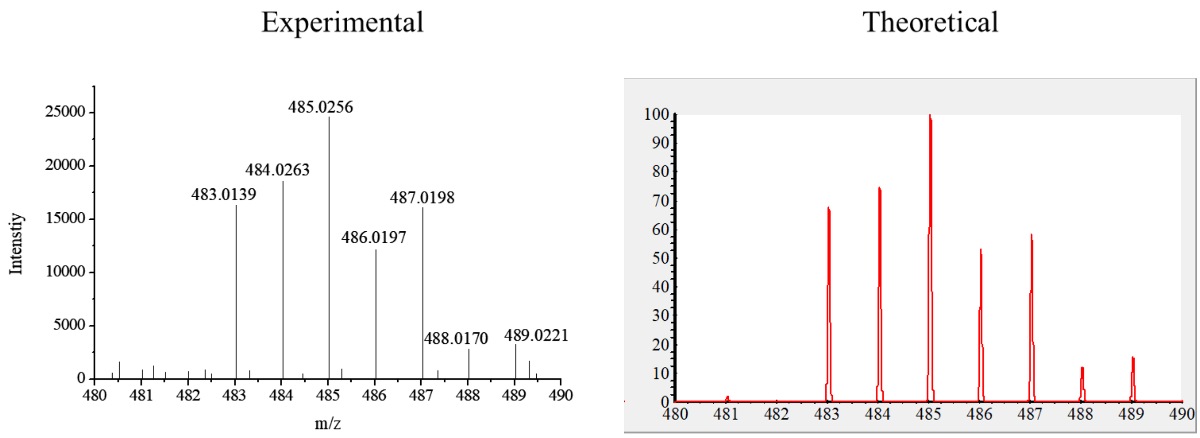

ESI-HRMS (positive ion mode), m/z. $[M+Na]^+$ calculated for $C_7H_{20}Cl_2N_2NaO_4Pt$: 485.0323, found: 485.0256

Figure S1. ESI-HRMS spectrum of complex *c,t,c*-[Pt(NH_3)$_2$(OCOOCH$_2$CH$_2$CH$_2$CH$_2$CH$_2$-CH$_3$)(OH)(Cl)$_2$] **1a**.

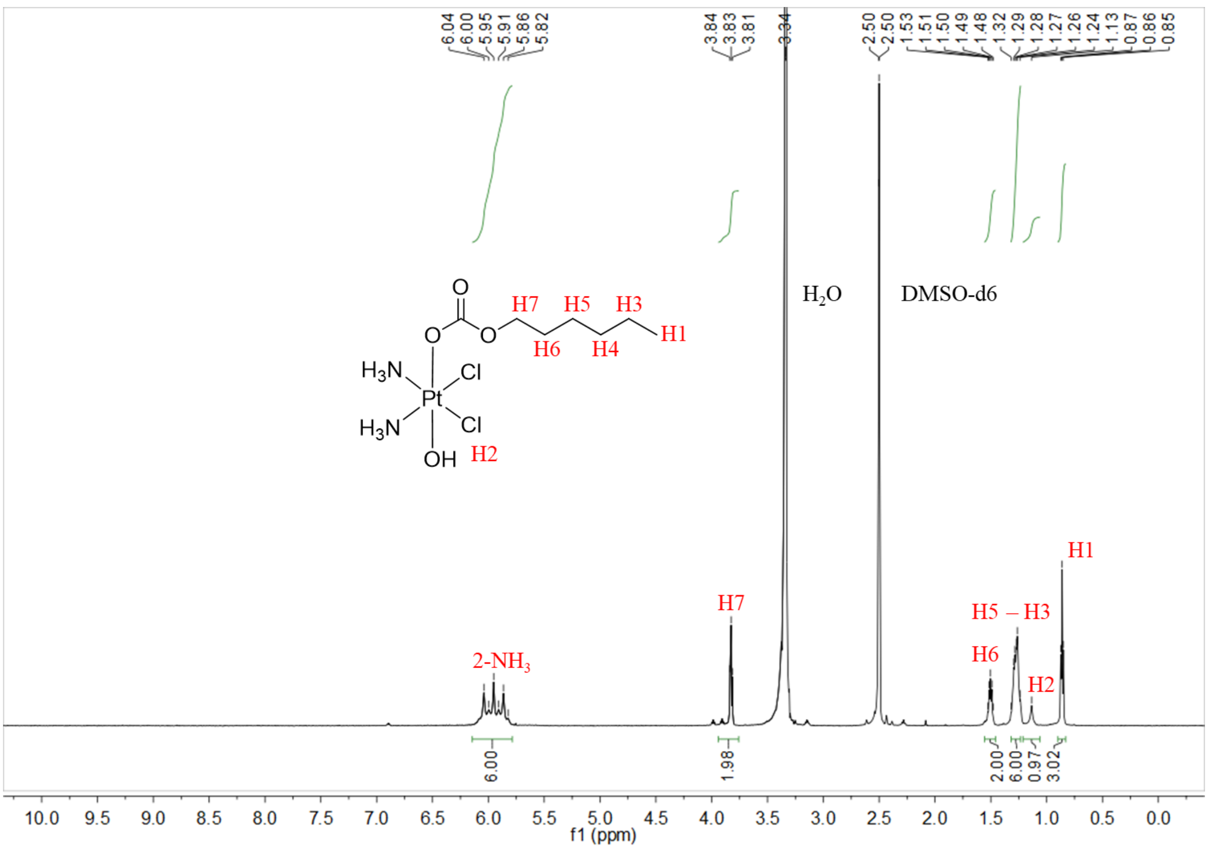

Figure S2. ^{1}H NMR spectrum of complex *c,t,c*-[Pt(NH_3)$_2$(OCOOCH$_2$CH$_2$CH$_2$CH$_2$CH$_2$CH$_3$)-(OH)(Cl)$_2$] **1a** in DMSO-*d*$_6$.

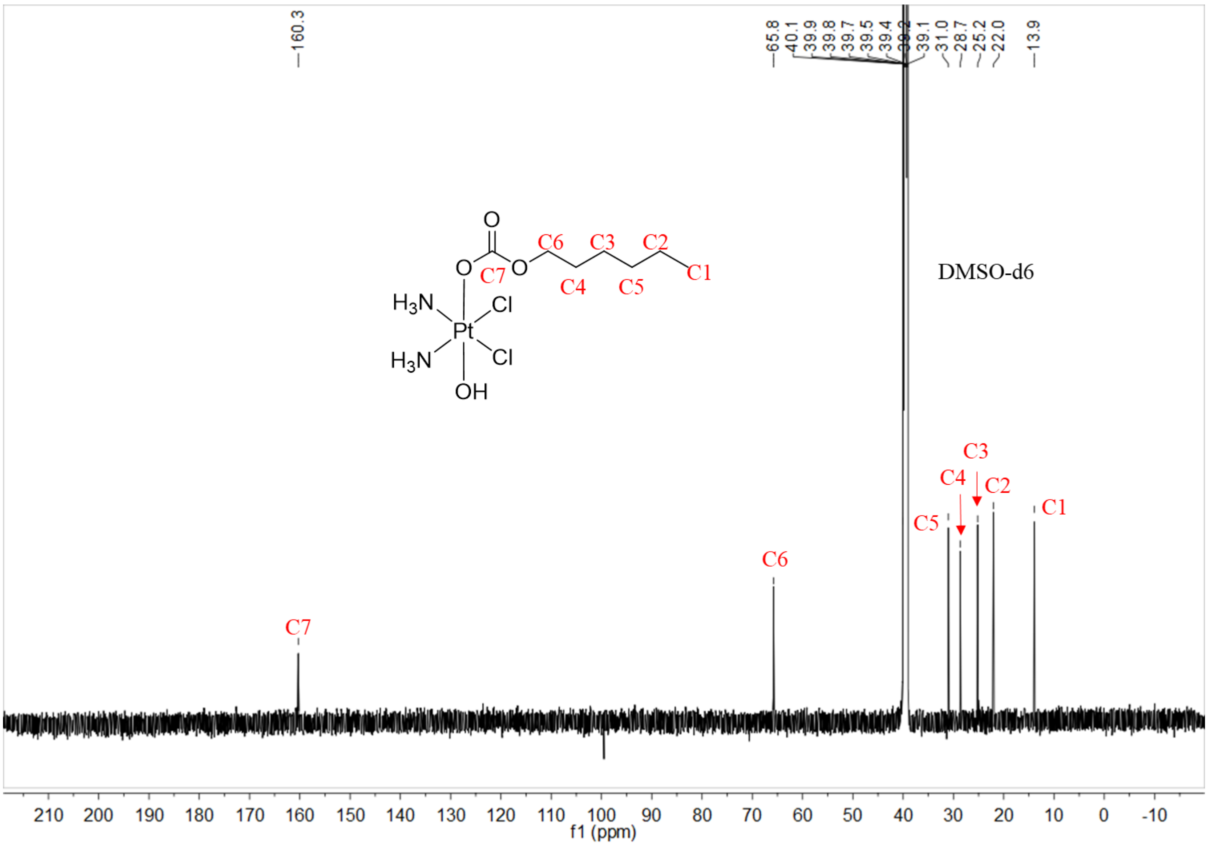

Figure S3. ^{13}C NMR spectrum of complex *c,t,c*-[Pt(NH_3)$_2$($OCOOCH_2CH_2CH_2CH_2CH_2CH_3$)-(OH)(Cl)$_2$] **1a** in DMSO-$d_6$.

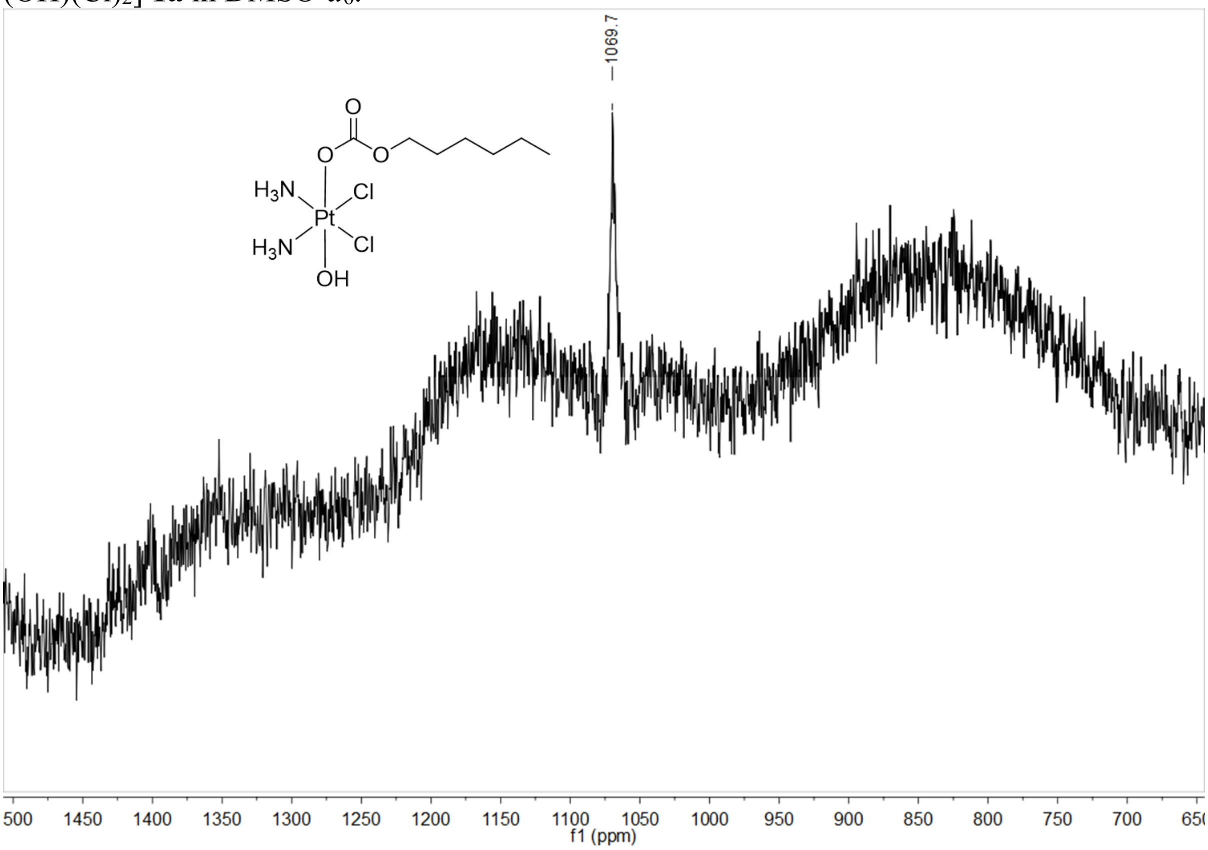

Figure S4. ^{195}Pt NMR spectrum of complex *c,t,c*-[Pt(NH_3)$_2$($OCOOCH_2CH_2CH_2CH_2CH_2$-CH_3)(OH)(Cl)$_2$] **1a** in DMSO-d_6.

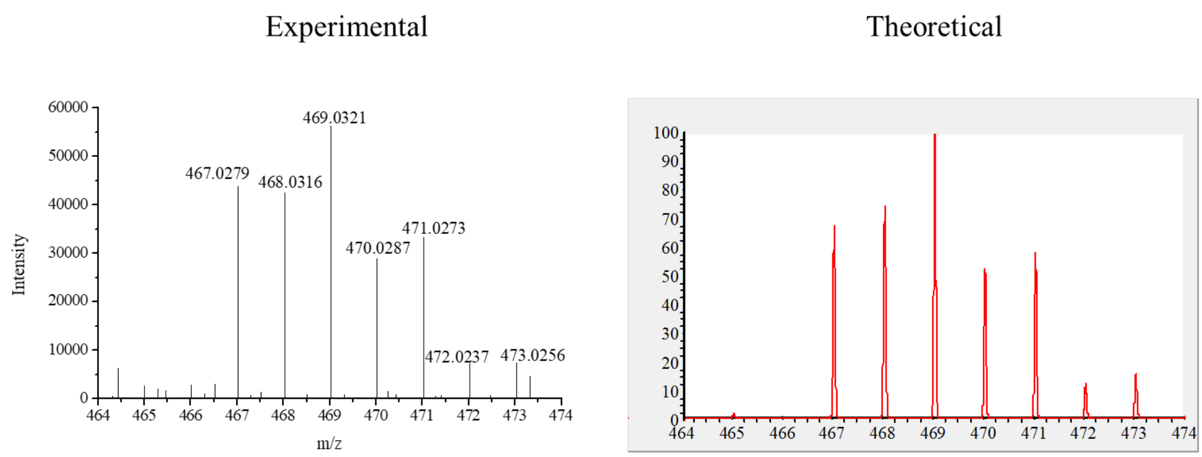

ESI-HRMS (positive ion mode), m/z. $[M+Na]^+$ calculated for $C_7H_{20}Cl_2N_2NaO_3Pt$: 469.0373, found: 469.0321

Figure S5. ESI-HRMS spectrum of complex *c,t,c*-$[Pt(NH_3)_2(OCOCH_2CH_2CH_2CH_2CH_2CH_3)(OH)(Cl)_2]$ **1b**.

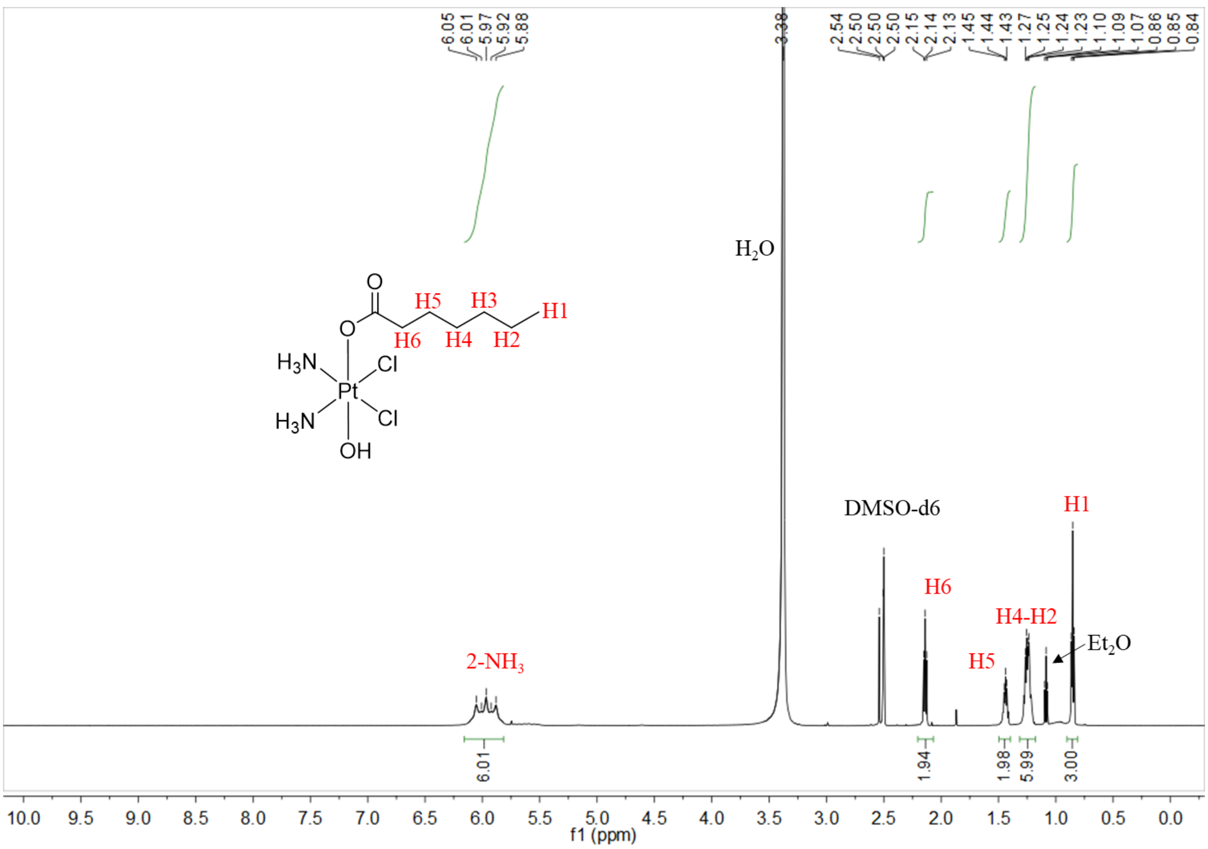

Figure S6. ^1H NMR spectrum of complex *c,t,c*-$[Pt(NH_3)_2(OCOCH_2CH_2CH_2CH_2CH_2CH_3)$-$(OH)(Cl)_2]$ **1b** in DMSO-d_6.

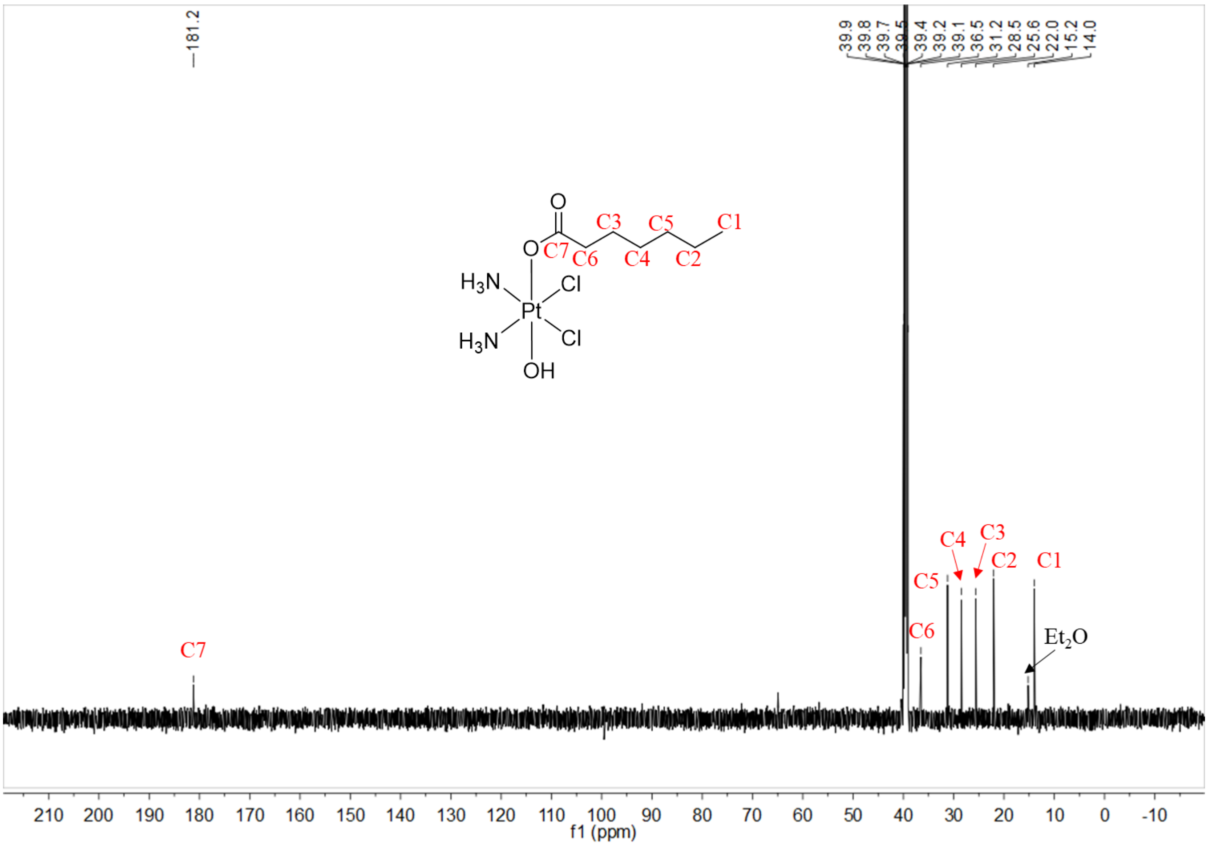

Figure S7. [13]C NMR spectrum of complex *c,t,c*-[Pt(NH_3)$_2$($OCOCH_2CH_2CH_2CH_2CH_2CH_3$)-(OH)($Cl$)$_2$] **1b** in DMSO-$d_6$.

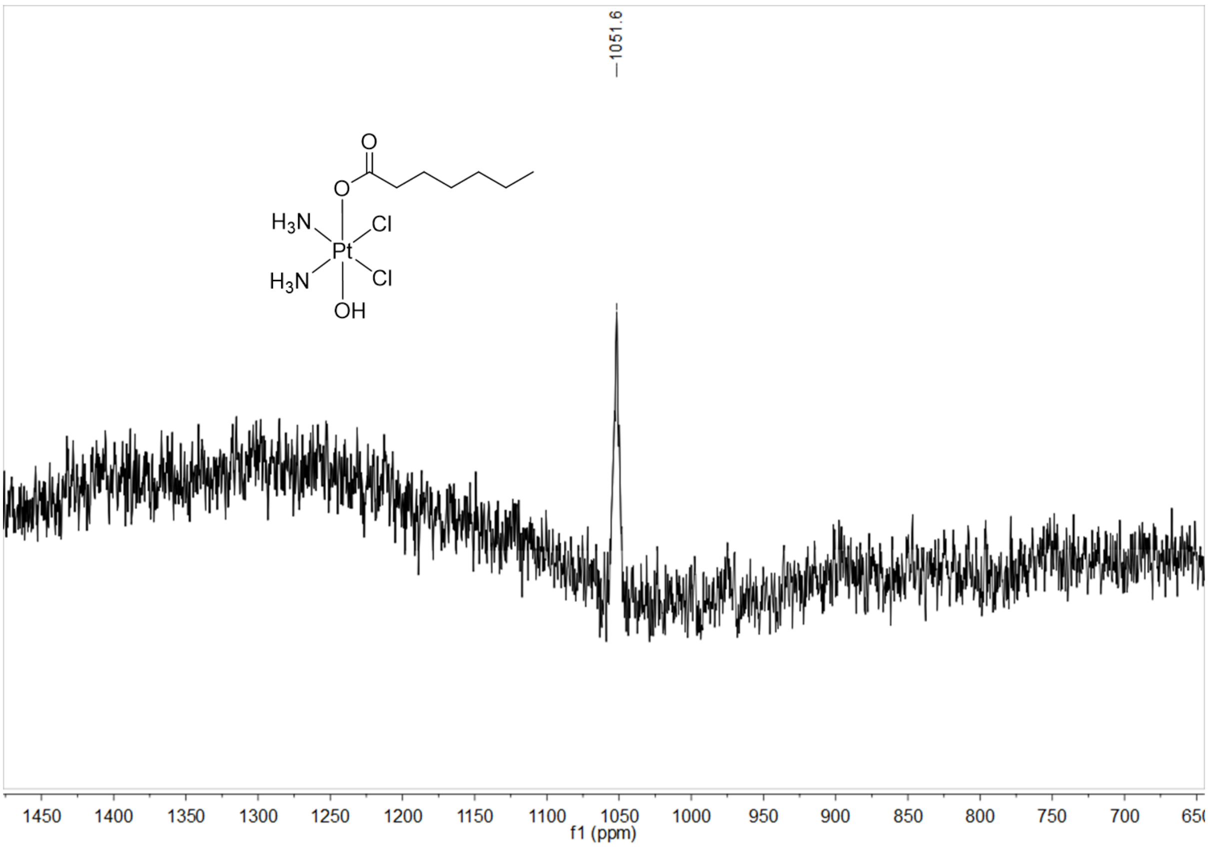

Figure S8. [195]Pt NMR spectrum of complex *c,t,c*-[Pt(NH_3)$_2$($OCOCH_2CH_2CH_2CH_2CH_2CH_3$)-(OH)($Cl$)$_2$] **1b** in DMSO-$d_6$.

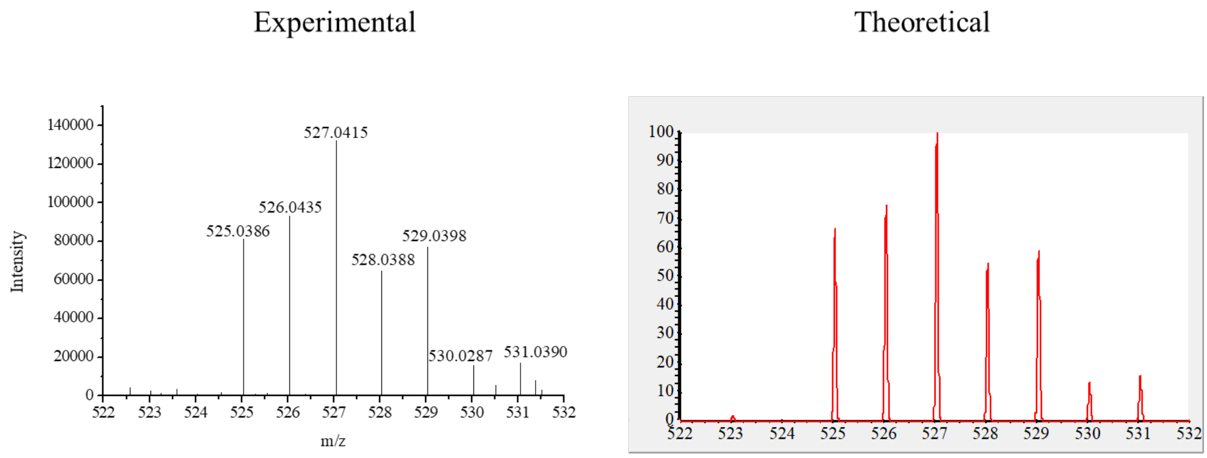

ESI-HRMS (positive ion mode), m/z. $[M+Na]^+$ calculated for $C_9H_{22}Cl_2N_2NaO_5Pt$: 527.0430, found: 527.0415

Figure S9. ESI-HRMS spectrum of complex *c,t,c*-[Pt(NH$_3$)$_2$(OCOOCH$_2$CH$_2$CH$_2$CH$_2$CH$_2$-CH$_3$)(OCOCH$_3$)(Cl)$_2$] **1a′**.

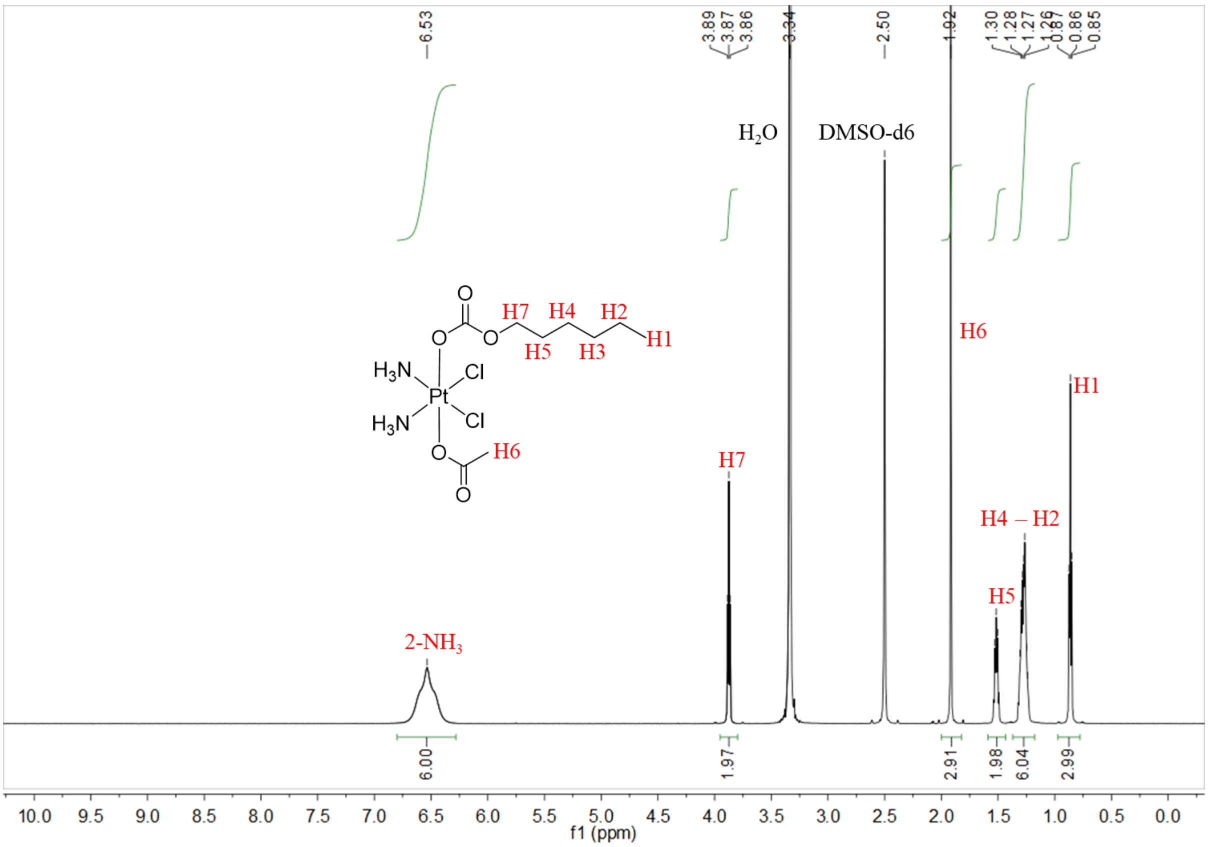

Figure S10. ^{1}H NMR spectrum of complex *c,t,c*-[Pt(NH$_3$)$_2$(OCOOCH$_2$CH$_2$CH$_2$CH$_2$CH$_2$CH$_3$)(OCOCH$_3$)(Cl)$_2$] **1a′** in DMSO-*d*$_6$.

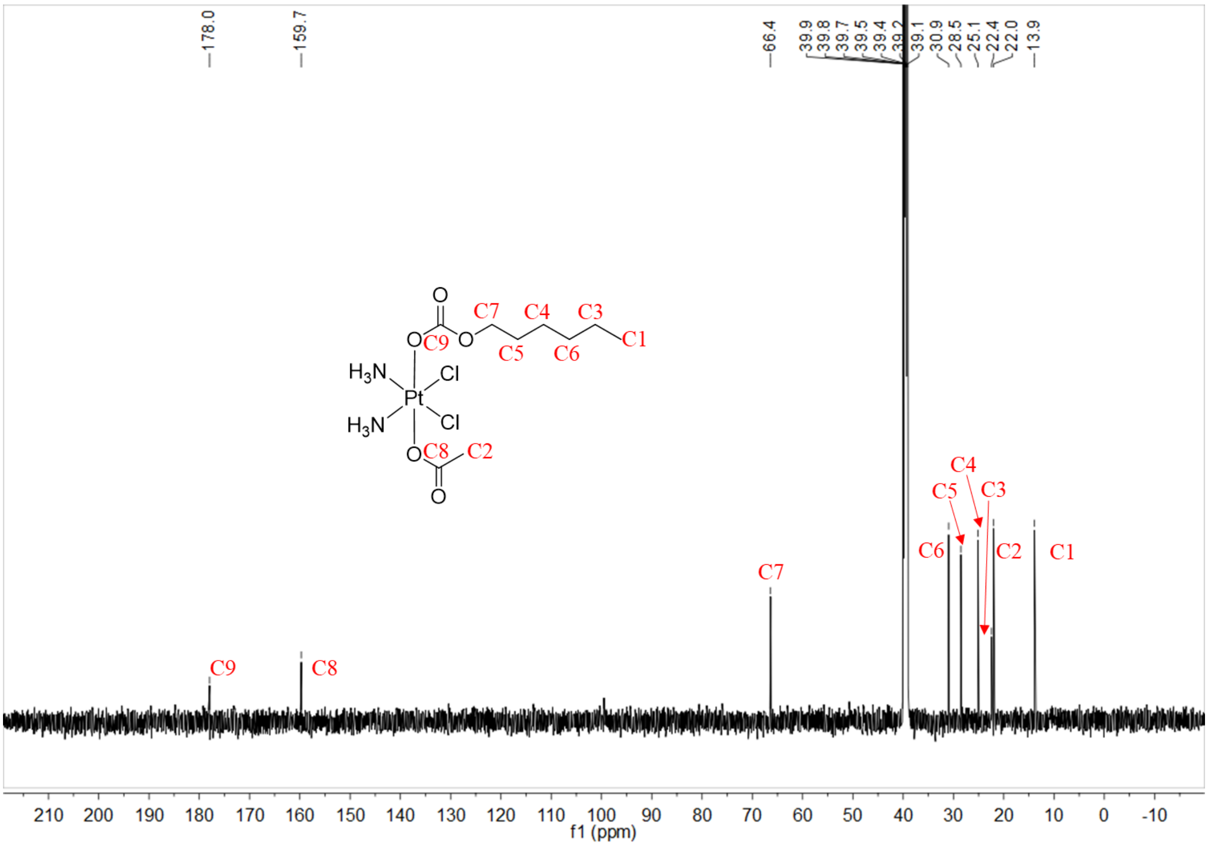

Figure S11. ^{13}C NMR spectrum of complex *c,t,c*-[Pt(NH$_3$)$_2$(OCOOCH$_2$CH$_2$CH$_2$CH$_2$CH$_2$-CH$_3$)(OCOCH$_3$)(Cl)$_2$] **1a′** in DMSO-*d*$_6$.

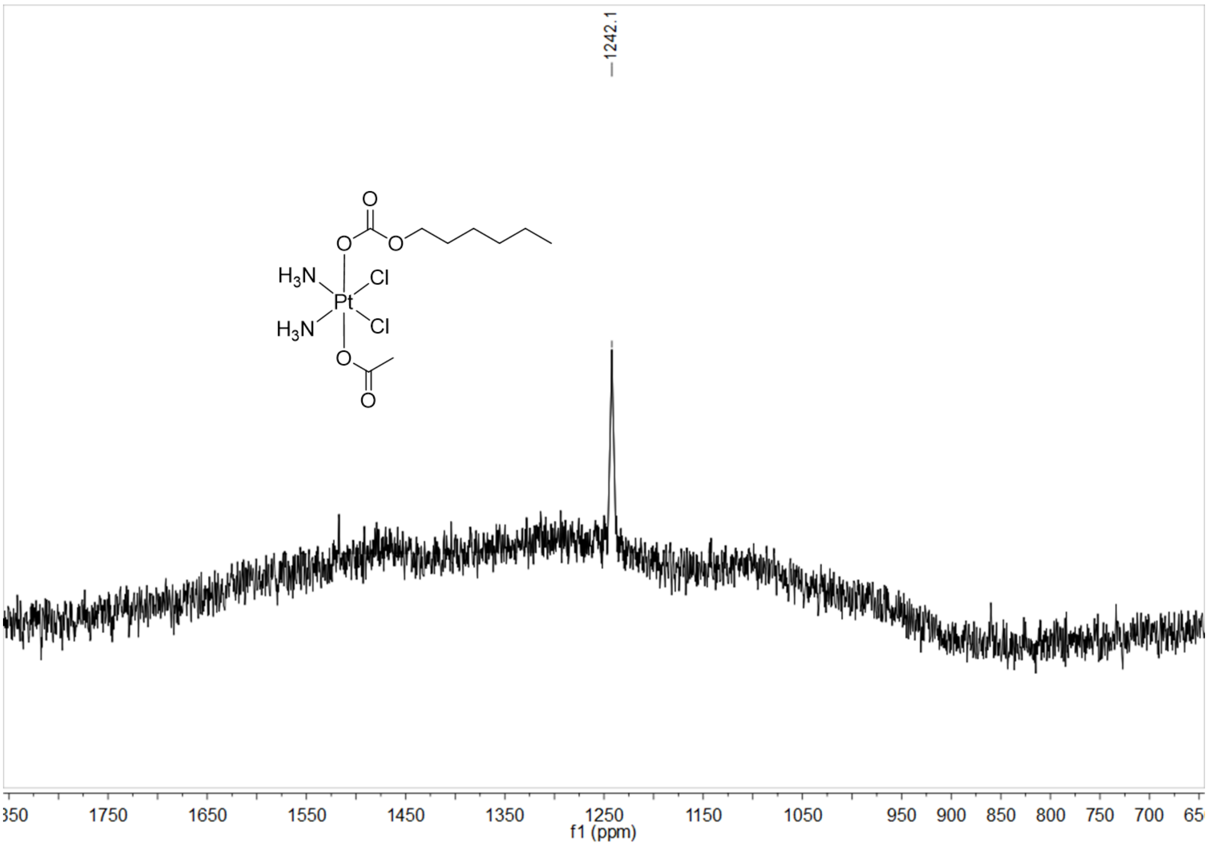

Figure S12. ^{195}Pt NMR spectrum of complex *c,t,c*-[Pt(NH$_3$)$_2$(OCOOCH$_2$CH$_2$CH$_2$-CH$_2$CH$_3$)(OCOCH$_3$)(Cl)$_2$] **1a′** in DMSO-*d*$_6$.

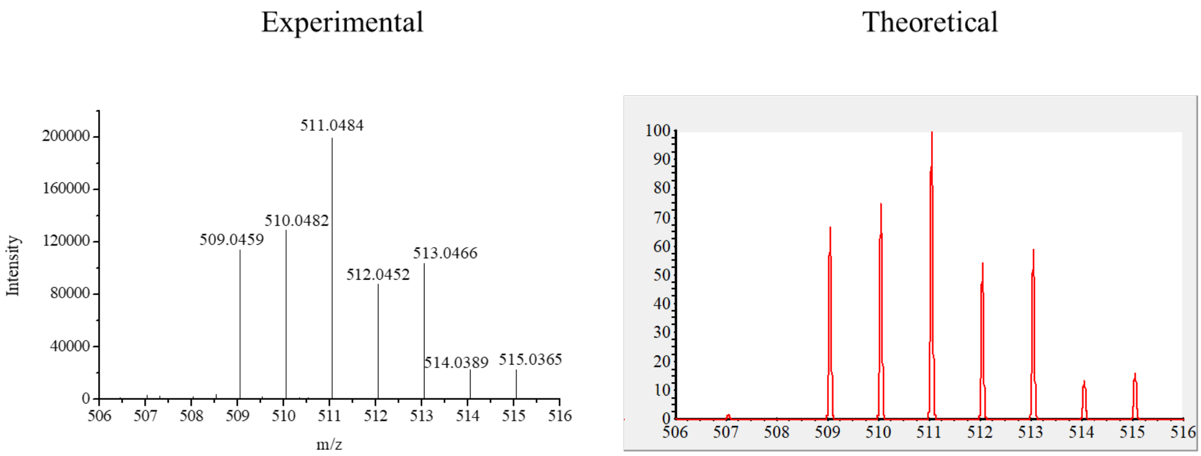

ESI-HRMS (positive ion mode), m/z. $[M+Na]^+$ calculated for $C_9H_{22}Cl_2N_2NaO_4Pt$: 511.0480, found: 511.0484

Figure S13. ESI-HRMS spectrum of complex *c,t,c*-[Pt(NH_3)$_2$($OCOCH_2CH_2CH_2CH_2CH_2$-CH_3)($OCOCH_3$)(Cl)$_2$] **1b′**.

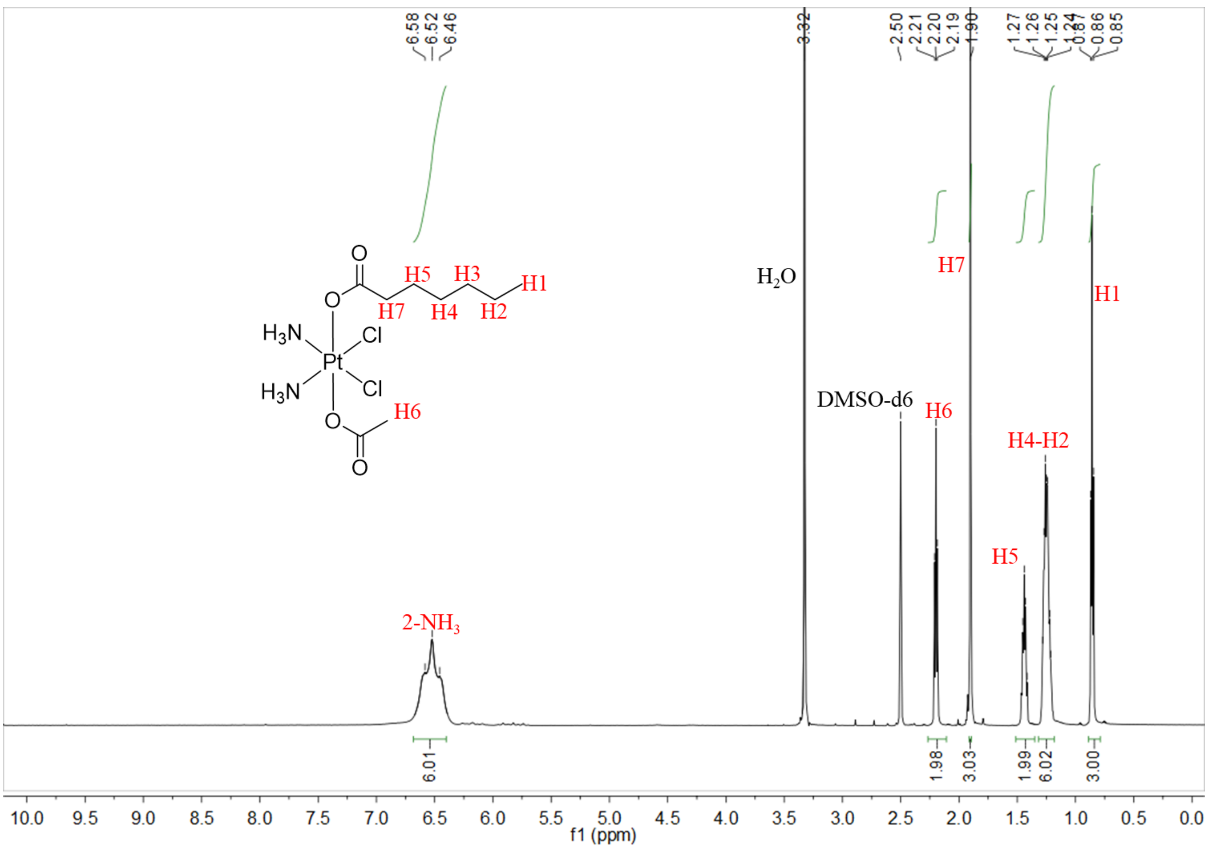

Figure S14. [1]H NMR spectrum of complex *c,t,c*-[Pt(NH_3)$_2$($OCOCH_2CH_2CH_2CH_2CH_2CH_3$)-($OCOCH_3$)($Cl$)$_2$] **1b′** in DMSO-$d_6$.

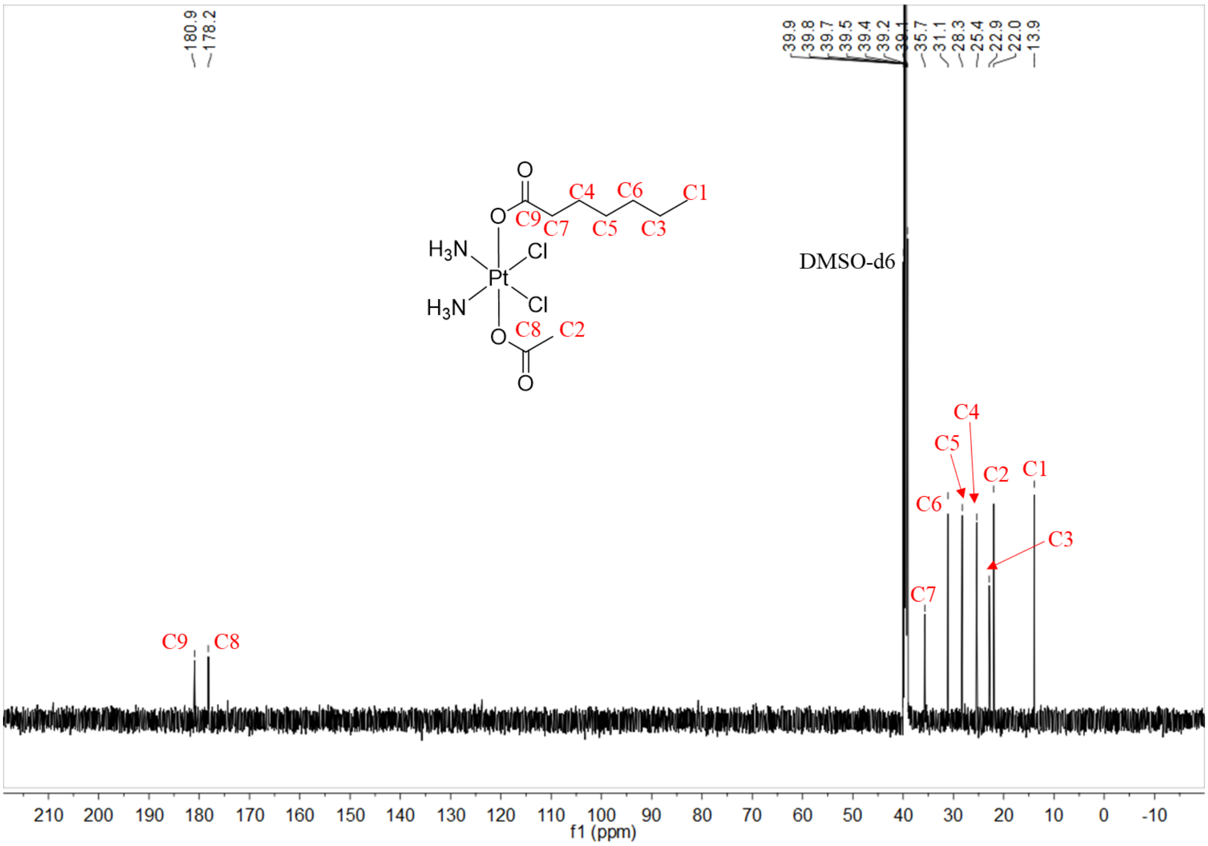

Figure S15. [13]C NMR spectrum of complex *c,t,c*-[Pt(NH_3)$_2$($OCOCH_2CH_2CH_2CH_2CH_2CH_3$)-($OCOCH_3$)(Cl)$_2$] **1b′** in DMSO-*d*$_6$.

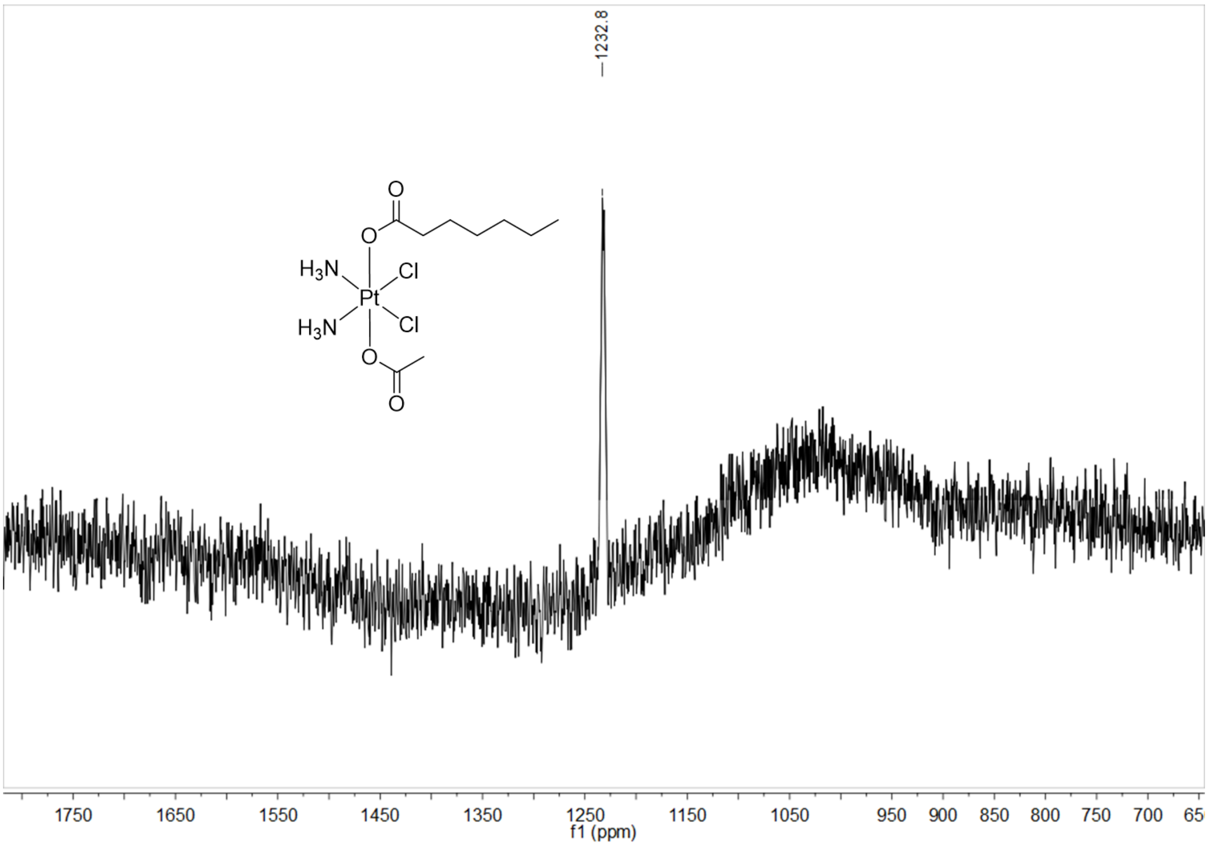

Figure S16. [195]Pt NMR spectrum of complex *c,t,c*-[Pt(NH_3)$_2$($OCOCH_2CH_2CH_2CH_2CH_2CH_3$) ($OCOCH_3$)(Cl)$_2$] **1b′** in DMSO-*d*$_6$.

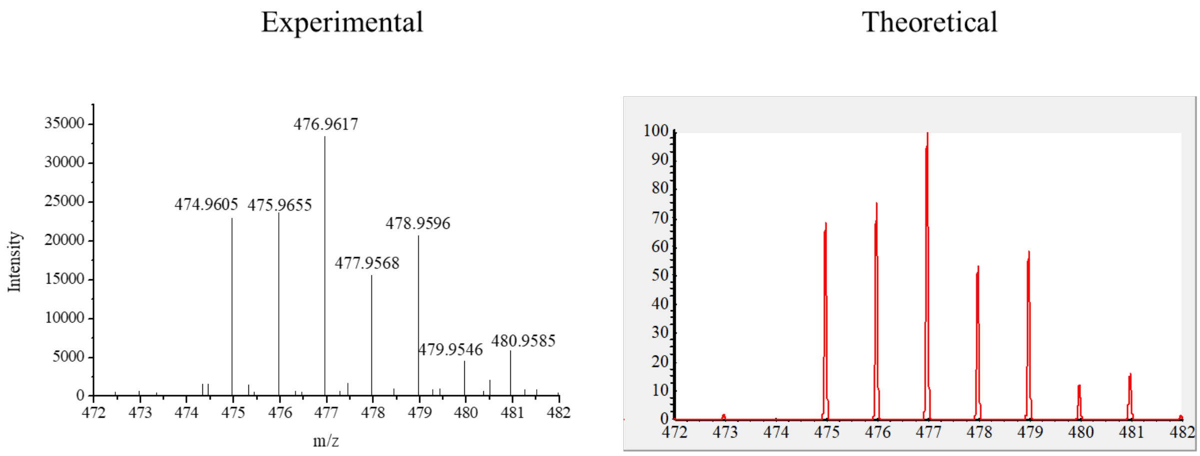

ESI-HRMS (positive ion mode), m/z. $[M+Na]^+$ calculated for $C_7H_{12}Cl_2N_2NaO_4Pt$: 476.9697, found: 476.9617

Figure S17. ESI-HRMS spectrum of complex *c,t,c*-[Pt(NH_3)$_2$(OCOOPh)(OH)(Cl)$_2$] **2a**.

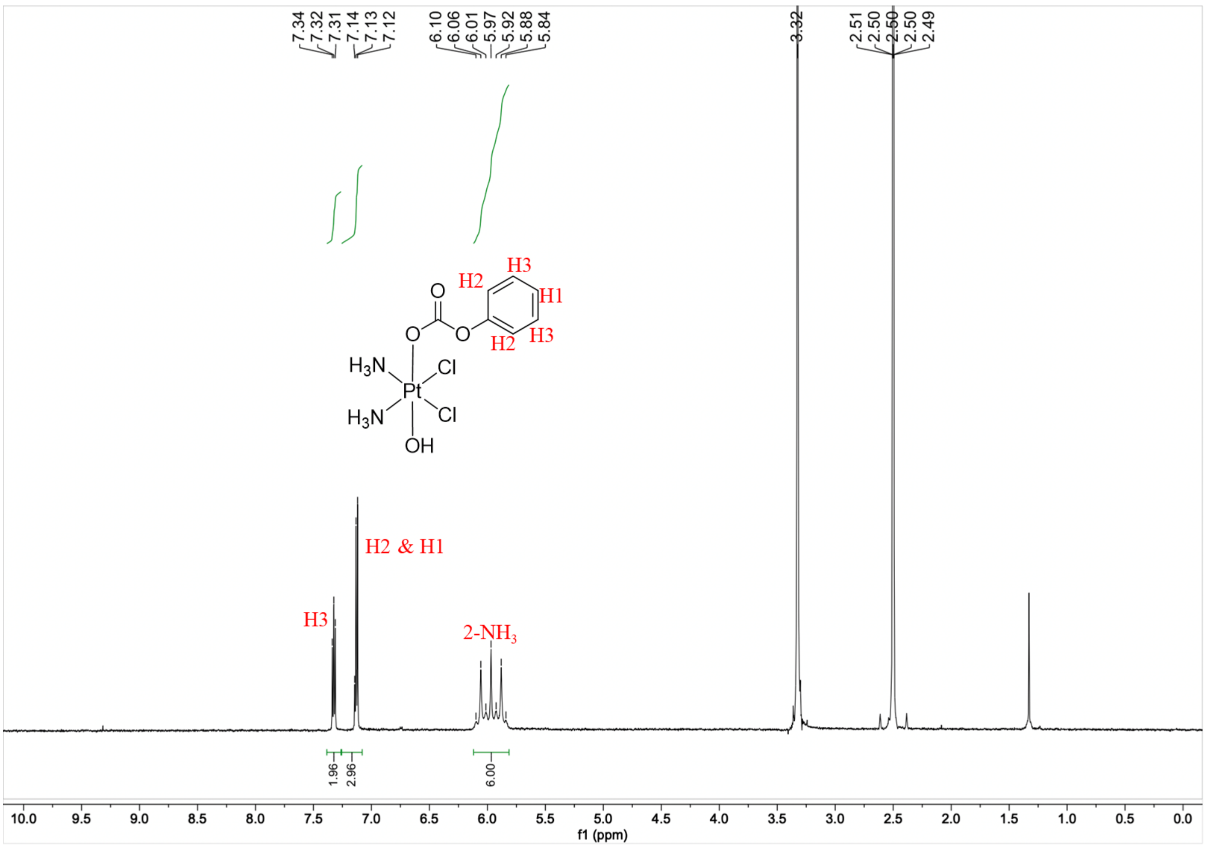

Figure S18. ^{1}H NMR spectrum of complex *c,t,c*-[Pt(NH_3)$_2$(OCOOPh)(OH)(Cl)$_2$] **2a** in DMSO-d_6.

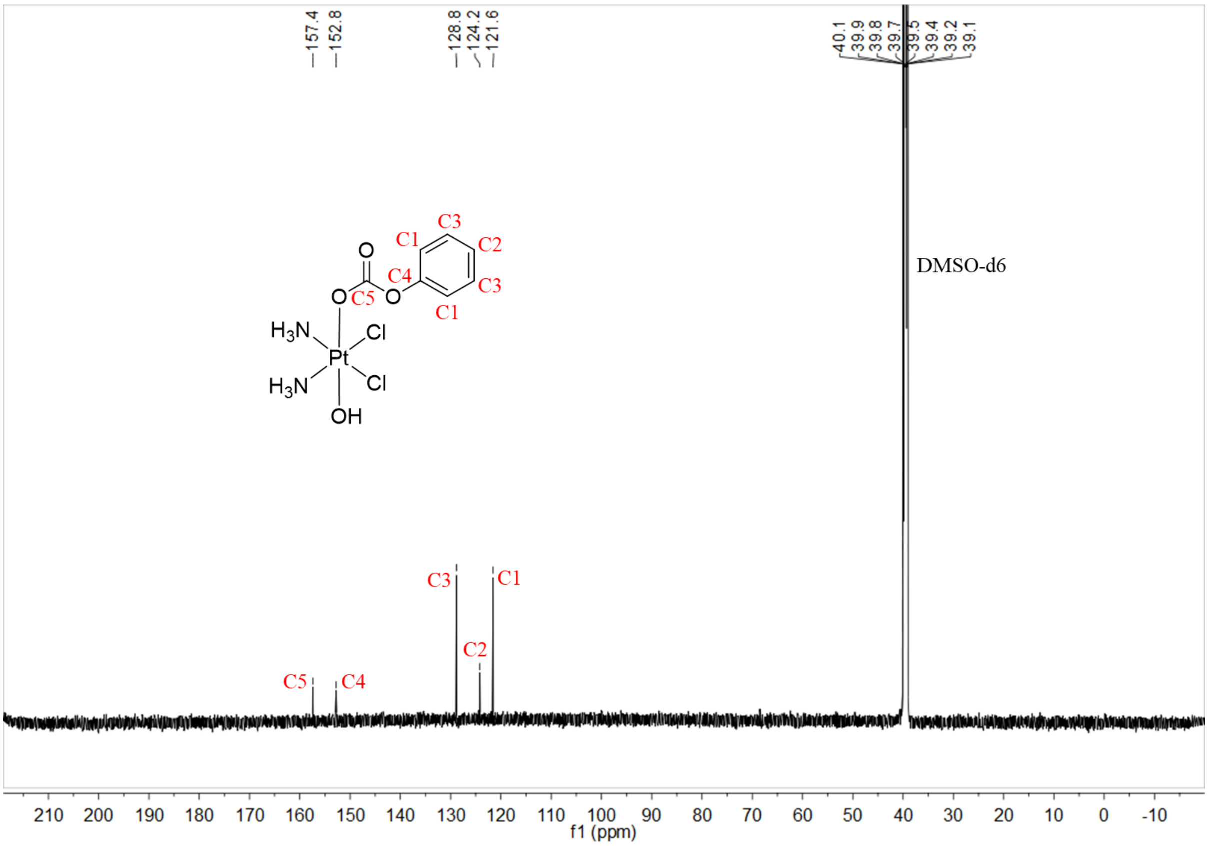

Figure S19. ^{13}C NMR spectrum of complex *c,t,c*-[Pt(NH_3)$_2$(OCOOPh)(OH)(Cl)$_2$] **2a** in DMSO-*d*$_6$.

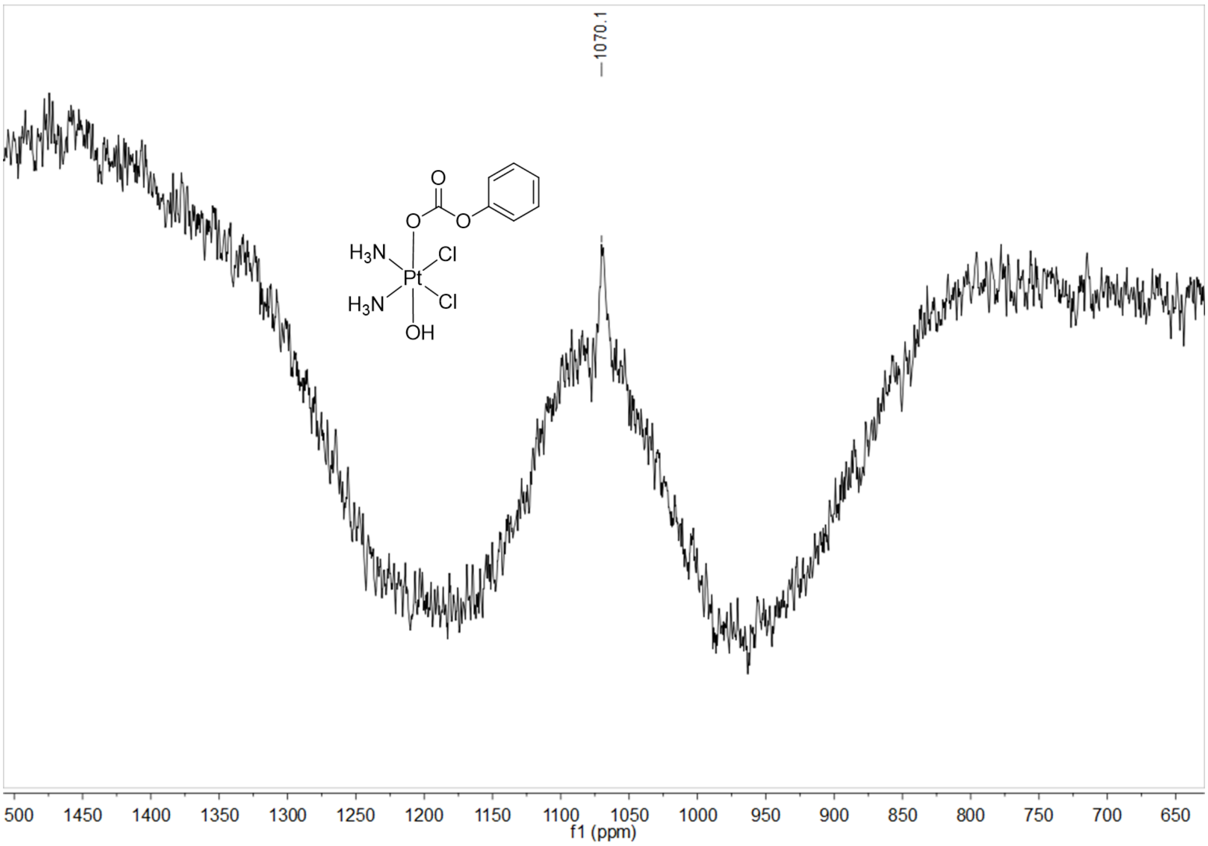

Figure S20. ^{195}Pt NMR spectrum of complex *c,t,c*-[Pt(NH_3)$_2$(OCOOPh)(OH)(Cl)$_2$] **2a** in DMSO-*d*$_6$.

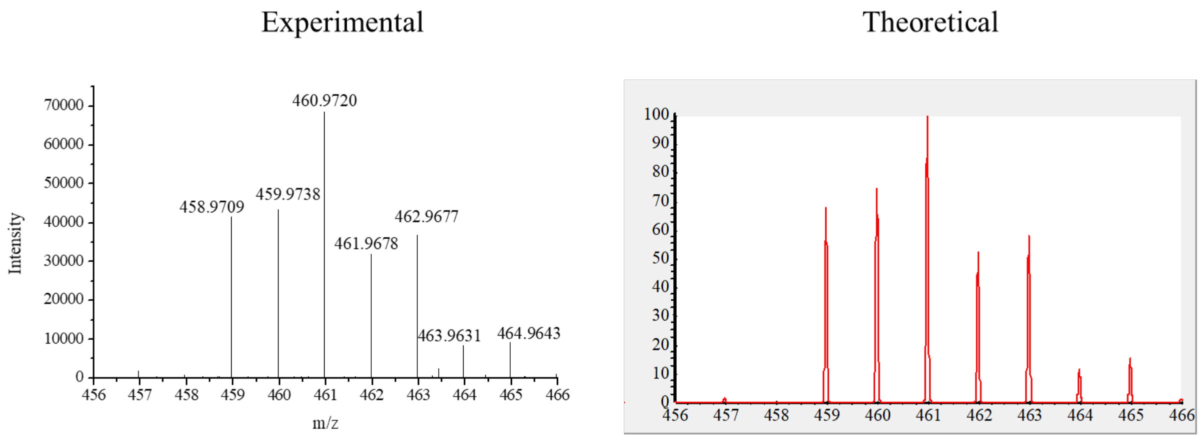

ESI-HRMS (positive ion mode), m/z. $[M+Na]^+$ calculated for $C_7H_{12}Cl_2N_2NaO_3Pt$: 460.9748, found: 460.9720

Figure S21. ESI-HRMS spectrum of complex *c,t,c*-[Pt(NH_3)$_2$(OCOPh)(OH)(Cl)$_2$] **2b**.

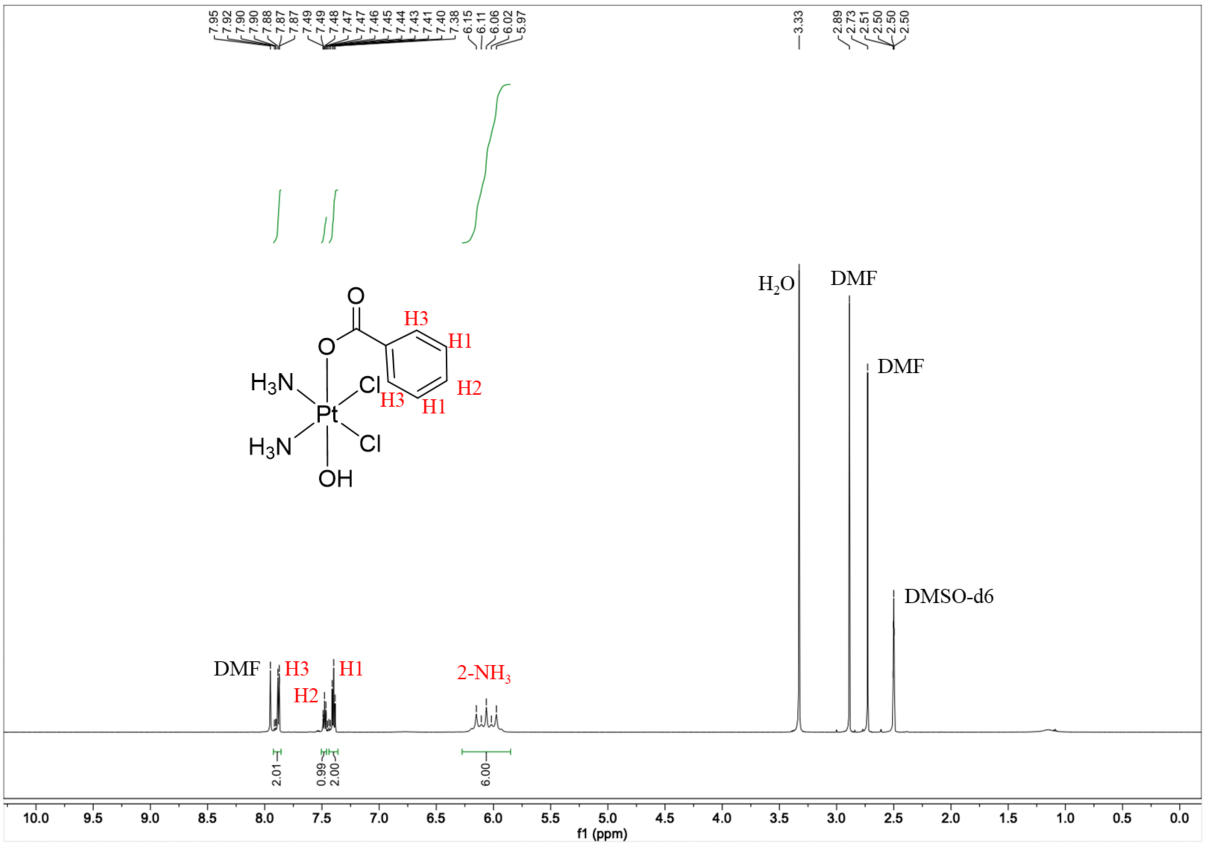

Figure S22. [1]H NMR spectrum of complex *c,t,c*-[Pt(NH_3)$_2$(OCOPh)(OH)(Cl)$_2$] **2b** in DMSO-*d*$_6$.

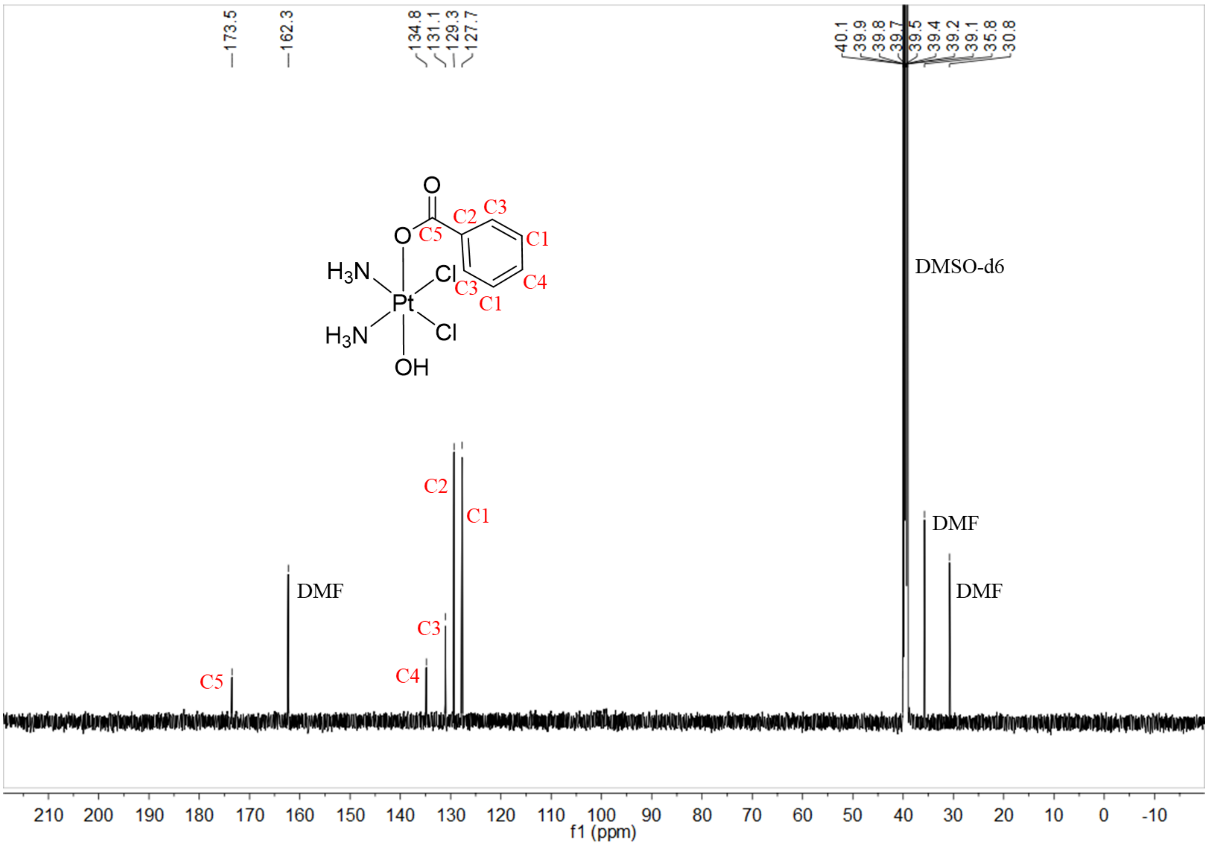

Figure S23. ^{13}C NMR spectrum of complex *c,t,c*-[Pt$(NH_3)_2$(OCOPh)(OH)$(Cl)_2$] **2b** in DMSO-*d*$_6$.

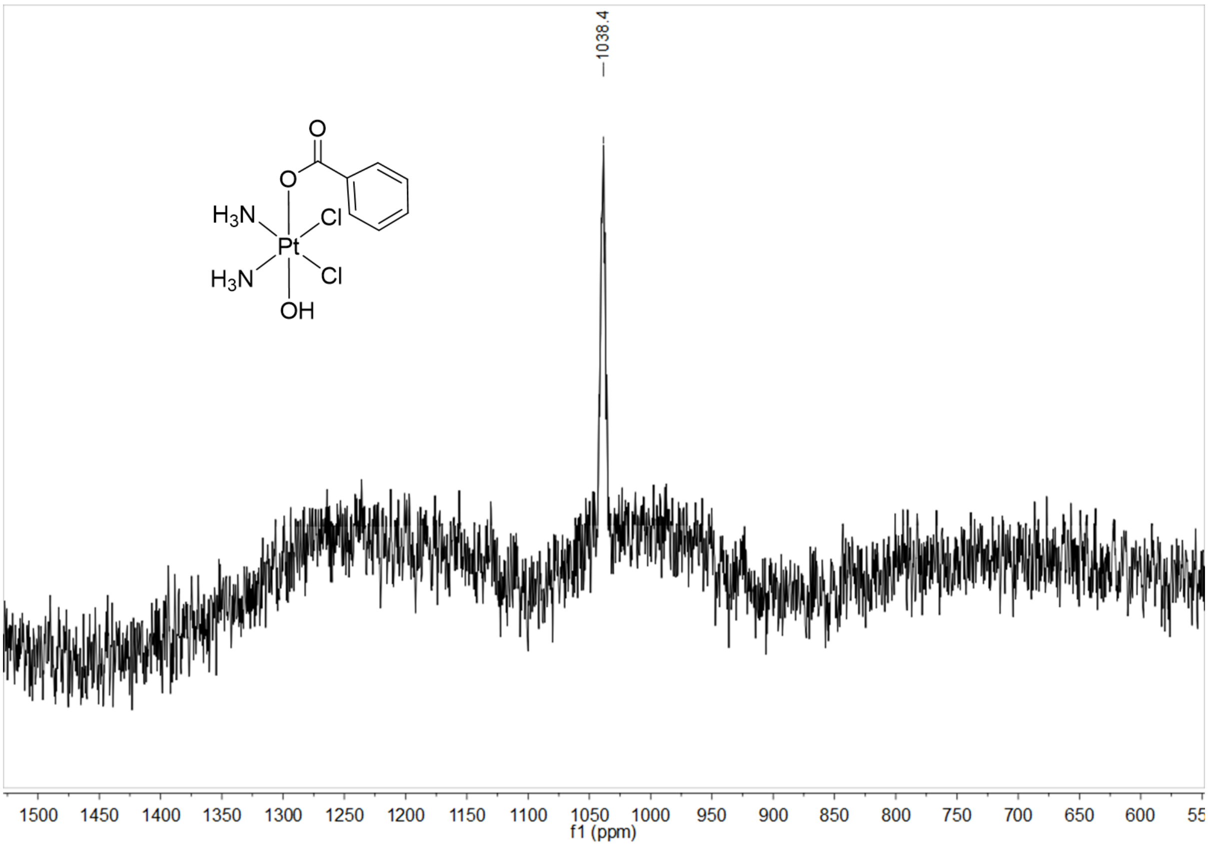

Figure S24. ^{195}Pt NMR spectrum of complex *c,t,c*-[Pt$(NH_3)_2$(OCOPh)(OH)$(Cl)_2$] **2b** in DMSO-*d*$_6$.

Experimental Theoretical

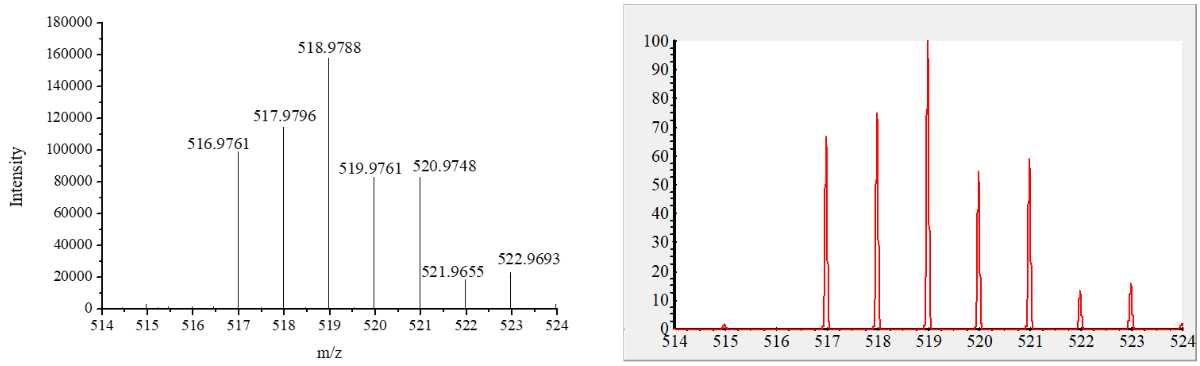

ESI-HRMS (positive ion mode), m/z. $[M+Na]^+$ calculated for $C_9H_{14}Cl_2N_2NaO_5Pt$: 518.9803, found: 518.9788

Figure S25. ESI-HRMS spectrum of complex *c,t,c*-[Pt(NH3)2(OCOOPh)(OCOCH3)(Cl)2] **2a'**.

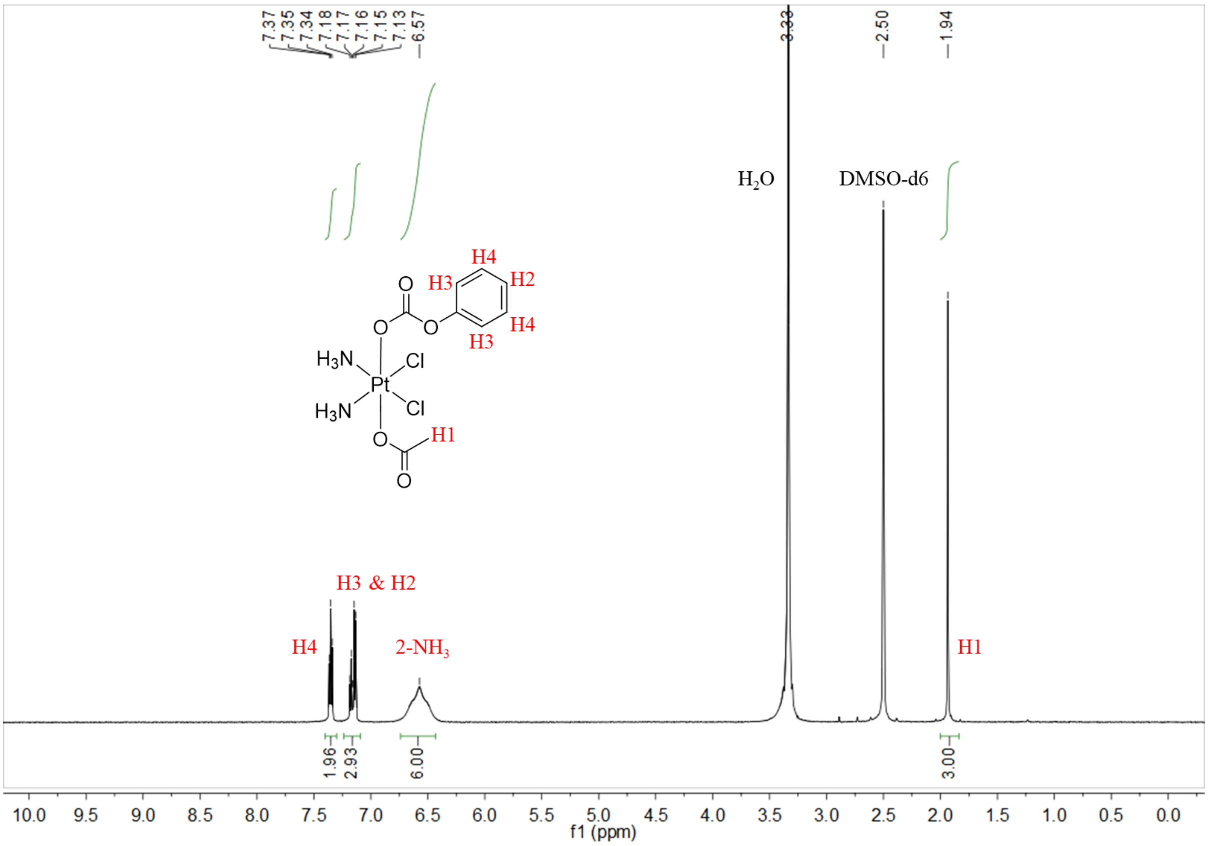

Figure S26. ^{1}H NMR spectrum of complex *c,t,c*-[Pt(NH3)2(OCOOPh)(OCOCH3)(Cl)2] **2a'** in DMSO-*d*6.

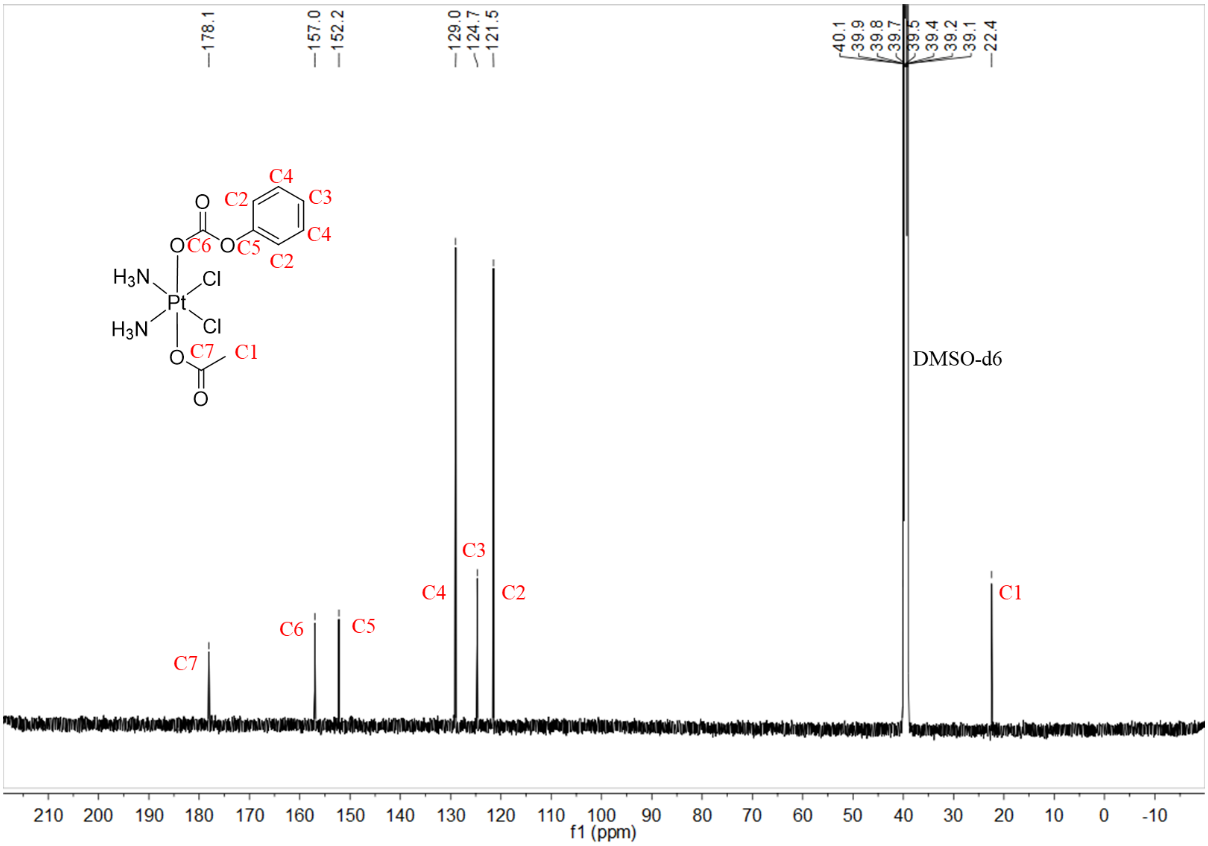

Figure S27. ^{13}C NMR spectrum of complex *c,t,c*-[Pt(NH_3)$_2$(OCOOPh)($OCOCH_3$)(Cl)$_2$] **2a'** in DMSO-d_6.

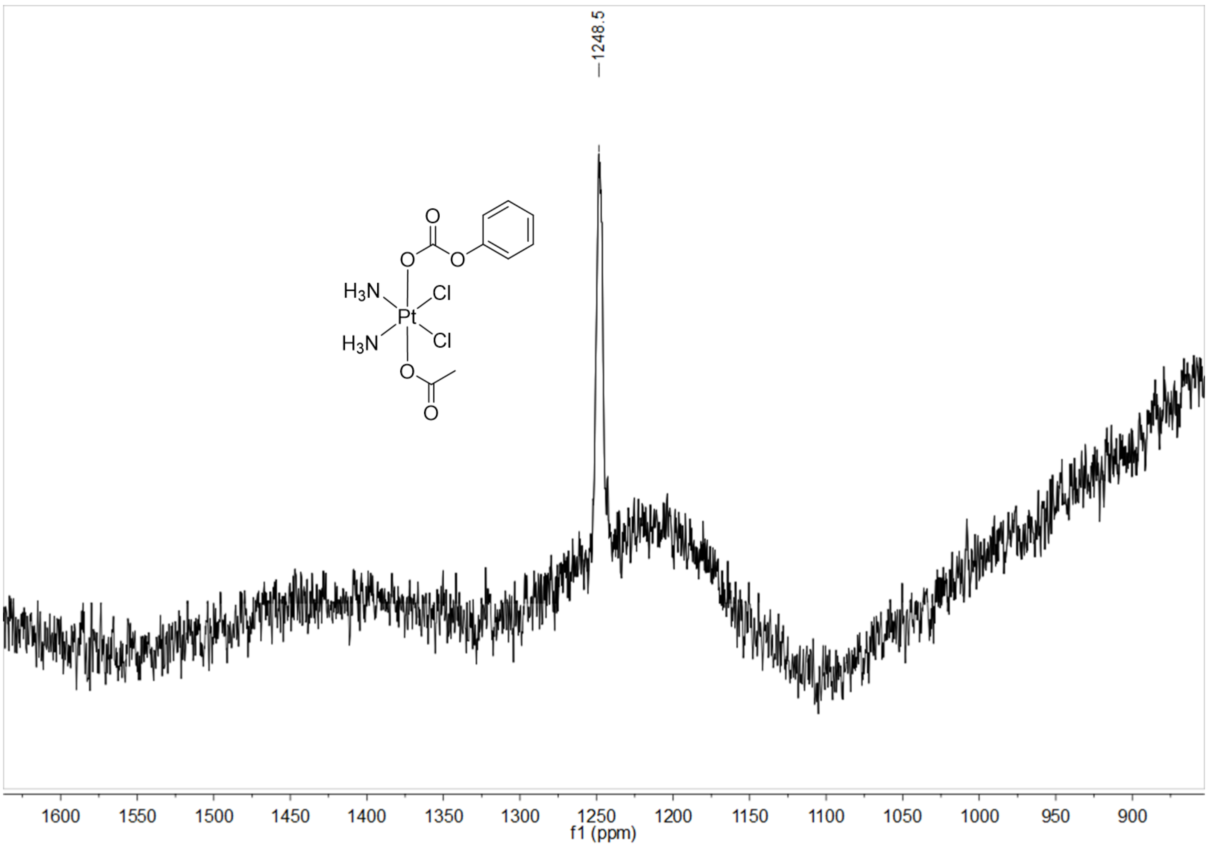

Figure S28. ^{195}Pt NMR spectrum of complex *c,t,c*-[Pt(NH_3)$_2$(OCOOPh)($OCOCH_3$)(Cl)$_2$] **2a'** in DMSO-d_6.

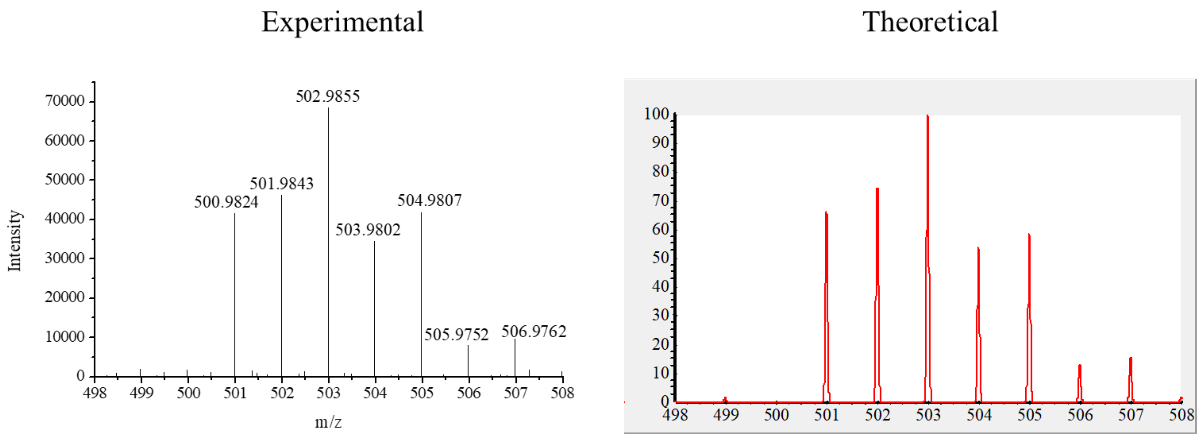

ESI-HRMS (positive ion mode), m/z. $[M+Na]^+$ calculated for $C_9H_{14}Cl_2N_2NaO_4Pt$: 502.9854, found: 502.9855

Figure S29. ESI-HRMS spectrum of complex *c,t,c*-[Pt$(NH_3)_2$(OCOPh)$(OCOCH_3)$$(Cl)_2$] **2b'**.

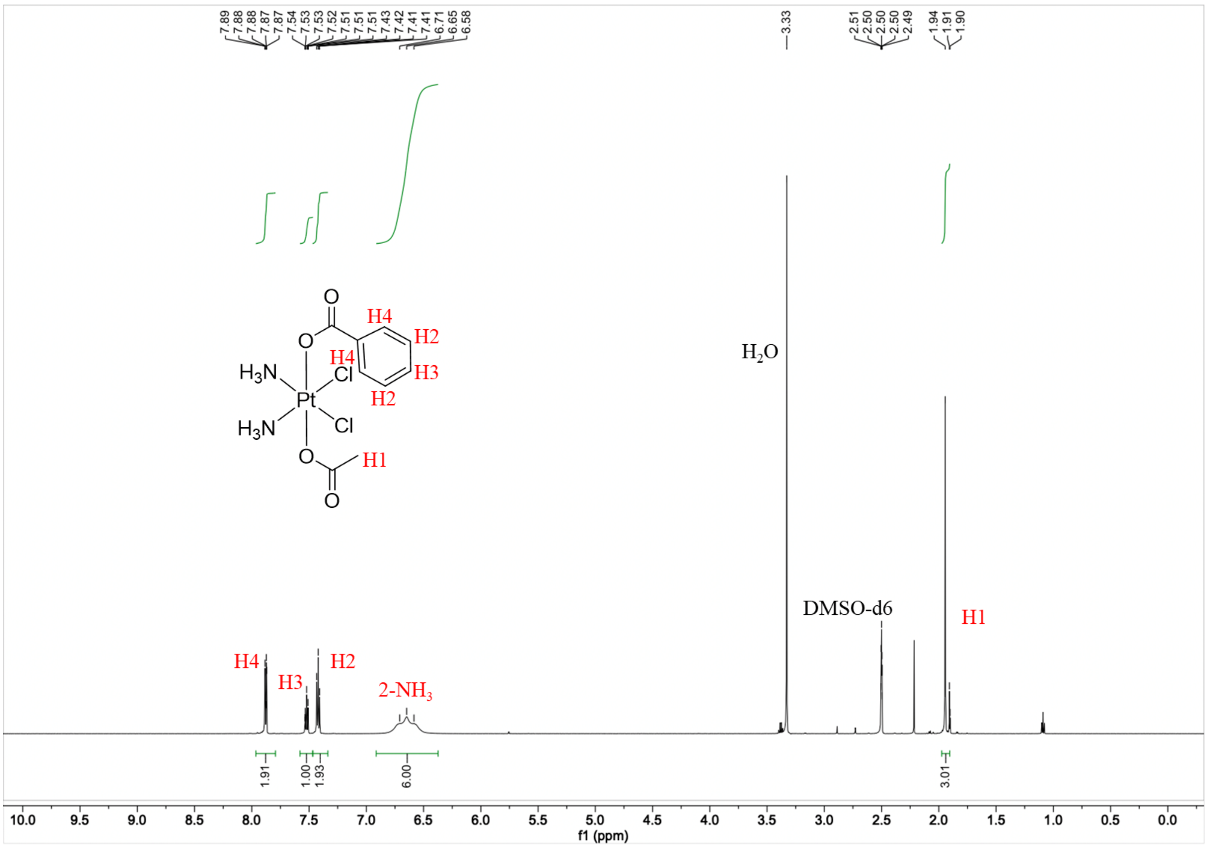

Figure S30. ^{1}H NMR spectrum of complex *c,t,c*-[Pt$(NH_3)_2$(OCOPh)$(OCOCH_3)$$(Cl)_2$] **2b'** in DMSO-$d_6$.

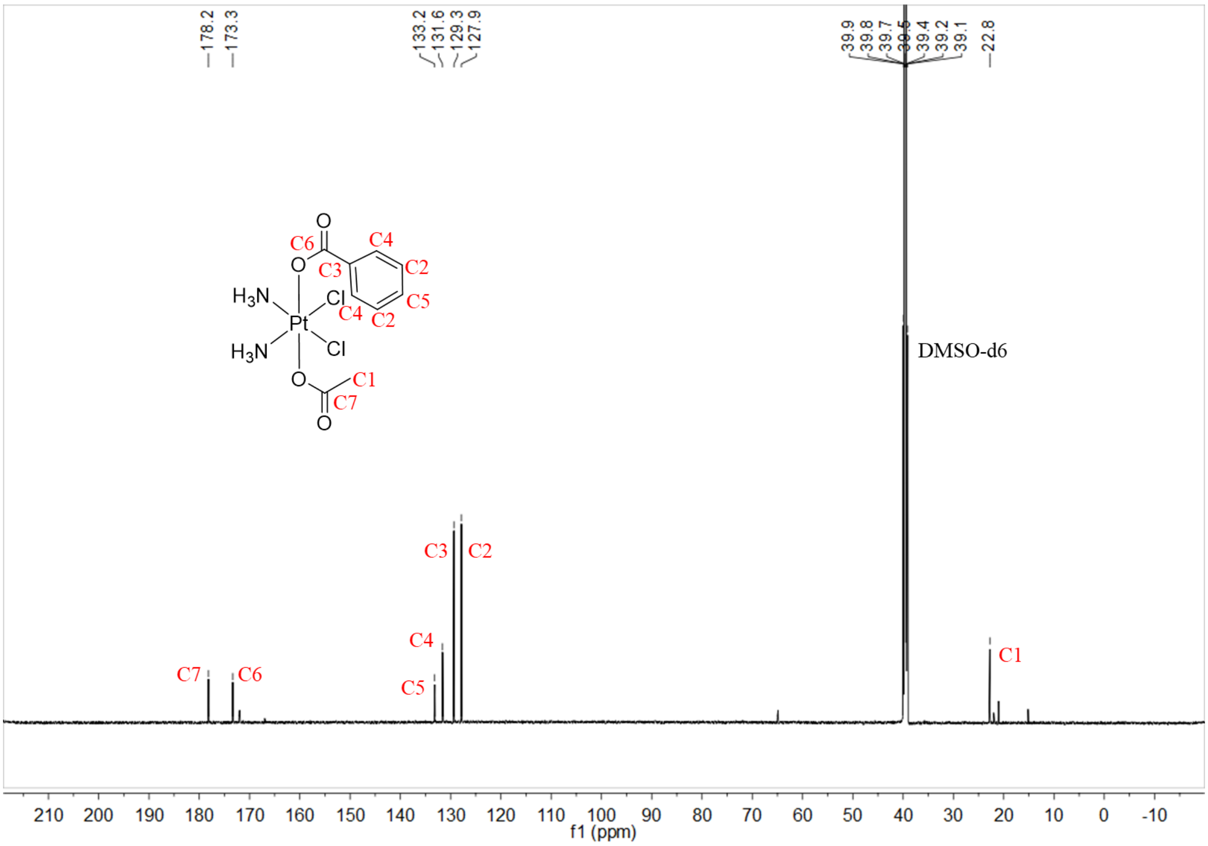

Figure S31. ^{13}C NMR spectrum of complex *c,t,c*-[Pt$(NH_3)_2$(OCOPh)$(OCOCH_3)(Cl)_2$] **2b'** in DMSO-d_6.

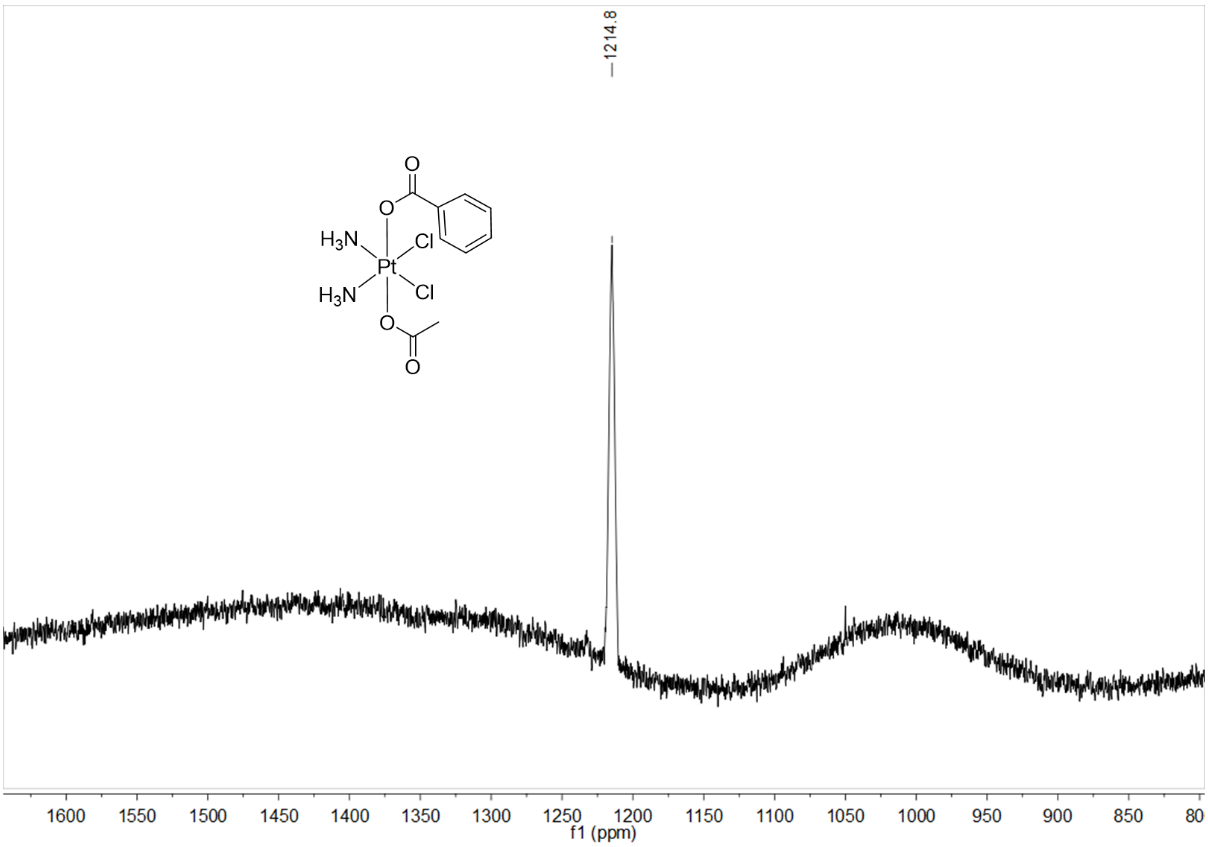

Figure S32. ^{13}C NMR spectrum of complex *c,t,c*-[Pt$(NH_3)_2$(OCOPh)$(OCOCH_3)(Cl)_2$] **2b'** in DMSO-d_6.

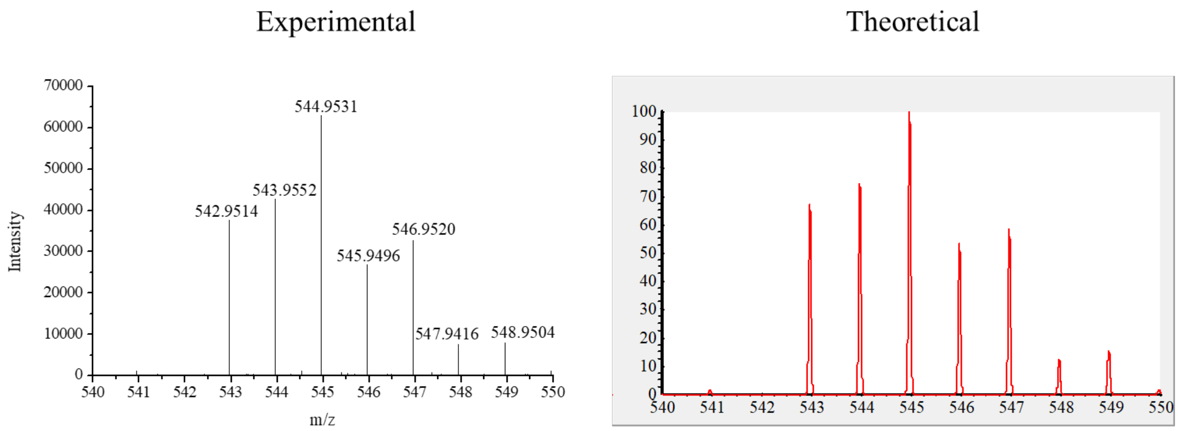

ESI-HRMS (positive ion mode), m/z. $[M+Na]^+$ calculated for $C_8H_{11}Cl_2F_3N_2NaO_4Pt$: 544.9571, found: 544.9531

Figure S33. ESI-HRMS spectrum of complex *c,t,c*-[Pt(NH$_3$)$_2$(OCOOPhCF$_3$)(OH)(Cl)$_2$] **3a**.

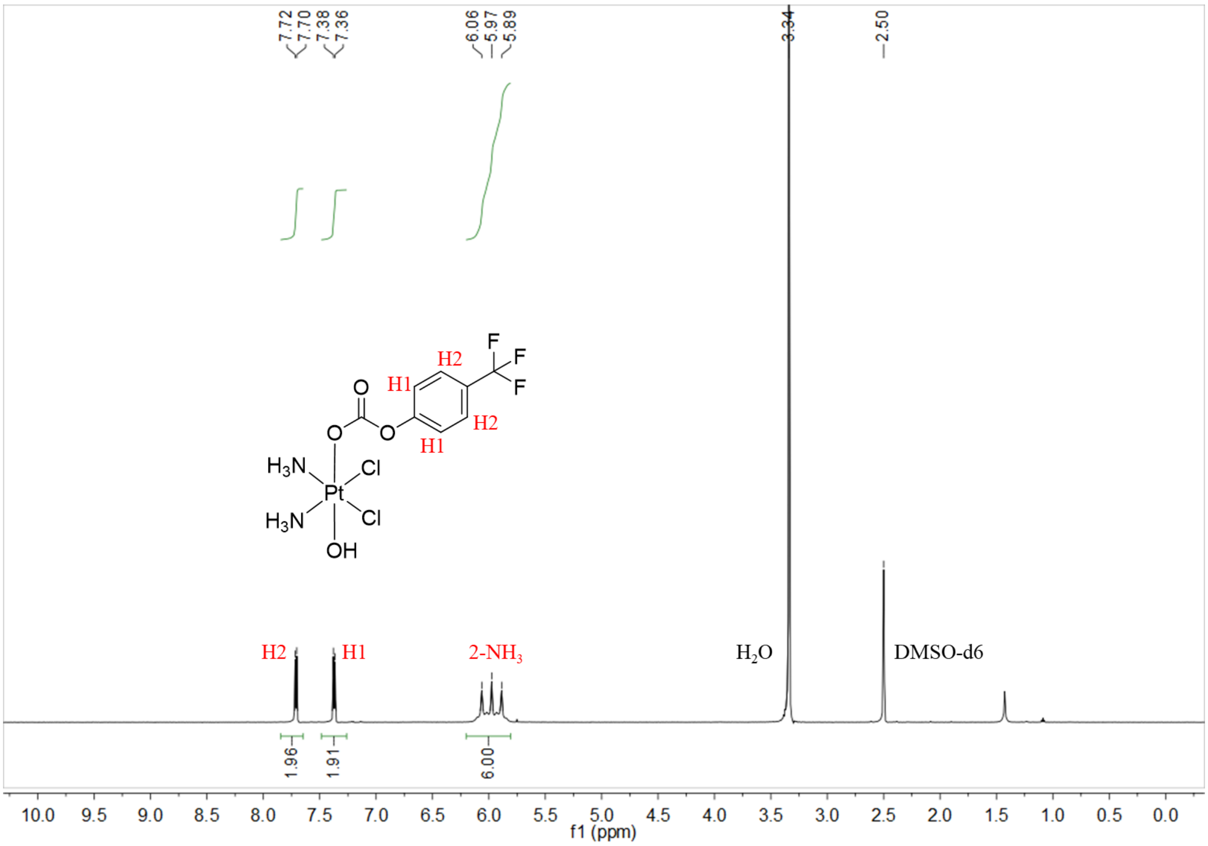

Figure S34. ^1H NMR spectrum of complex *c,t,c*-[Pt(NH$_3$)$_2$(OCOOPhCF$_3$)(OH)(Cl)$_2$] **3a** in DMSO-*d*$_6$.

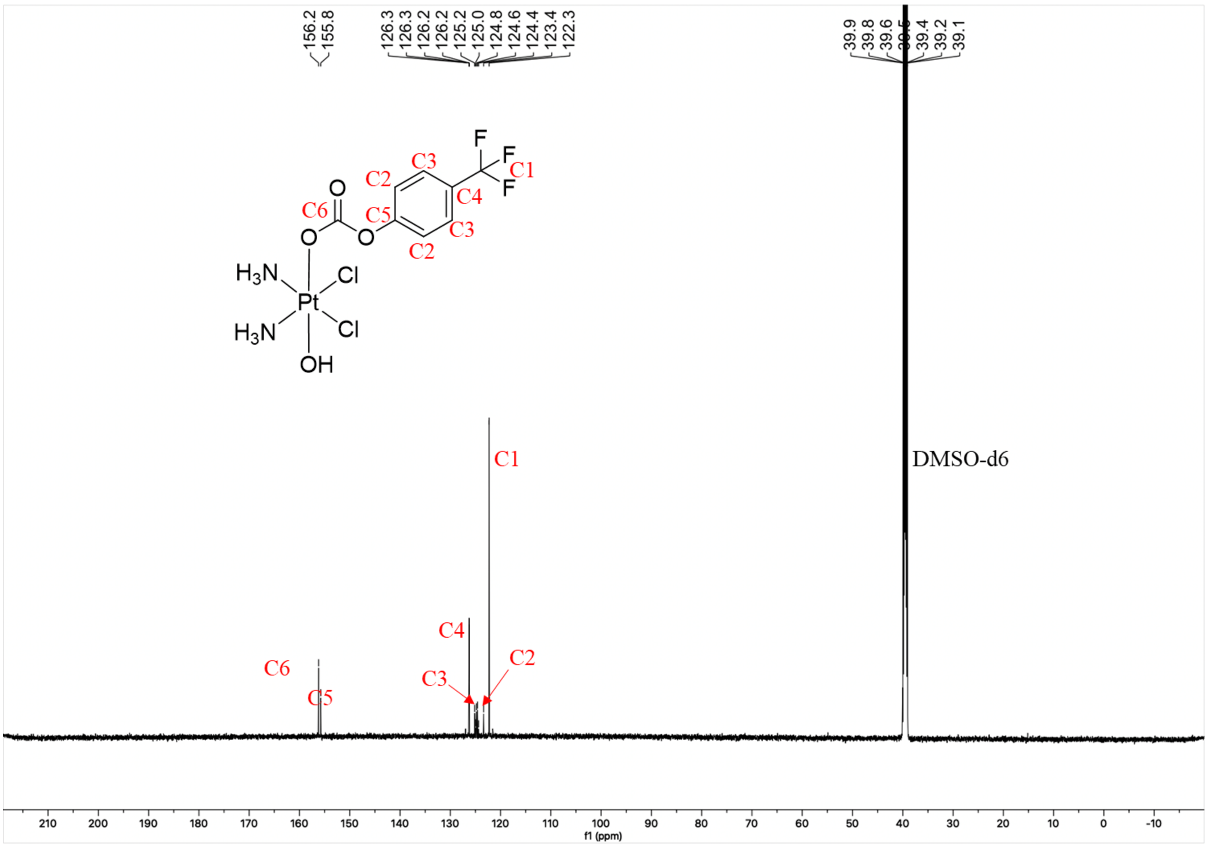

Figure S35. [13]C NMR spectrum of complex *c,t,c*-[Pt(NH3)2(OCOOPhCF3)(OH)(Cl)2] **3a** in DMSO-d_6.

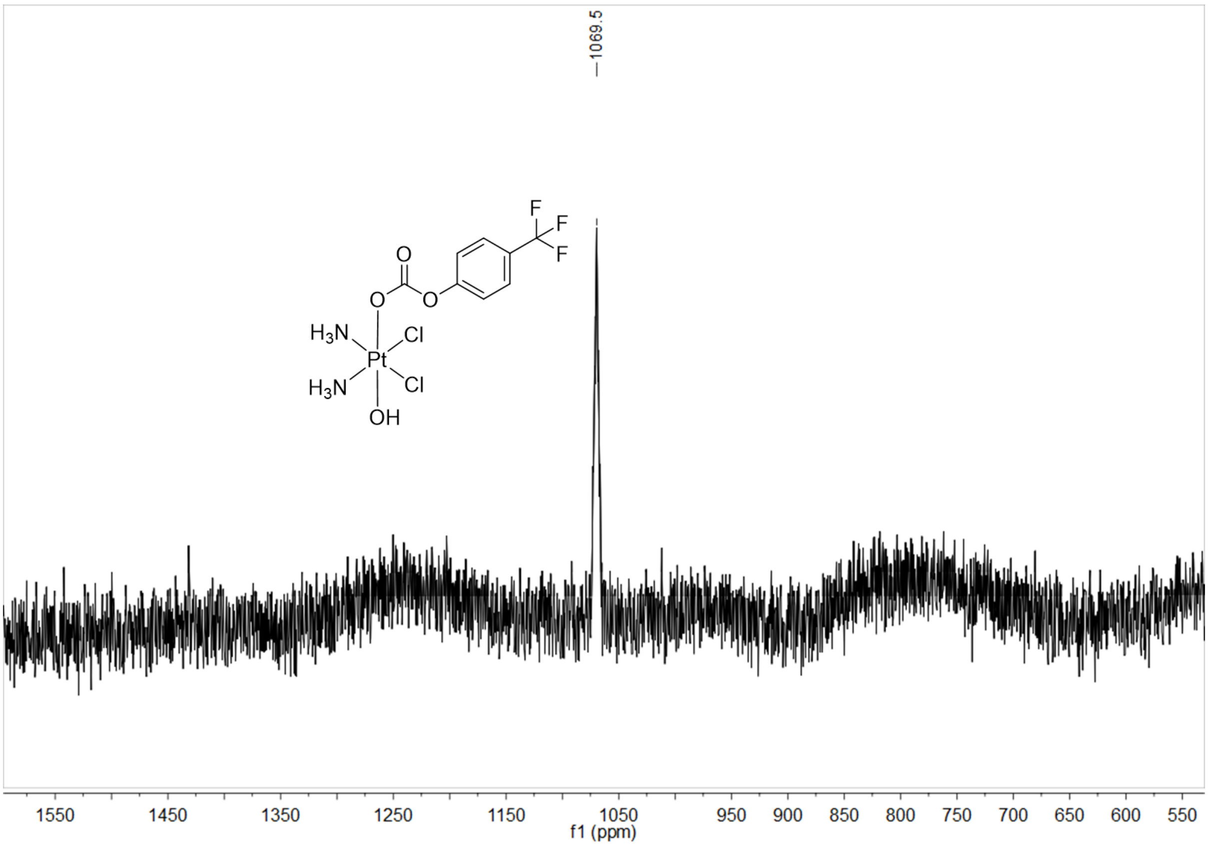

Figure S36. [195]Pt NMR spectrum of complex *c,t,c*-[Pt(NH3)2(OCOOPhCF3)(OH)(Cl)2] **3a** in DMSO-d_6.

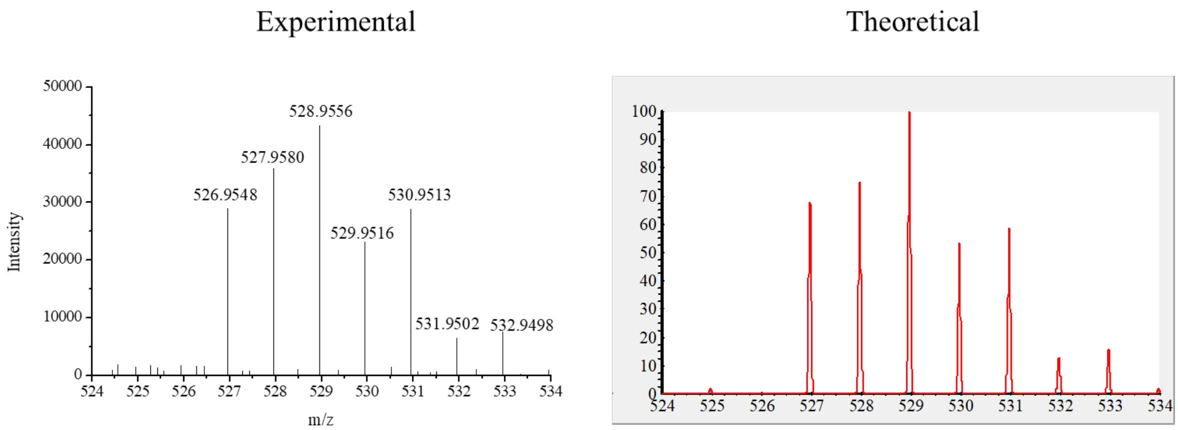

ESI-HRMS (positive ion mode), m/z. $[M+Na]^+$ calculated for $C_8H_{11}Cl_2F_3N_2NaO_3Pt$: 528.9622, found: 528.9556

Figure S37. ESI-HRMS spectrum of complex *c,t,c*-[Pt(NH$_3$)$_2$(OCOOPhCF$_3$)(OH)(Cl)$_2$] **3b**.

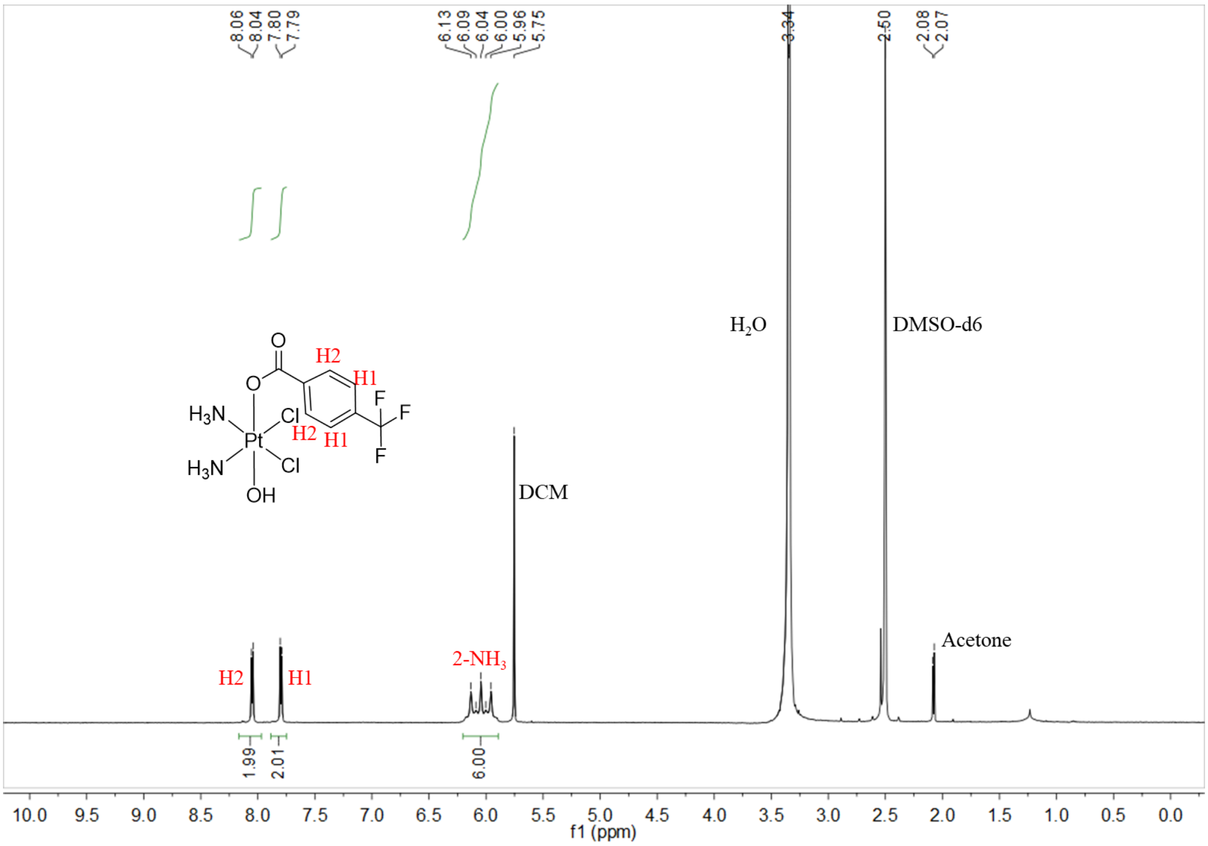

Figure S38. ^1H NMR spectrum of complex *c,t,c*-[Pt(NH$_3$)$_2$(OCOPhCF$_3$)(OH)(Cl)$_2$] **3b** in DMSO-*d*$_6$.

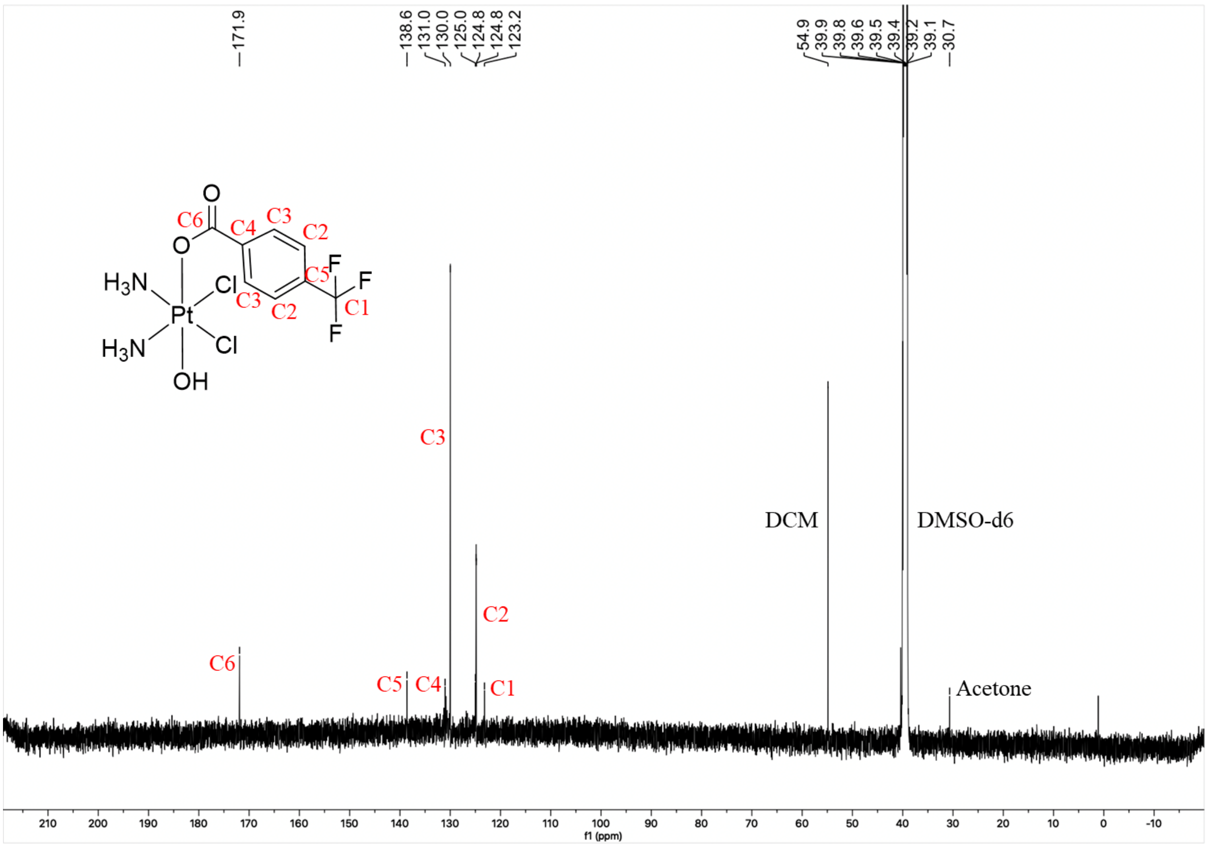

Figure S39. ^{13}C NMR spectrum of complex *c,t,c*-[Pt(NH_3)$_2$(OCOPhCF_3)(OH)(Cl)$_2$] **3b** in DMSO-d_6.

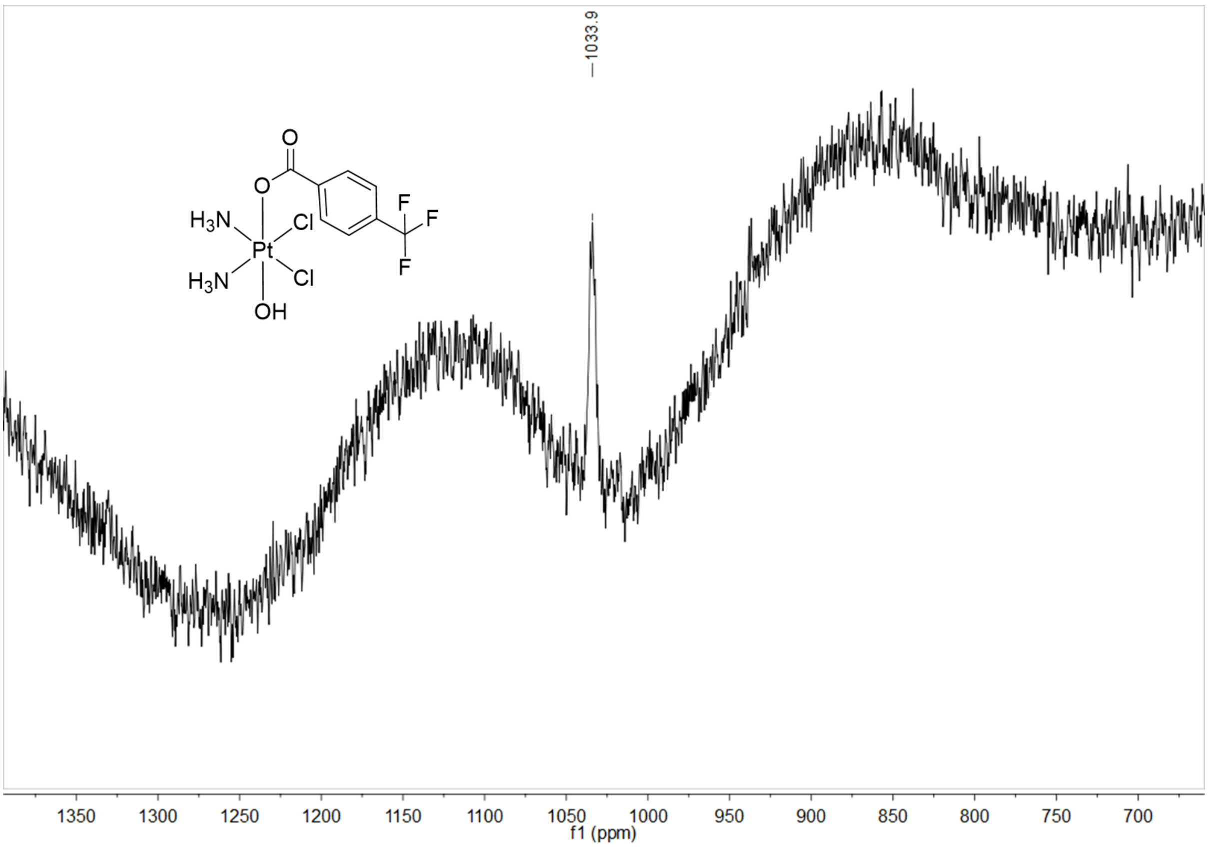

Figure S40. ^{195}Pt NMR spectrum of complex *c,t,c*-[Pt(NH_3)$_2$(OCOPhCF_3)(OH)(Cl)$_2$] **3b** in DMSO-d_6.

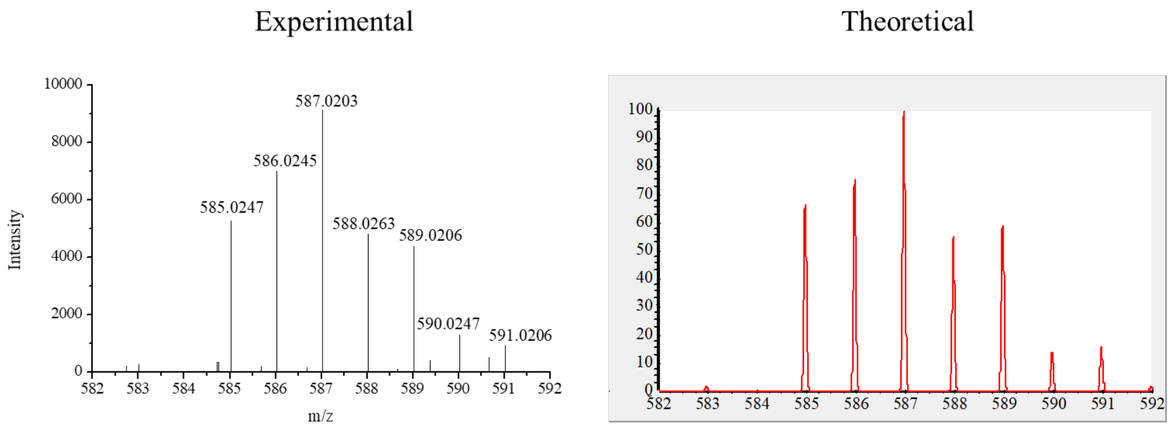

ESI-HRMS (positive ion mode), m/z. $[M+Na]^+$ calculated for $C_{10}H_{13}Cl_2F_3N_2NaO_5Pt$: 586.9678, found: 587.0203

Figure S41. ESI-HRMS spectrum of complex *c,t,c*-[Pt(NH_3)$_2$($OCOOPhCF_3$)($OCOCH_3$)(Cl)$_2$] **3a'**.

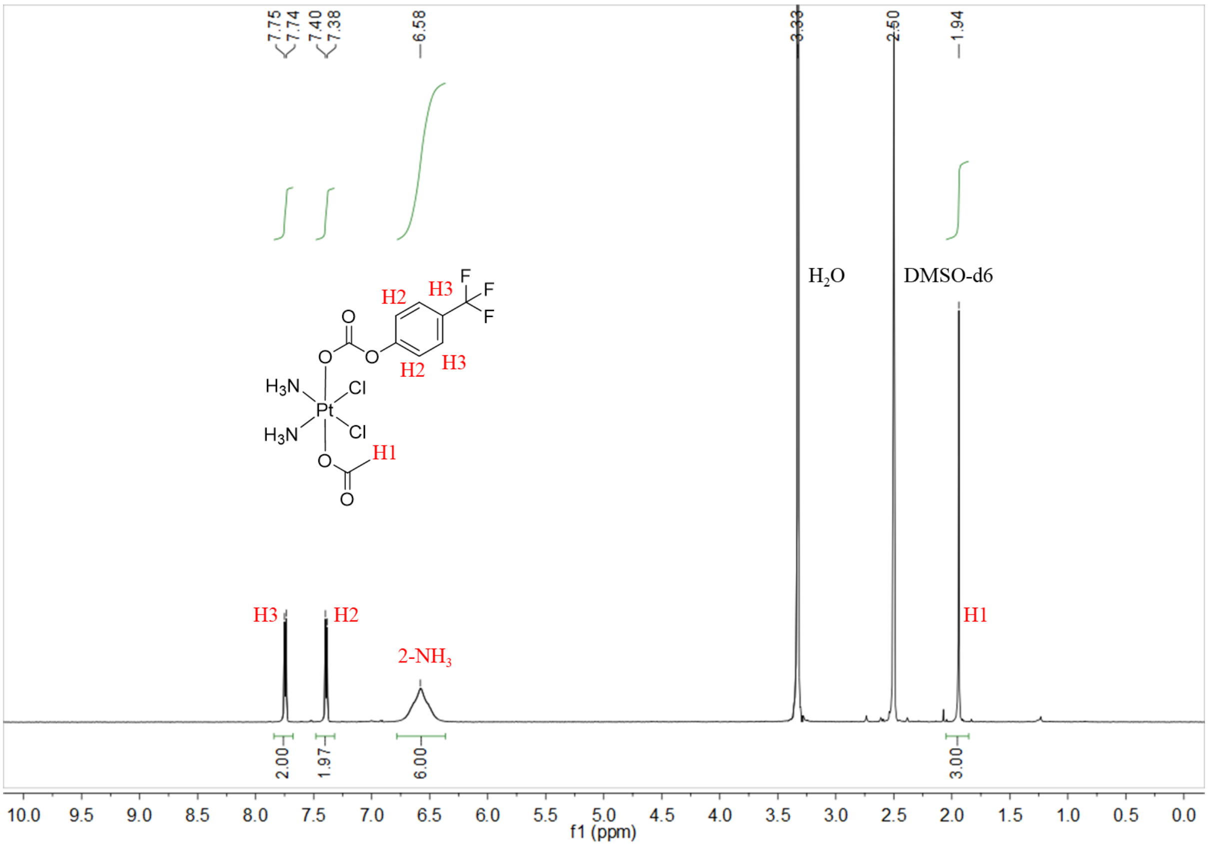

Figure S42. ^{1}H NMR spectrum of complex *c,t,c*-[Pt(NH_3)$_2$($OCOOPhCF_3$)($OCOCH_3$)(Cl)$_2$] **3a'** in DMSO-d_6.

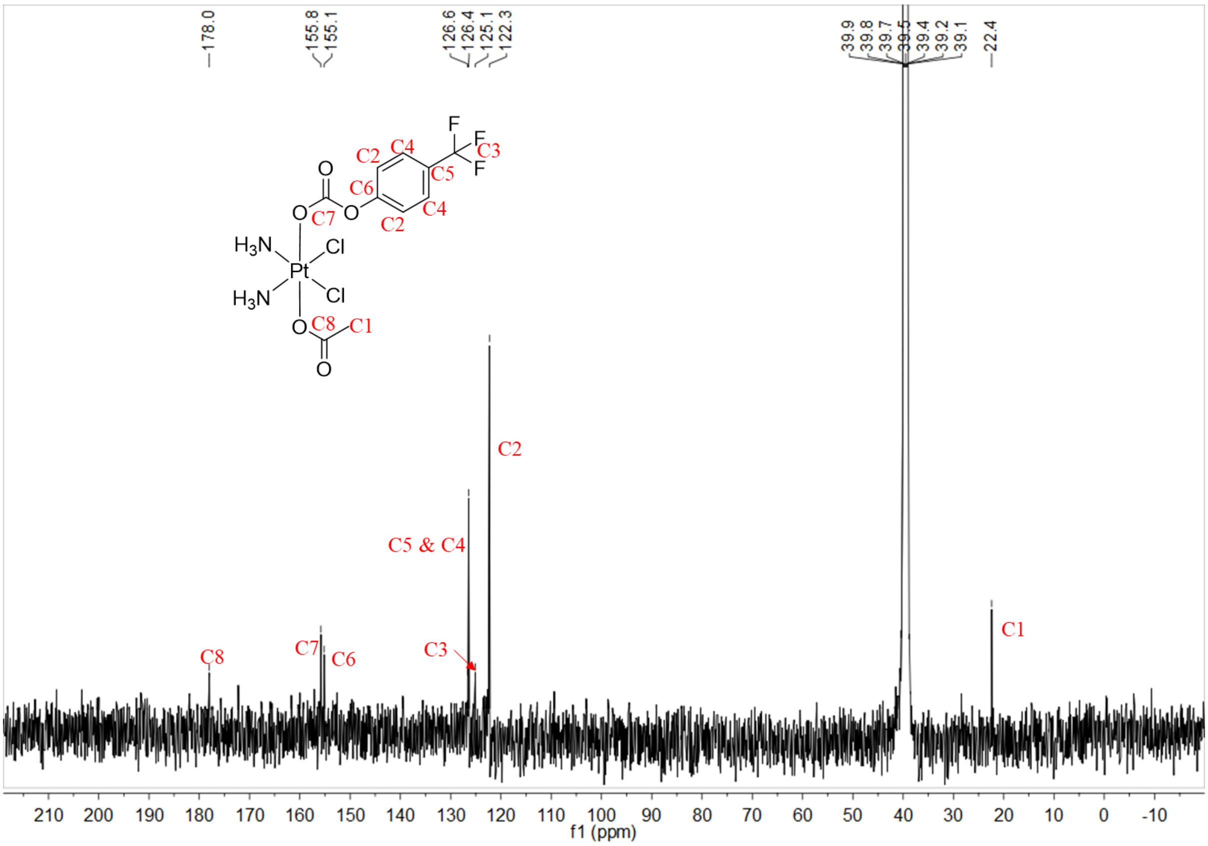

Figure S43. ^{13}C NMR spectrum of complex *c,t,c*-[Pt(NH_3)$_2$(OCOOPhCF$_3$)(OCOCH$_3$)(Cl)$_2$] **3a'** in DMSO-d_6.

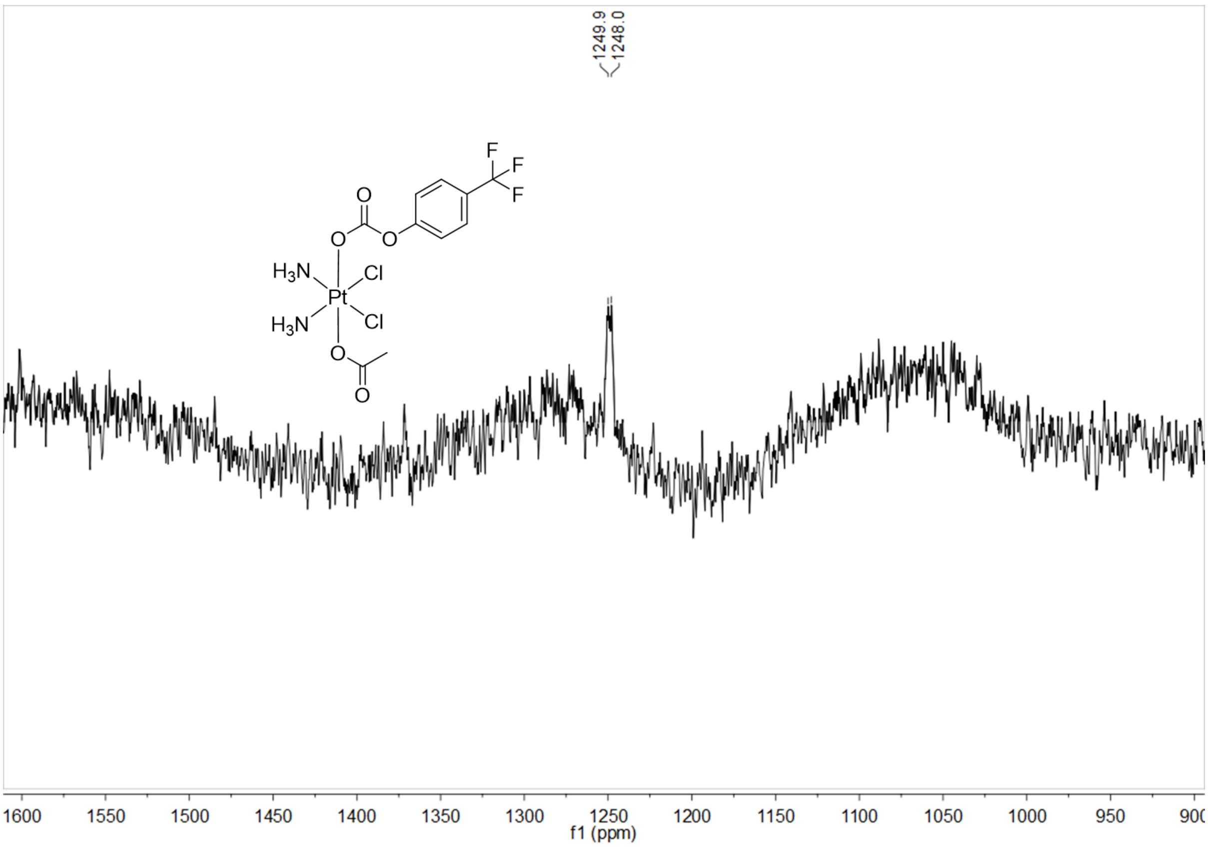

Figure S44. ^{195}Pt NMR spectrum of complex *c,t,c*-[Pt(NH_3)$_2$(OCOOPhCF$_3$)(OCOCH$_3$)(Cl)$_2$] **3a'** in DMSO-d_6.

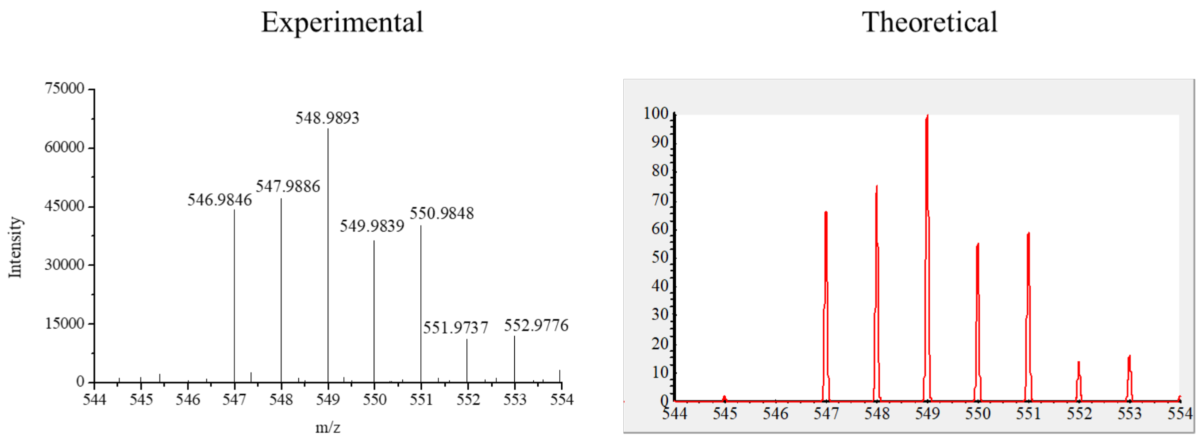

ESI-HRMS (positive ion mode), m/z. $[M+H]^+$ calculated for $C_{10}H_{14}Cl_2F_3N_2O_4Pt$: 548.9909, found: 548.9893

Figure S45. ESI-HRMS spectrum of complex *c,t,c*-[Pt(NH_3)$_2$(OCOPhCF_3)(OCOCH_3)(Cl)$_2$] **3b'**.

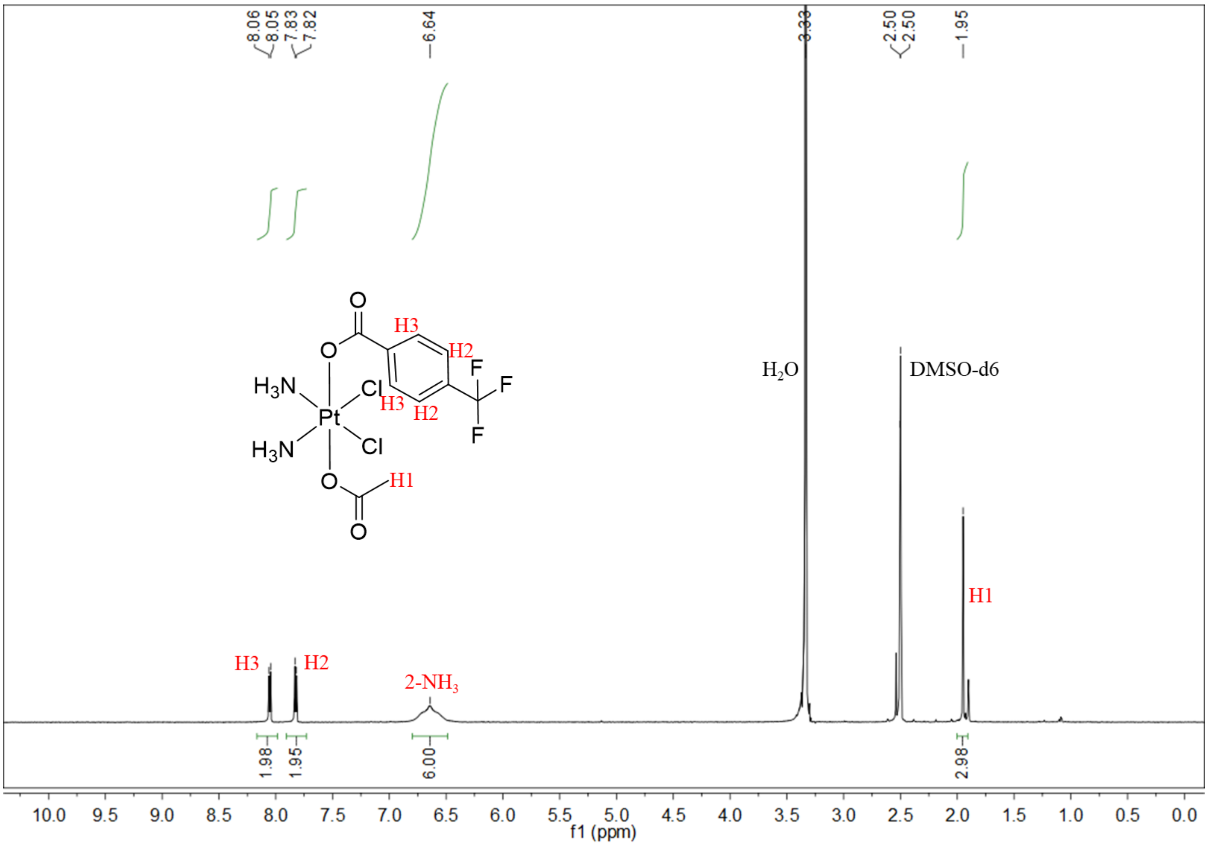

Figure S46. ^{1}H NMR spectrum of complex *c,t,c*-[Pt(NH_3)$_2$(OCOPhCF_3)(OCOCH_3)(Cl)$_2$] **3b'** in DMSO-d_6.

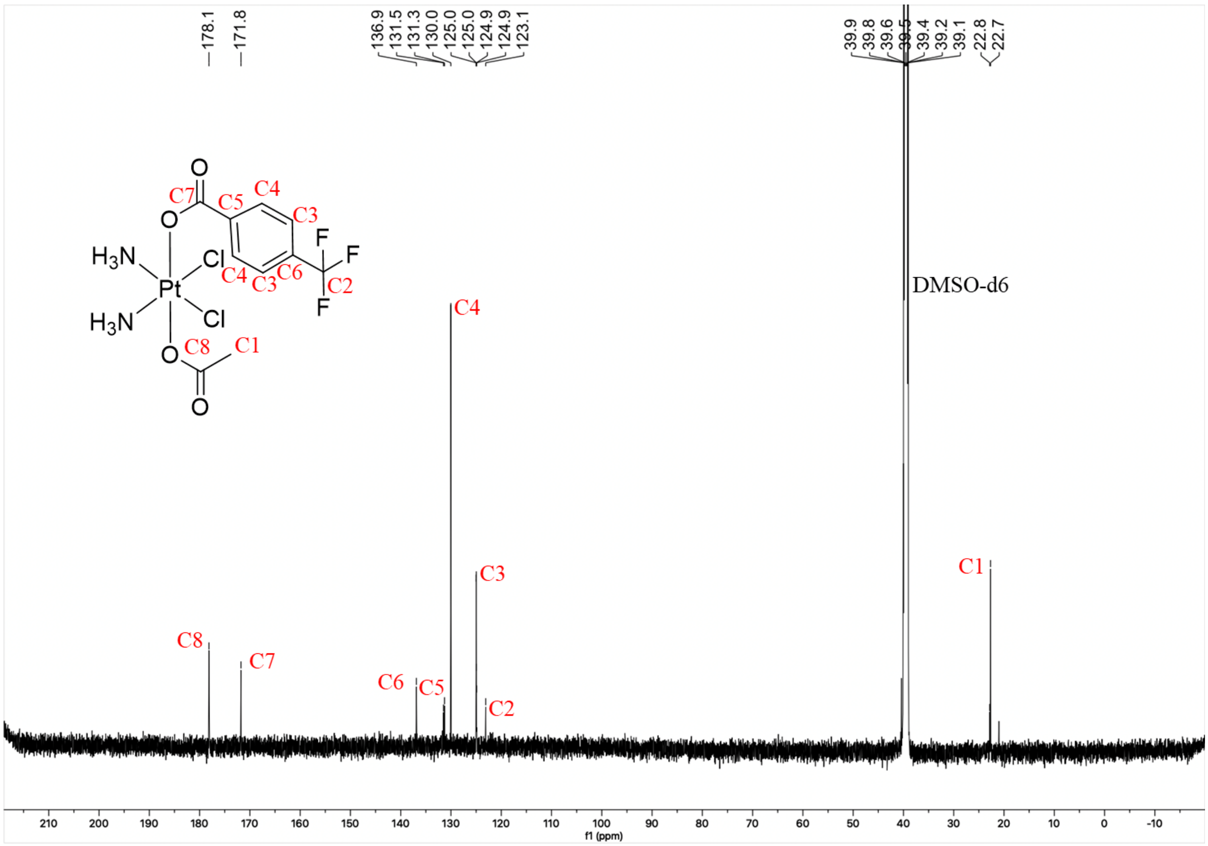

Figure S47. ^{13}C NMR spectrum of complex *c,t,c*-[Pt(NH_3)$_2$($OCOPhCF_3$)($OCOCH_3$)(Cl)$_2$] **3b'** in DMSO-d_6.

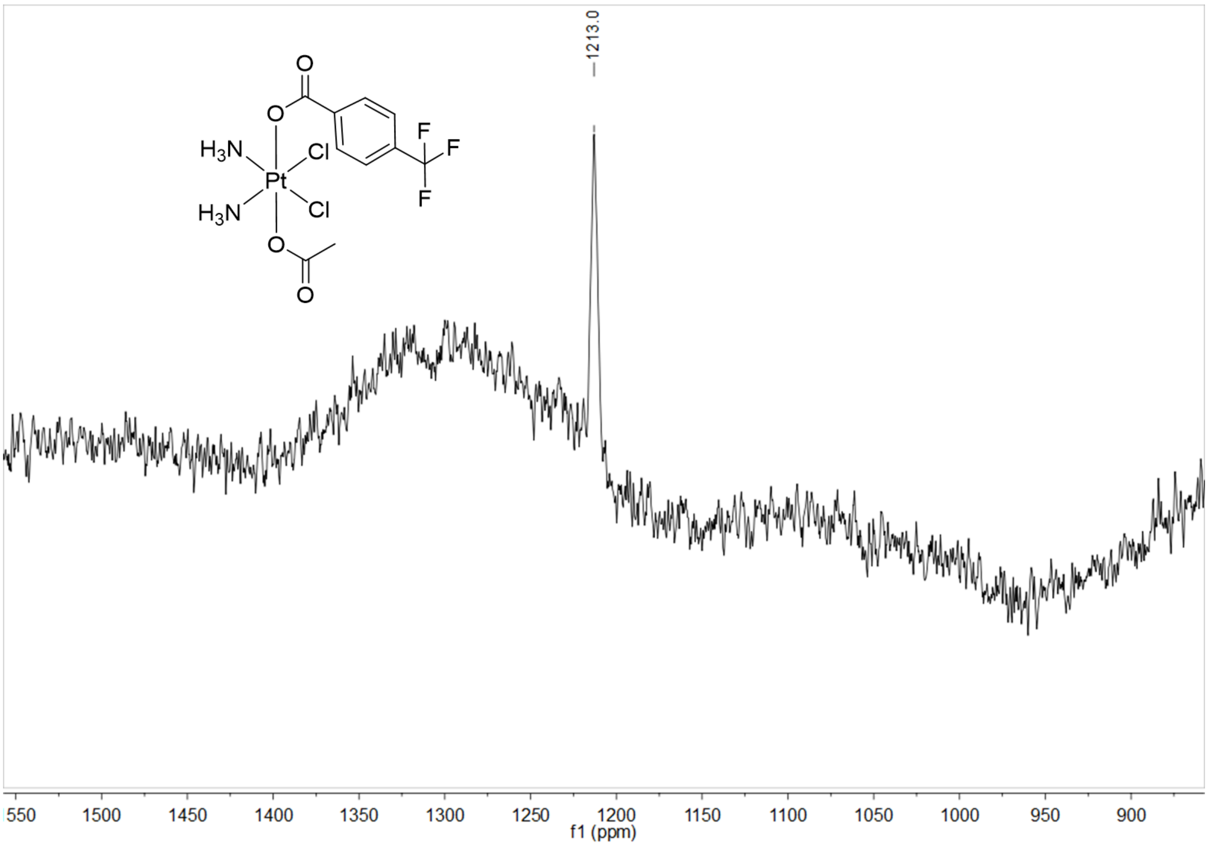

Figure S48. ^{13}C NMR spectrum of complex *c,t,c*-[Pt(NH_3)$_2$($OCOPhCF_3$)($OCOCH_3$)(Cl)$_2$] **3b'** in DMSO-d_6.

Complex **1a**

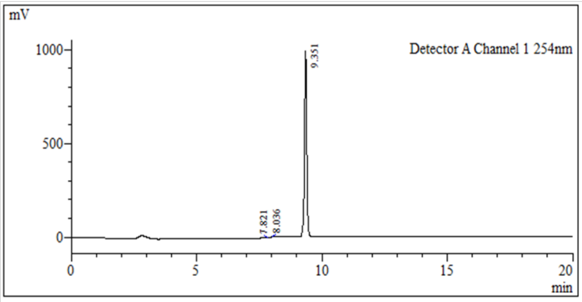

Detector A Channel 1 254nm

Peak#	Ret. Time	USP Width	Area	Height	Area%
1	7.821	0.160	7863	1276	0.125
2	8.036	0.143	24075	4841	0.383
3	9.351	0.177	6257414	987098	99.492
Total			6289352	993214	100.000

Complex **1b**

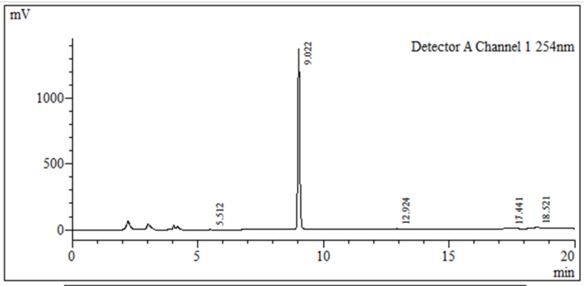

Detector A Channel 1 254nm

Peak#	Ret. Time	USP Width	Area	Height	Area%
1	5.512	0.224	5122	651	0.068
2	9.022	0.158	7443694	1364073	98.100
3	12.924	0.342	19133	1239	0.252
4	17.441	0.677	14430	580	0.190
5	18.521	0.327	105502	9022	1.390
Total			7587882	1375566	100.000

Complex **1a'**

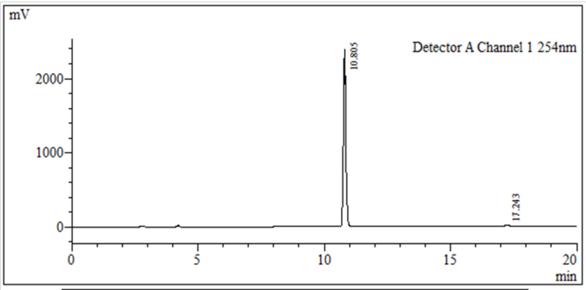

Detector A Channel 1 254nm

Peak#	Ret. Time	USP Width	Area	Height	Area%
1	10.805	0.187	15945565	2377828	98.918
2	17.243	0.633	174362	7401	1.082
Total			16119927	2385229	100.000

Complex **1b'**

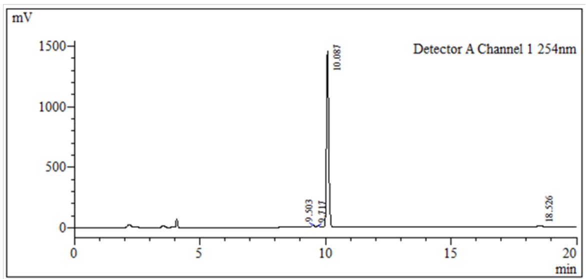

Detector A Channel 1 254nm

Peak#	Ret. Time	USP Width	Area	Height	Area%
1	9.503	0.207	157993	20809	1.660
2	9.717	0.210	115735	15012	1.216
3	10.087	0.179	9151398	1449148	96.166
4	18.526	0.356	91085	7057	0.957
Total			9516211	1492026	100.000

Figure S49. HPLC analysis for the purity of Pt(IV) complexes **1a**, **1b**, **1a'**, and **1b'**.

Complex **2a**

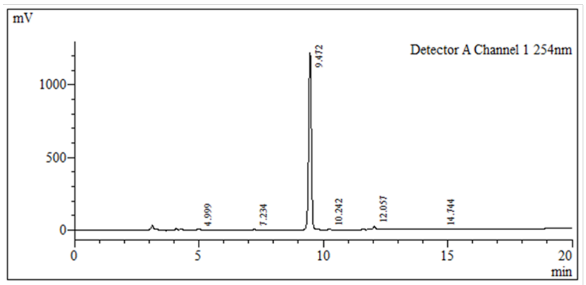

Detector A Channel 1 254nm

Peak#	Ret. Time	USP Width	Area	Height	Area%
1	4.999	0.219	58558	7049	0.631
2	7.234	0.210	21648	2900	0.233
3	9.472	0.203	9018882	1221838	97.110
4	10.242	0.163	15981	2841	0.172
5	12.057	0.192	163109	20466	1.756
6	14.744	0.177	9064	1290	0.098
Total			9287241	1256383	100.000

Complex **2b**

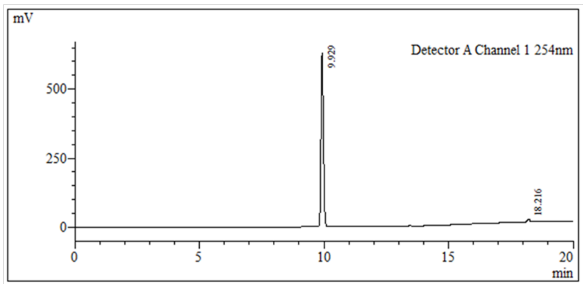

Detector A Channel 1 254nm

Peak#	Ret. Time	USP Width	Area	Height	Area%
1	9.929	0.189	4221140	629800	98.505
2	18.216	0.173	64063	10150	1.495
Total			4285203	639950	100.000

Complex **2a'**

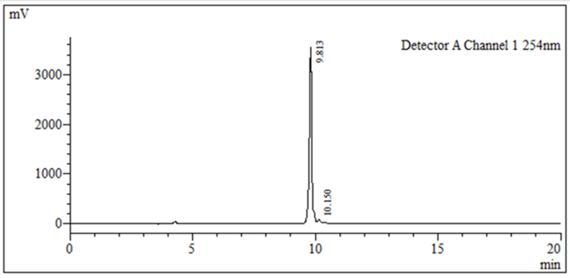

Detector A Channel 1 254nm

Peak#	Ret. Time	USP Width	Area	Height	Area%
1	9.813	0.176	23755272	3512240	98.961
2	10.150	0.141	249374	52748	1.039
Total			24004646	3564989	100.000

Complex **2b'**

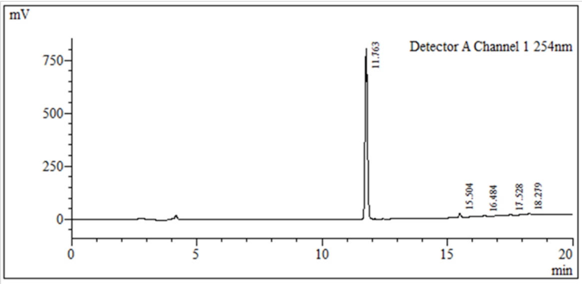

Detector A Channel 1 254nm

Peak#	Ret. Time	USP Width	Area	Height	Area%
1	11.763	0.183	5181412	801627	96.615
2	15.504	0.150	86169	16841	1.607
3	16.484	0.209	22718	3028	0.424
4	17.528	0.165	24914	4327	0.465
5	18.279	0.166	47758	8102	0.891
Total			5362970	833925	100.000

Figure S50. HPLC analysis for the purity of Pt(IV) complexes **2a**, **2b**, **2a'**, and **2b'**.

Complex **3a**

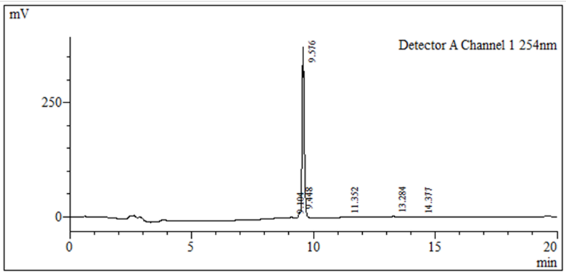

Detector A Channel 1 254nm

Peak#	Ret. Time	USP Width	Area	Height	Area%
1	9.104	0.167	8849	1508	0.400
2	9.448	0.089	10755	3078	0.486
3	9.576	0.168	2130658	363657	96.280
4	11.352	0.465	17401	960	0.786
5	13.284	0.217	18160	2333	0.821
6	14.377	0.845	27166	803	1.228
Total			2212989	372339	100.000

Complex **3b**

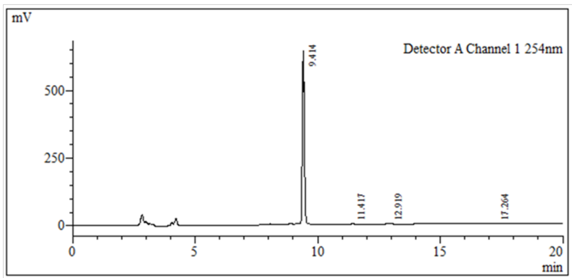

Detector A Channel 1 254nm

Peak#	Ret. Time	USP Width	Area	Height	Area%
1	9.414	0.162	3582688	636336	98.263
2	11.417	0.182	5126	813	0.141
3	12.919	0.287	30459	3003	0.835
4	17.264	0.775	27759	917	0.761
Total			3646032	641069	100.000

Complex **3a'**

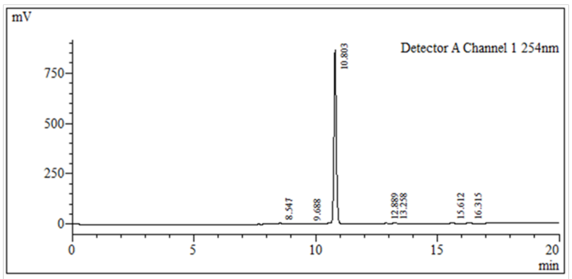

Detector A Channel 1 254nm

Peak#	Ret. Time	USP Width	Area	Height	Area%
1	8.547	0.188	20214	3011	0.346
2	9.688	0.161	4530	815	0.078
3	10.803	0.188	5776500	858899	98.953
4	12.889	0.222	8600	1087	0.147
5	13.258	0.212	17624	2366	0.302
6	15.612	0.230	5432	664	0.093
7	16.315	0.263	4694	494	0.080
Total			5837592	867336	100.000

Complex **3b'**

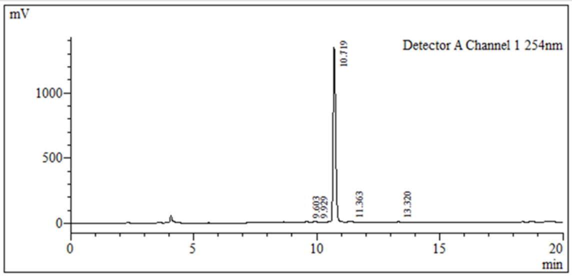

Detector A Channel 1 254nm

Peak#	Ret. Time	USP Width	Area	Height	Area%
1	9.603	0.297	23511	2174	0.257
2	9.929	0.160	22040	4008	0.241
3	10.719	0.189	9051448	1333666	99.073
4	11.363	0.177	18909	3107	0.207
5	13.320	0.219	20207	1905	0.221
Total			9136114	1344861	100.000

Figure S51. HPLC analysis for the purity of Pt(IV) complexes **3a**, **3b**, **3a'**, and **3b'**.

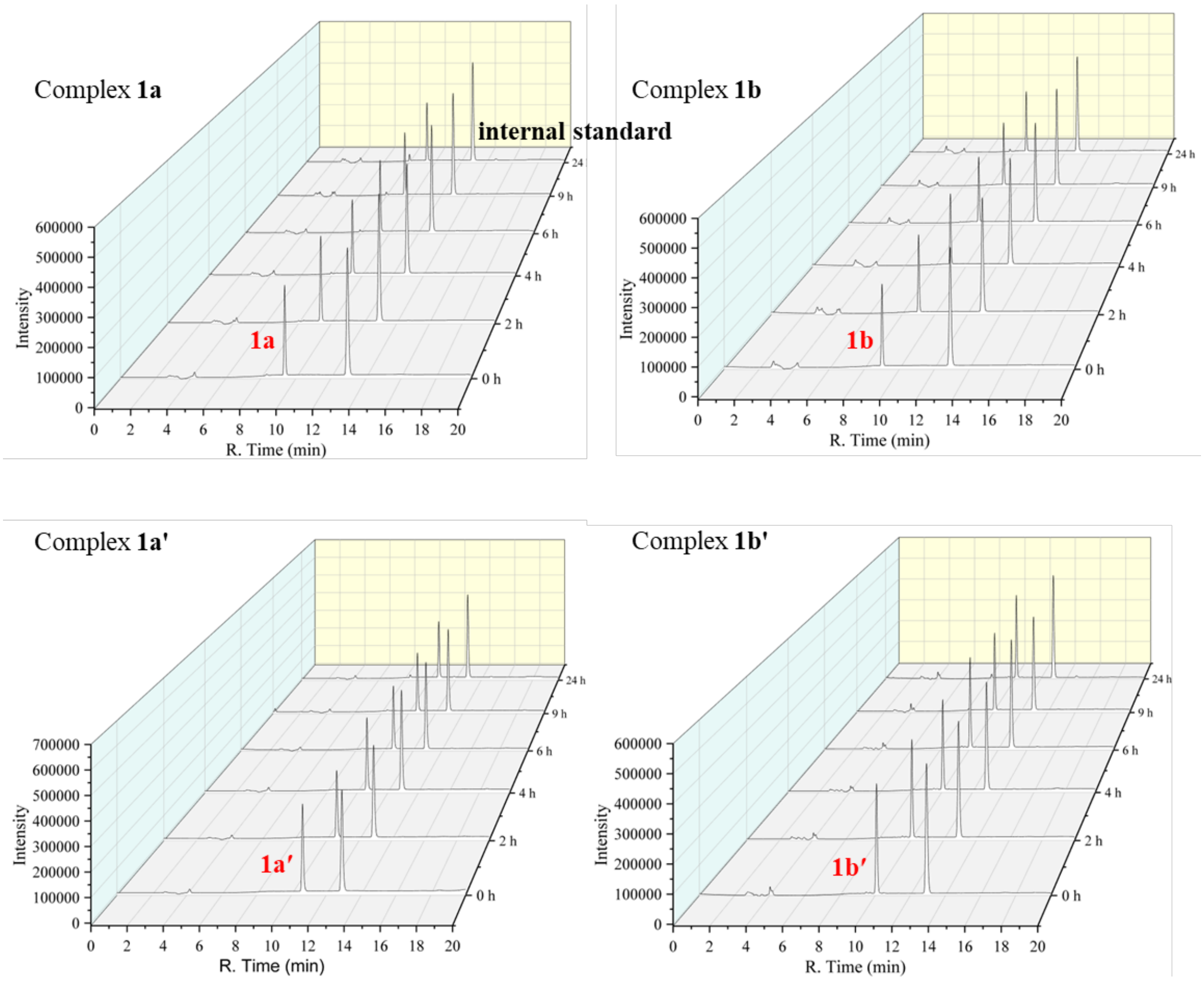

Figure S52. HPLC chromatograms of Pt(IV) complexes **1a**, **1b**, **1a'**, and **1b'** in PBS buffer (pH = 7.4) at 37 °C from 0 to 24 h.

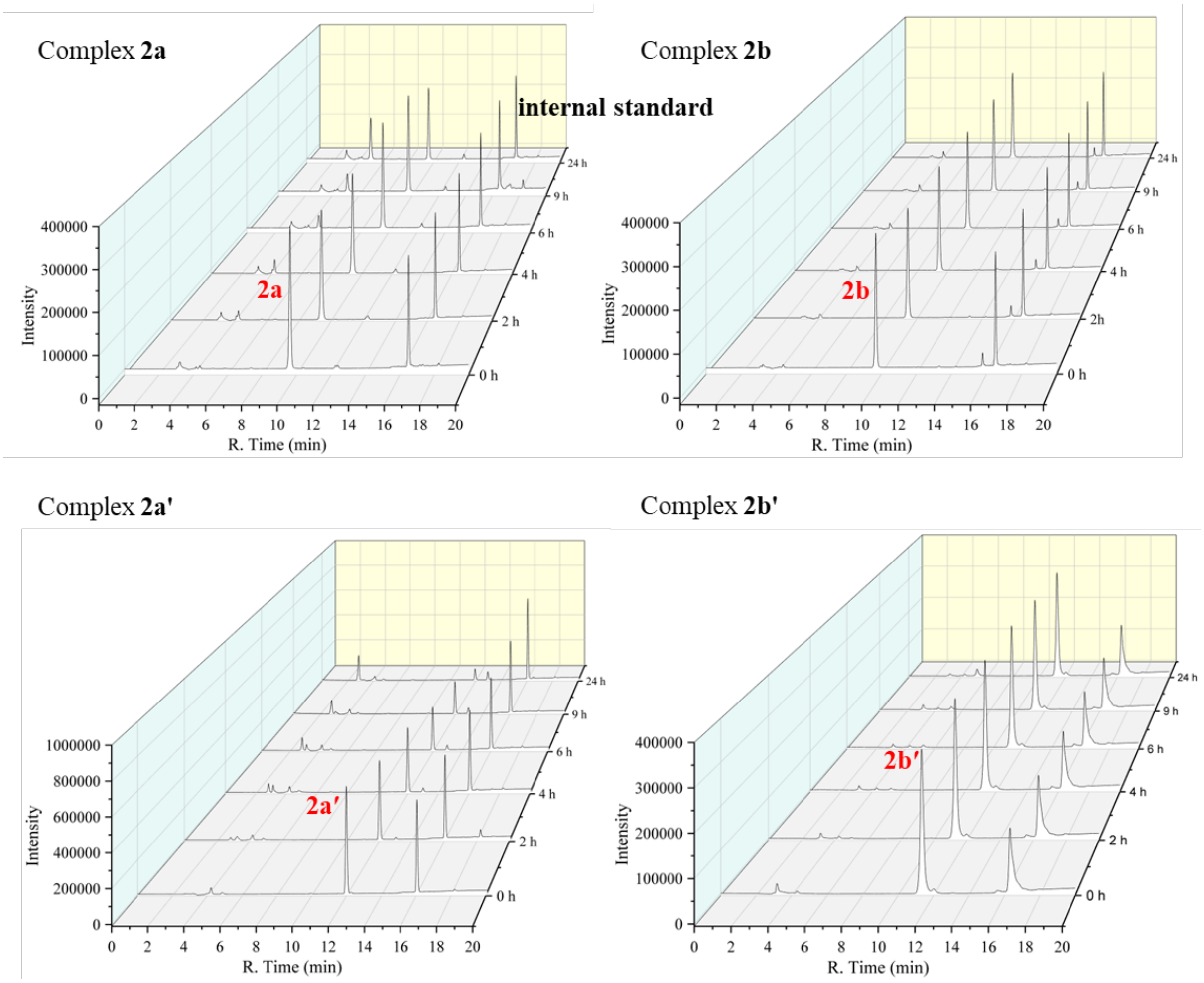

Figure S53. HPLC chromatograms of Pt(IV) complexes **2a**, **2b**, **2a'**, and **2b'** in PBS buffer (pH = 7.4) at 37 °C from 0 to 24 h.

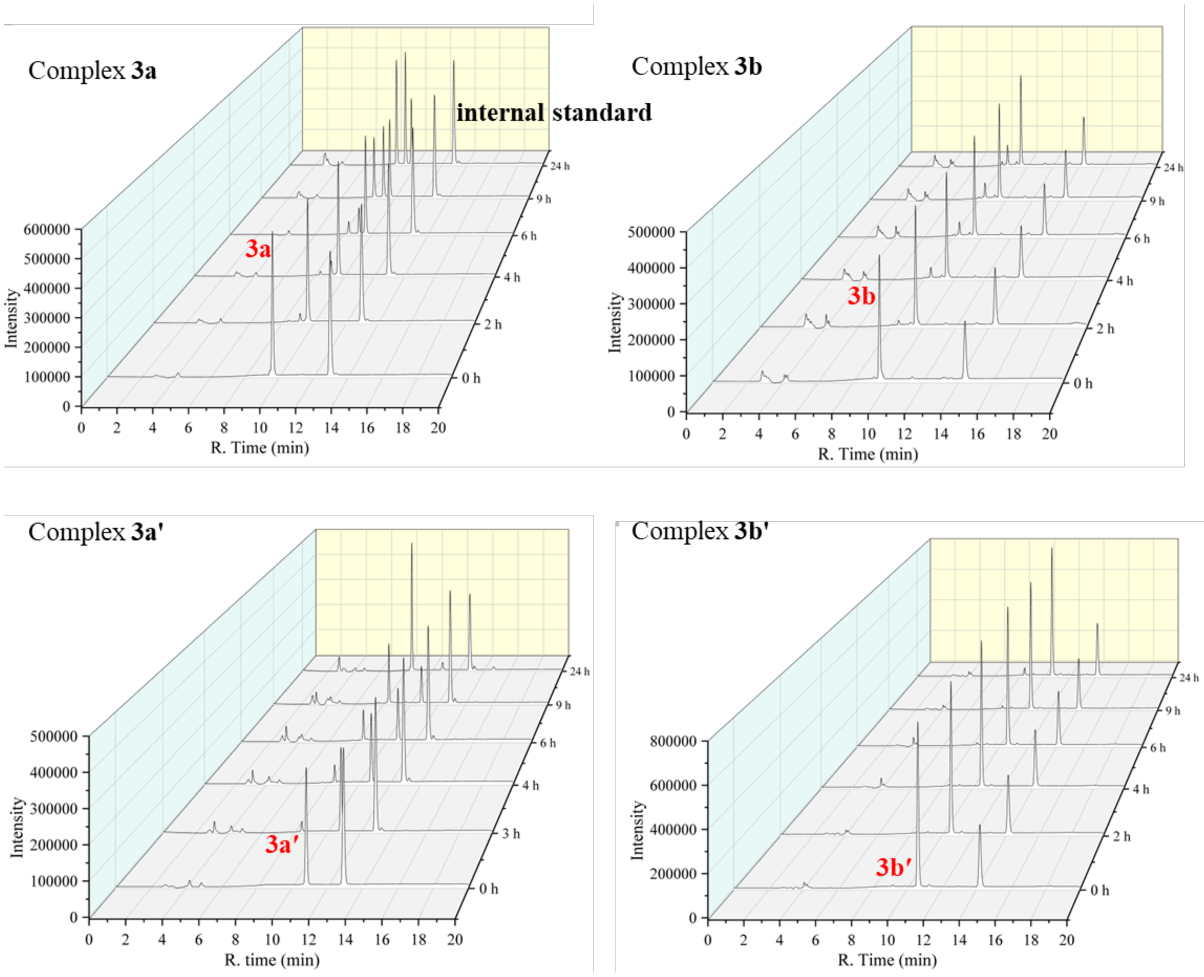

Figure S54. HPLC chromatograms of Pt(IV) complexes **3a**, **3b**, **3a'**, and **3b'** in PBS buffer (pH = 7.4) at 37 °C from 0 to 24 h.

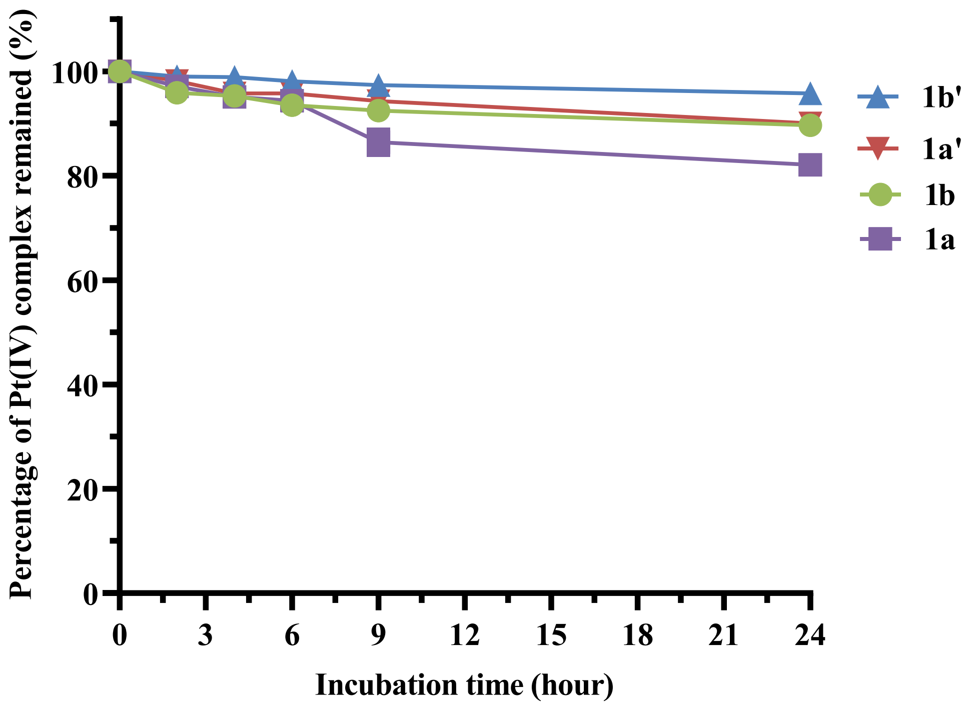

Figure S55. The decay profiles of the Pt(IV) complexes **1a**, **1b**, **1a′**, and **1b′** in PBS buffer (pH 7.4) at 37 °C within 24 hours.

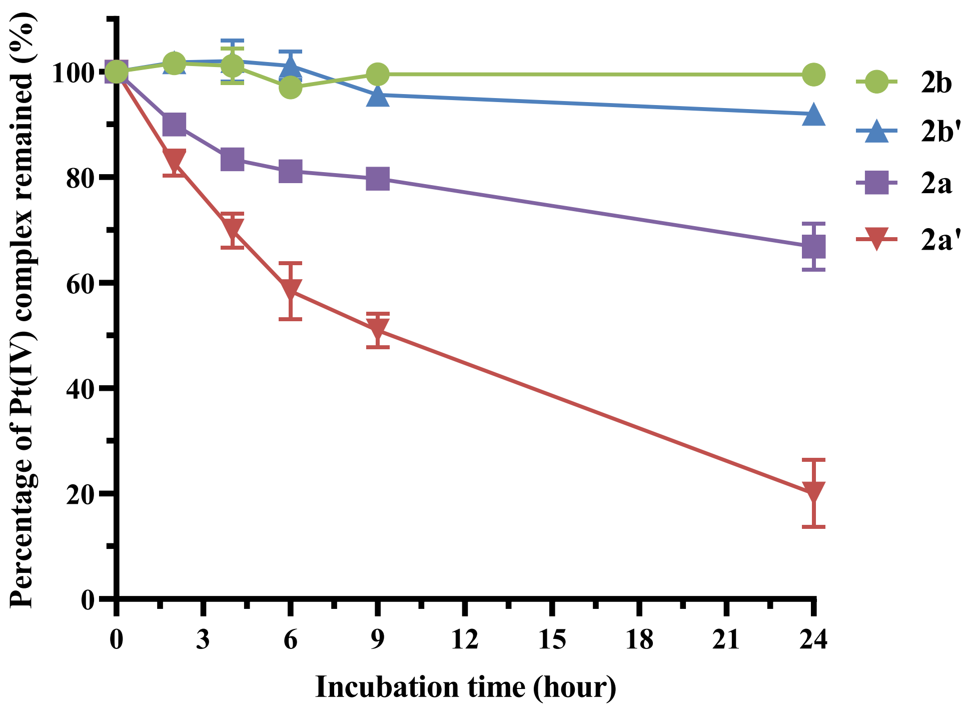

Figure S56. The decay profiles of the Pt(IV) complexes **2a**, **2b**, **2a′**, and **2b′** in PBS buffer (pH 7.4) at 37 °C within 24 hours.

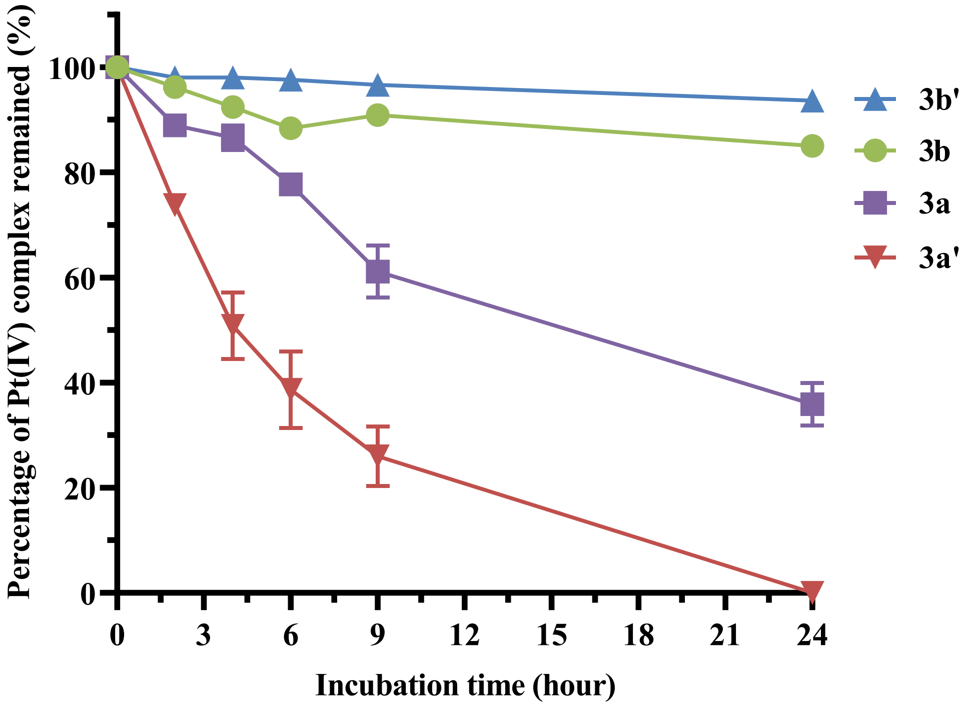

Figure S57. The decay profiles of the Pt(IV) complexes **3a**, **3b**, **3a′**, and **3b′** in PBS buffer (pH 7.4) at 37 °C within 24 hours.

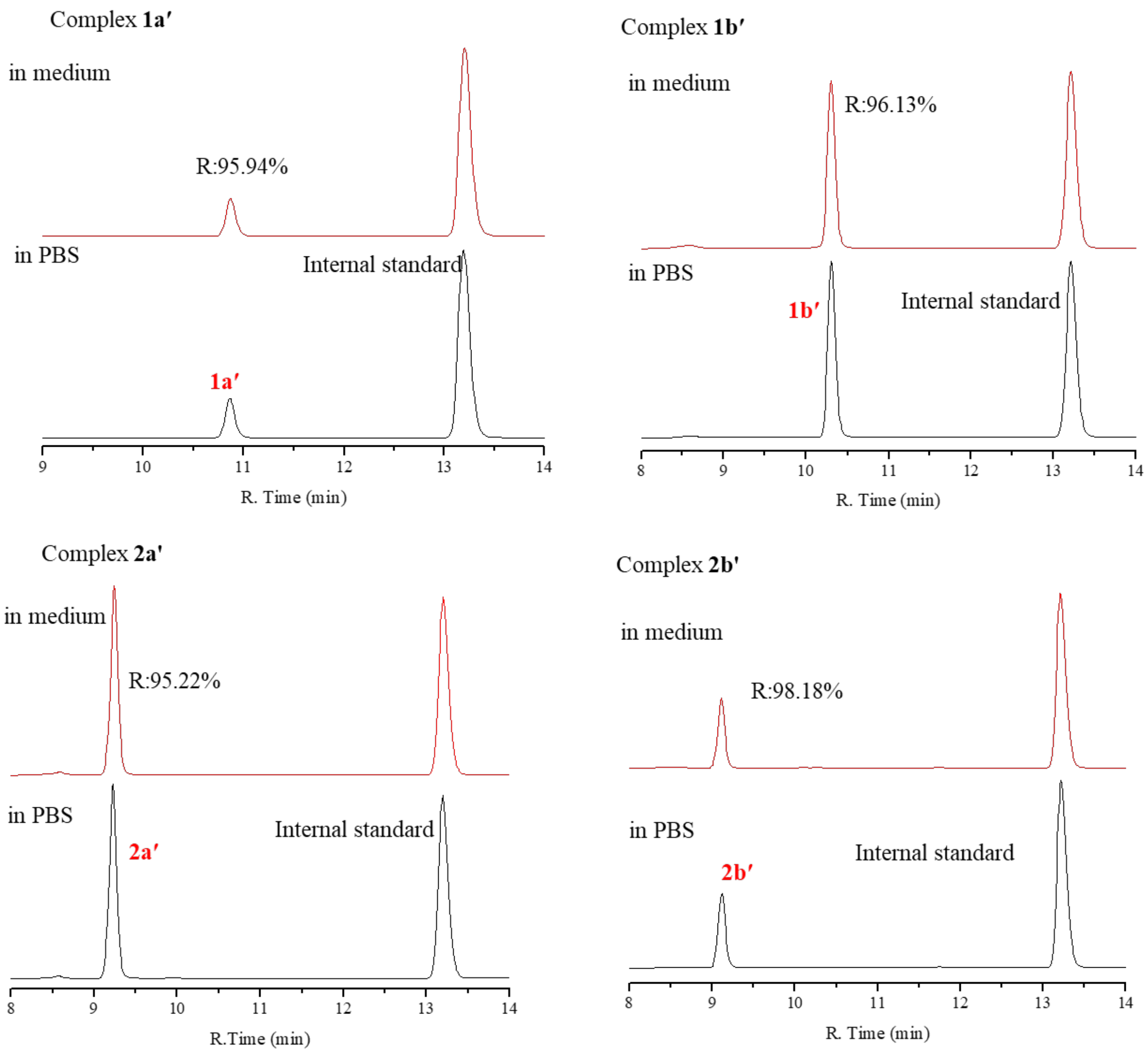

Figure S58. HPLC chromatograms of Pt(IV) complexes **1a'**, **1b'**, **2a'**, and **2b'** in medium and PBS. The recovery rate (R) of complex was obtained by using the following equation: $R = (A_{Pt(IV)\ in\ medium}/A_{internal\ standard\ in\ medium})/(A_{Pt(IV)\ in\ PBS}/A_{internal\ standard\ in\ PBS})$, where $A_{Pt(IV)\ in\ medium}$, and $A_{Pt(IV)\ in\ PBS}$ are the integrated areas of HPLC peaks of Pt(IV) complexes recovered from medium and in PBS at a wavelength of 254 nm, respectively; $A_{internal\ standard\ in\ medium}$, and $A_{internal\ standard\ in\ PBS}$ are the integrated area of HPLC peaks of internal standard obtained in medium and PBS at a wavelength of 254 nm, respectively.

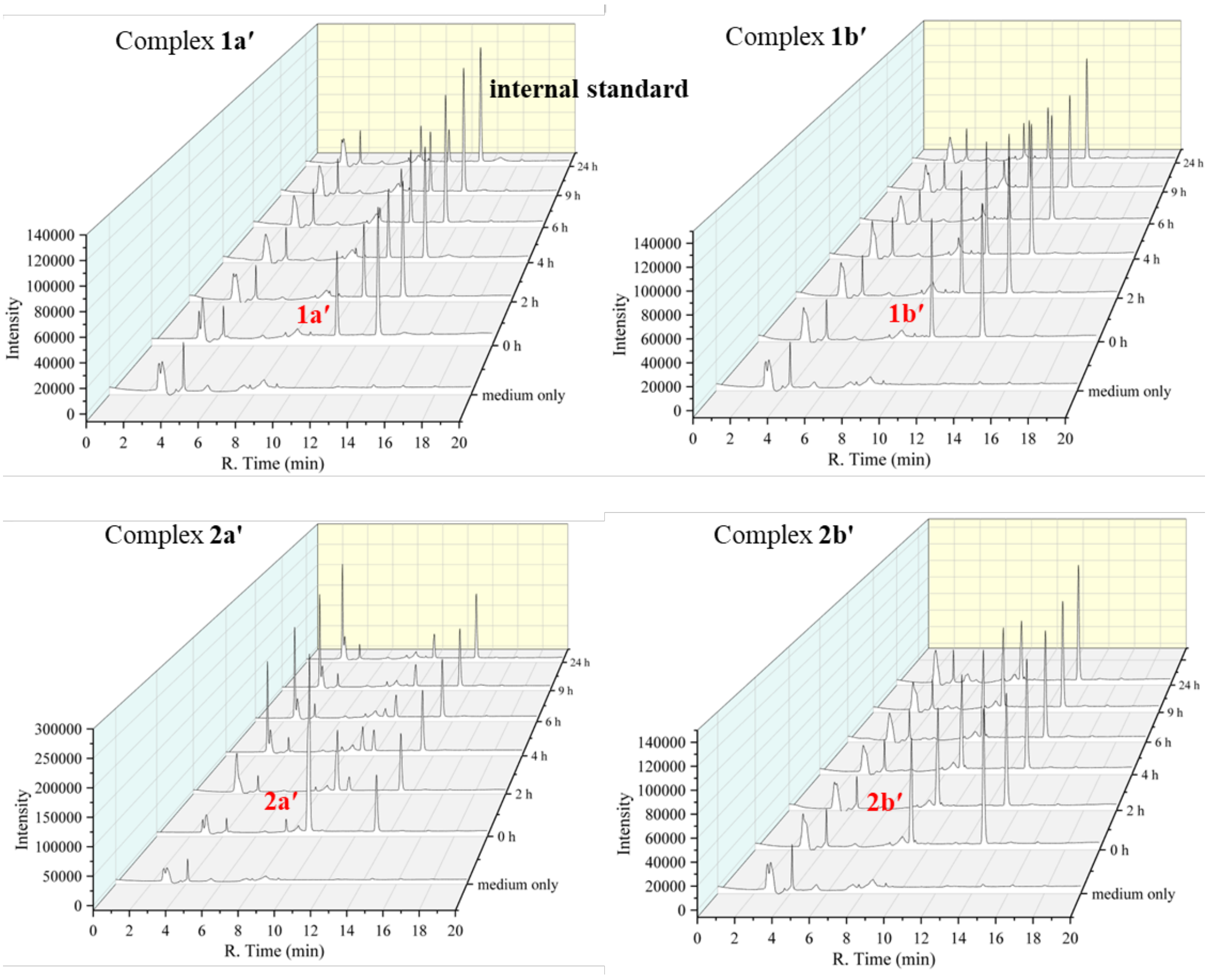

Figure S59. HPLC chromatograms of Pt(IV) complexes **1a'**, **1b'**, **2a'**, and **2b'** in complete medium at 37 °C from 0 to 24 h.

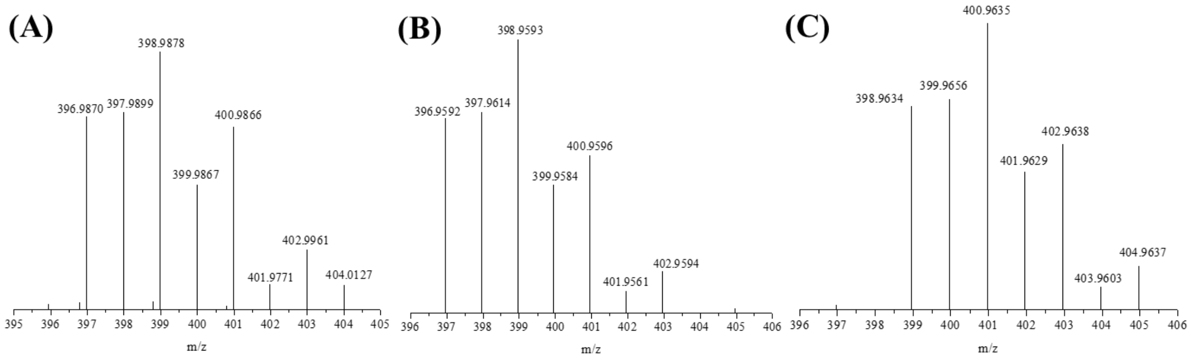

(D) Proposed hydrolysis pathway of **3a′**

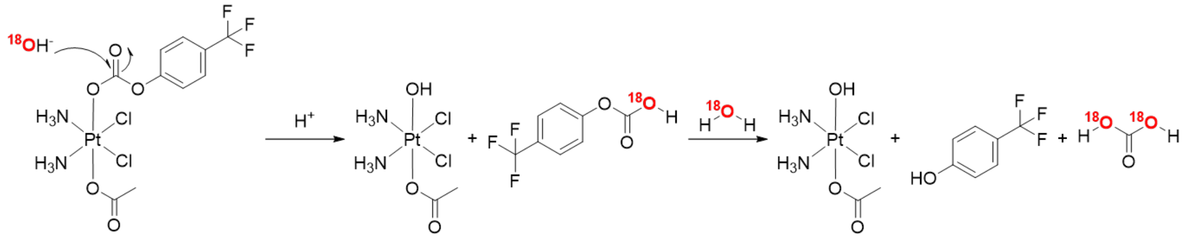

Figure S60. (A) HRMS spectrum of *c,t,c*-[Pt(NH_3)$_2$(OCOOPhCF_3)(OCOCH_3)(Cl)$_2$] **3a'** in PBS-buffered $H_2{}^{18}O$ after 24 h, confirming that only {*c,t,c*-[Pt(NH_3)$_2$(^{16}OH)(OCOCH_3)(Cl)$_2$] + Na}$^+$ was formed; (B) Simulated ESI-MS spectrum of {*c,t,c*-[Pt(NH_3)$_2$(^{16}OH)(OCOCH_3)(Cl)$_2$] + Na}$^+$; (C) simulated ESI-MS spectrum of {*c,t,c*-[Pt(NH_3)$_2$(^{18}OH)(OCOCH_3)(Cl)$_2$] + Na}$^+$; (D) the possible hydrolytic pathway of **3a'**: an attack of the $^{18}OH^-$ on the carbonyl carbon, leading to the formation of Pt-^{16}OH.

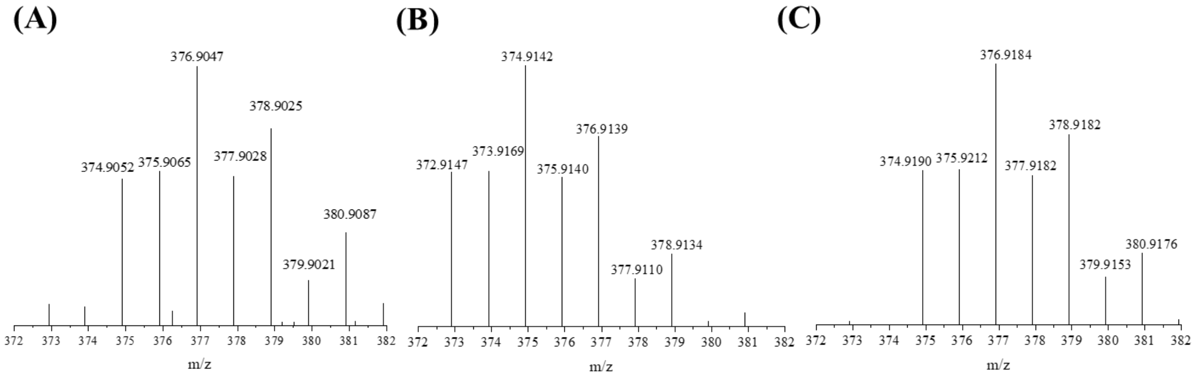

(D) Proposed hydrolysis pathway of *c,t,c*-[Pt(NH_3)$_2$(acetato)Cl(Cl)$_2$]

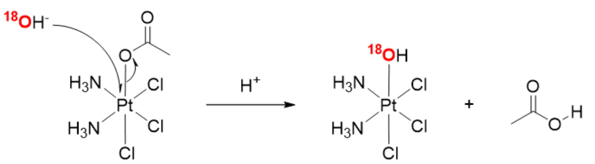

Figure S61. (A) HRMS spectrum of *c,t,c*-[Pt(NH_3)$_2$(OCOCH_3)Cl(Cl)$_2$] in PBS-buffered $H_2{}^{18}O$ after 24 h, confirming that only {*c,t,c*-[Pt(NH_3)$_2$(^{18}OH)Cl(Cl)$_2$] + Na}$^+$ was formed; (B) simulated ESI-MS spectrum of {*c,t,c*-[Pt(NH_3)$_2$(^{16}OH)Cl(Cl)$_2$] + Na}$^+$; (C) simulated ESI-MS spectrum of {*c,t,c*-[Pt(NH_3)$_2$(^{18}OH)Cl(Cl)$_2$] + Na}$^+$; (D) the possible hydrolytic pathway of *c,t,c*-[Pt(NH_3)$_2$(OCOCH_3)Cl(Cl)$_2$]: a direct attack from $^{18}OH^-$ to the centre of Pt(IV) complex, resulting in the break of Pt(IV)-O(COCH_3) bond and formation of the Pt-^{18}OH bond.

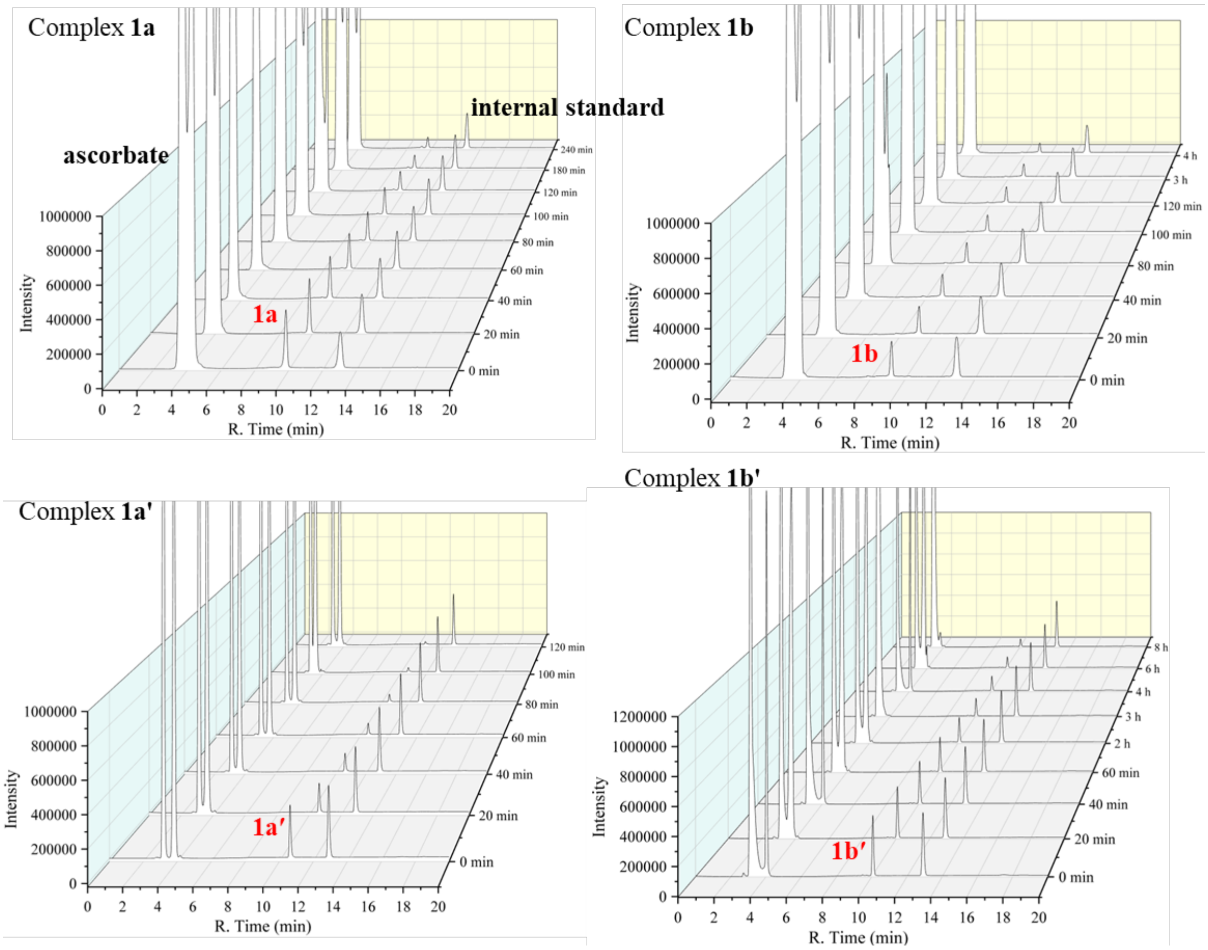

Figure S62. HPLC chromatograms for the reduction test of Pt(IV) complexes **1a**, **1b**, **1a'**, and **1b'** in a PBS buffer (pH = 7.4) containing 20 equiv. ascorbate.

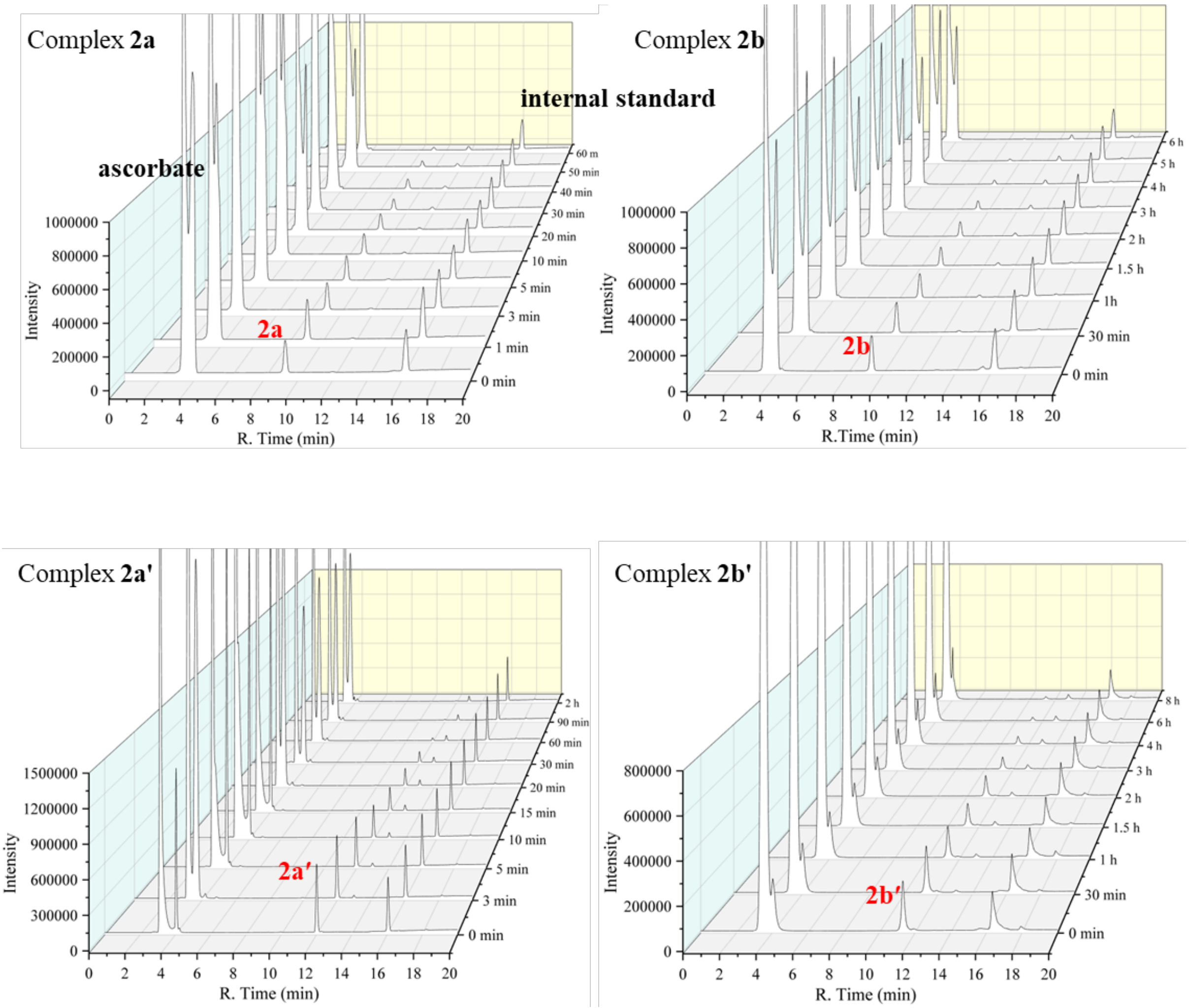

Figure S63. HPLC chromatograms for the reduction test of Pt(IV) complexes **2a**, **2b**, **2a'** and **2b'** in a PBS buffer (pH = 7.4) containing 20 equiv. ascorbate.

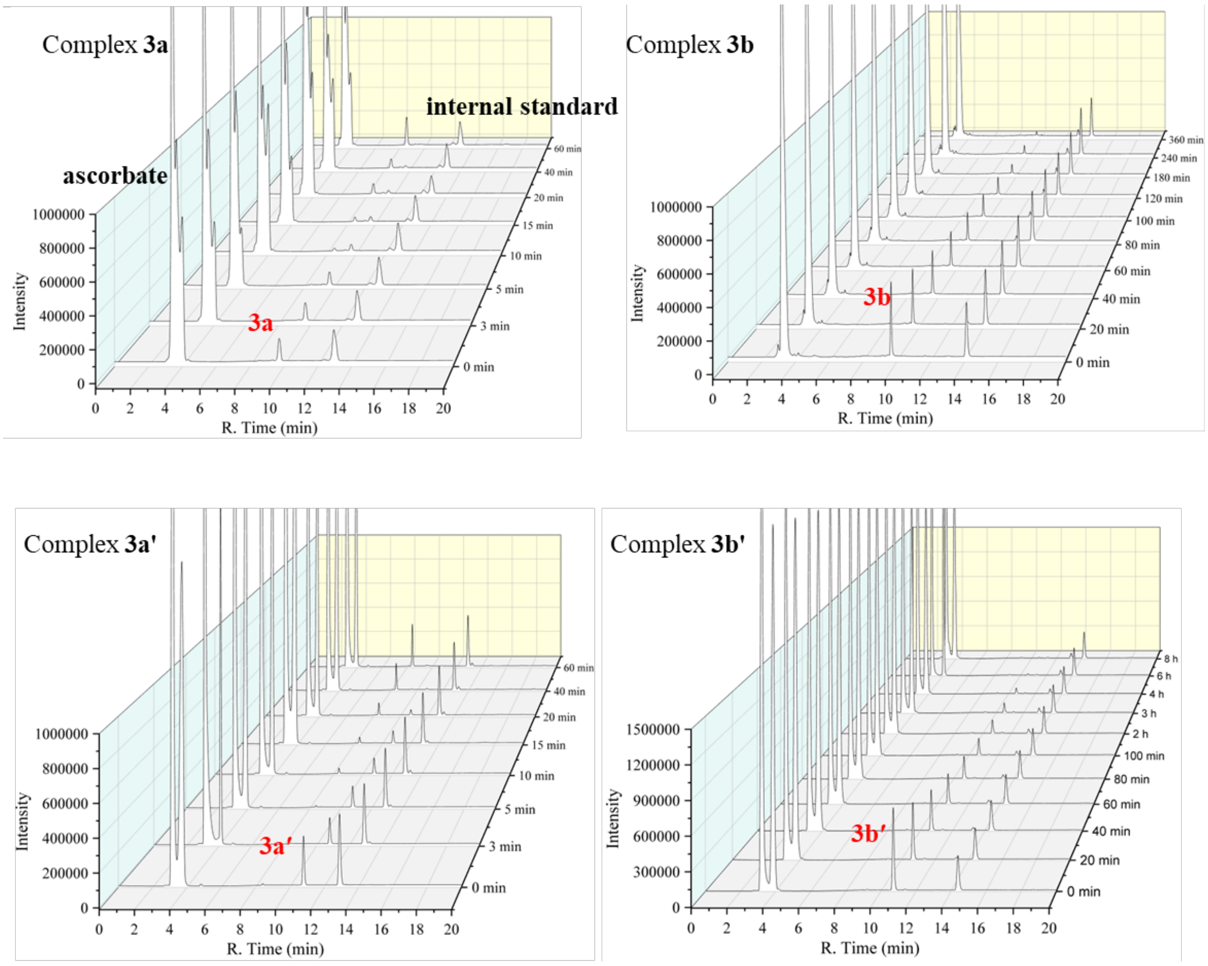

Figure S64. HPLC chromatograms for the reduction test of Pt(IV) complexes **3a**, **3b**, **3a'** and **3b'** in a PBS buffer (pH = 7.4) containing 20 equiv. ascorbate.

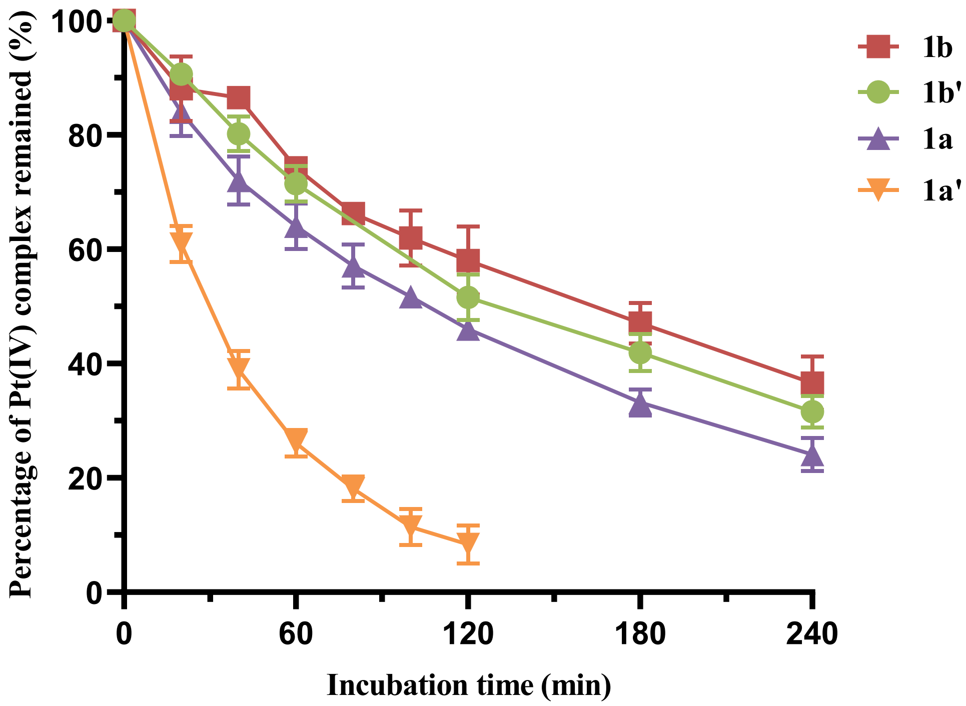

Figure S65. The decay profiles of the Pt(IV) complexes **1a**, **1b**, **1a′**, and **1b′** in PBS buffer (pH 7.4) at 37 °C with excess amount of sodium ascorbate.

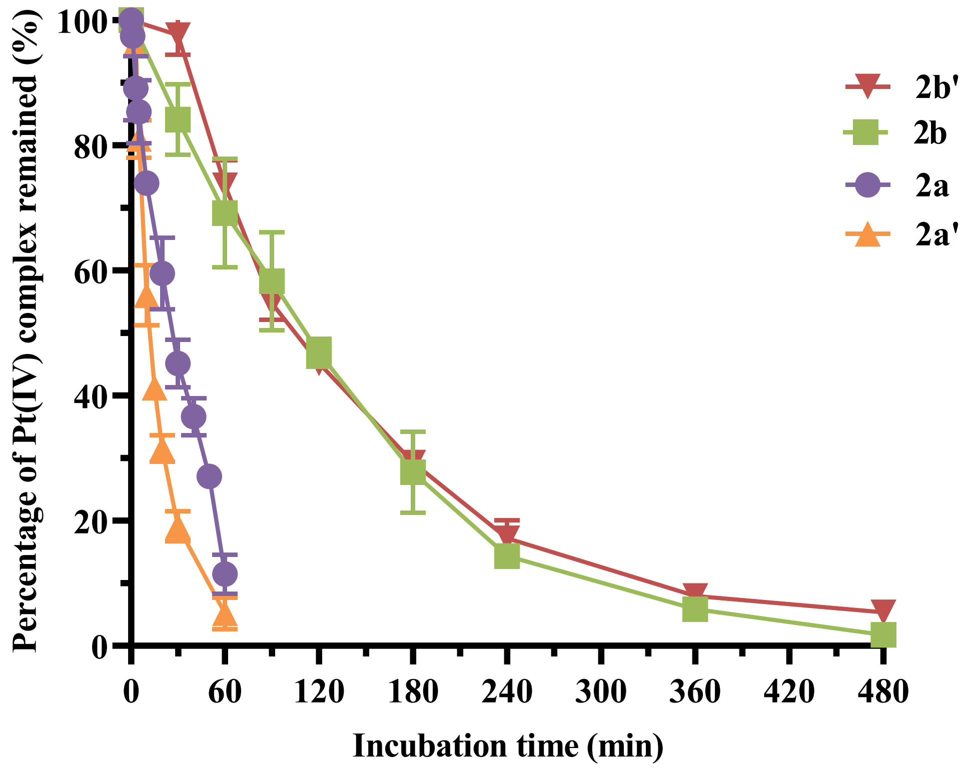

Figure S66. The decay profiles of the Pt(IV) complexes **2a**, **2b**, **2a′**, and **2b′** in PBS buffer (pH 7.4) at 37 °C with excess amount of sodium ascorbate.

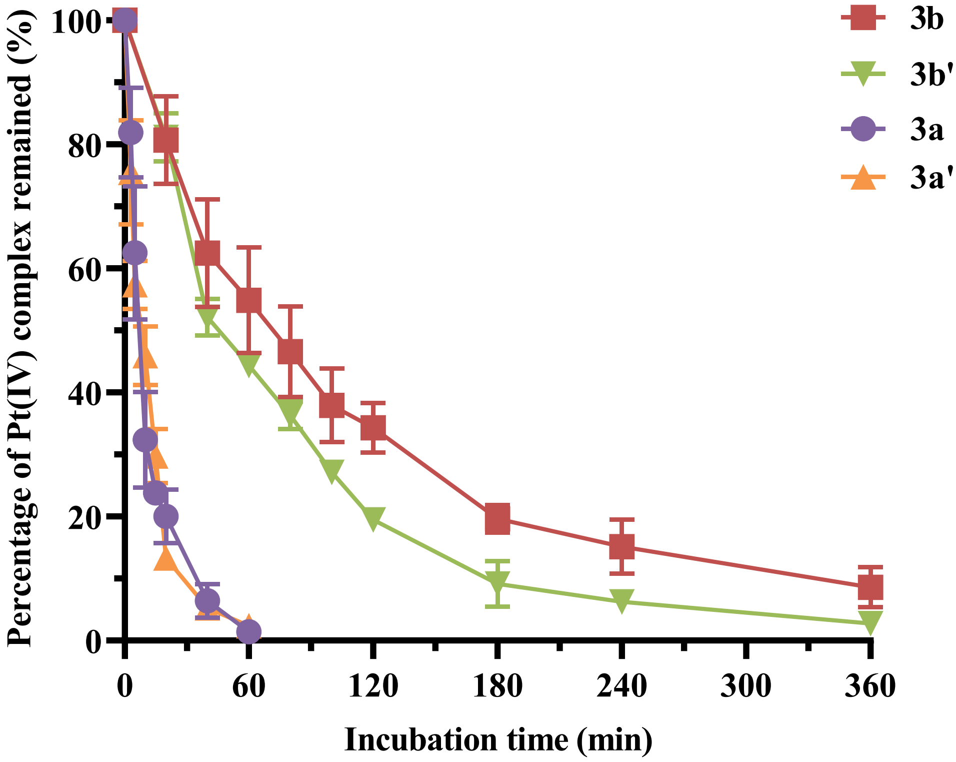

Figure S67. The decay profiles of the Pt(IV) complexes **3a**, **3b**, **3a′**, and **3b′** in PBS buffer (pH 7.4) at 37 °C with excess amount of sodium ascorbate.

Complex **1a**

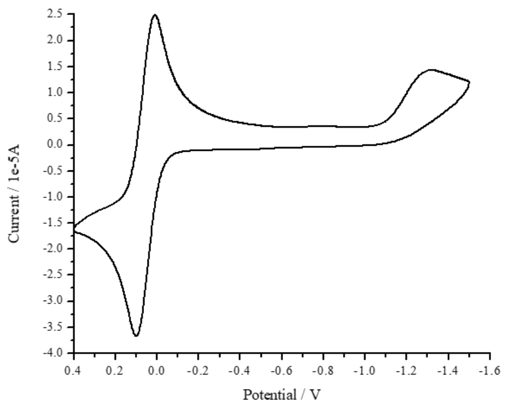

Complex **1b**

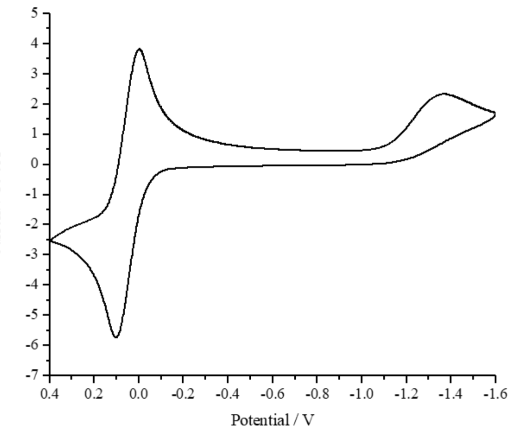

Complex **1a'**

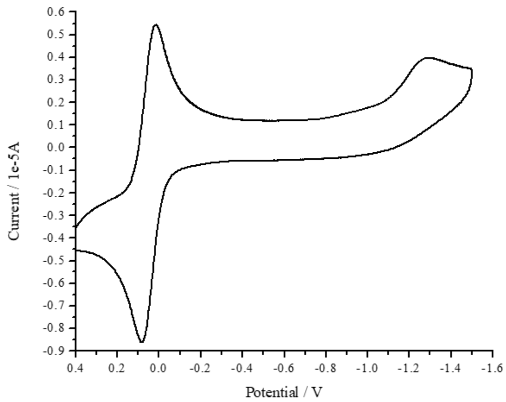

Complex **1b'**

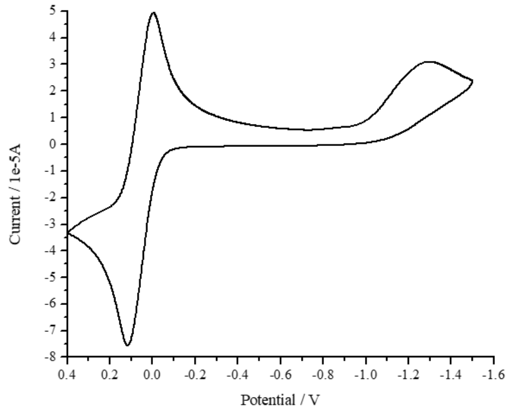

Figure S68. Cyclic voltammograms of complexes **1a**, **1b**, **1a′**, and **1b′** with ferrocene as internal reference.

Complex **2a**

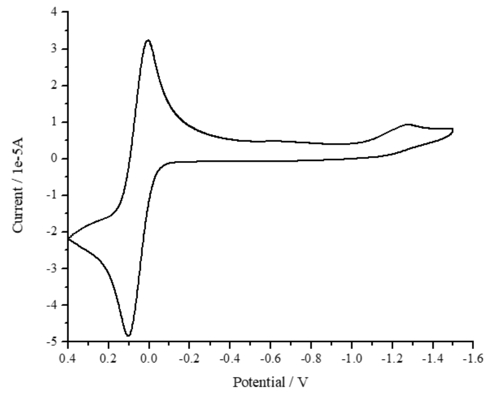

Complex **2b**

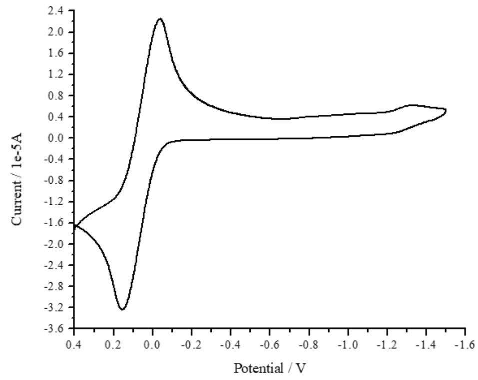

Complex **2a'**

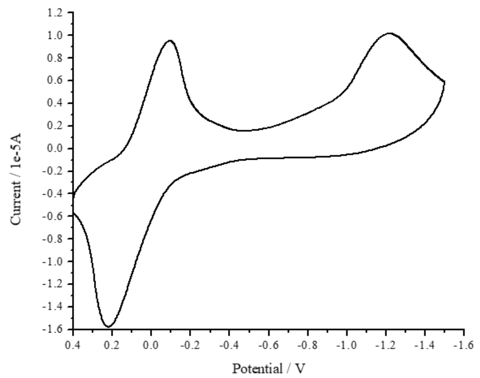

Complex **2b'**

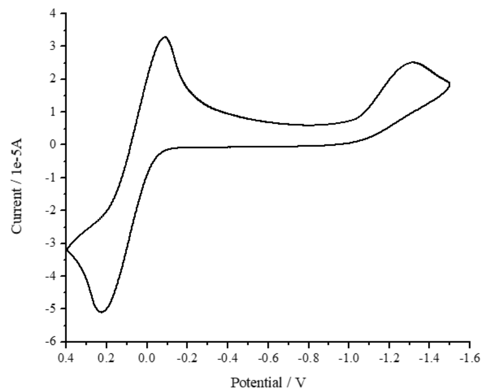

Figure S69. Cyclic voltammograms of complexes **2a**, **2b**, **2a′**, and **2b′** with ferrocene as internal reference.

Complex **3a**

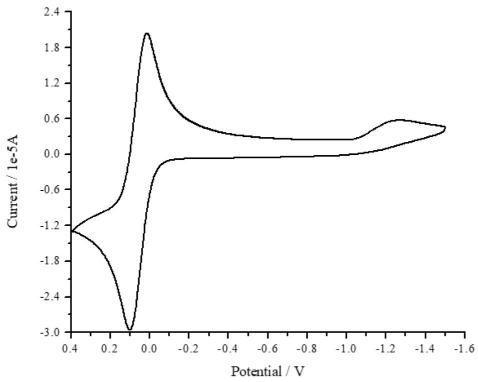

Complex **3b**

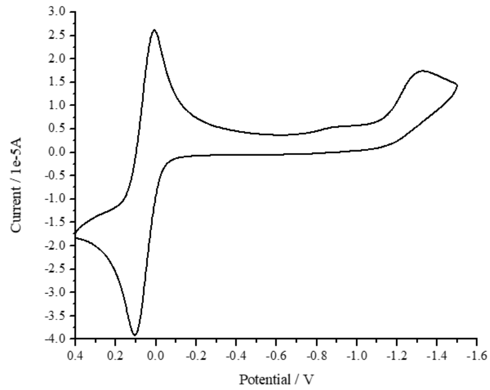

Complex **3a'**

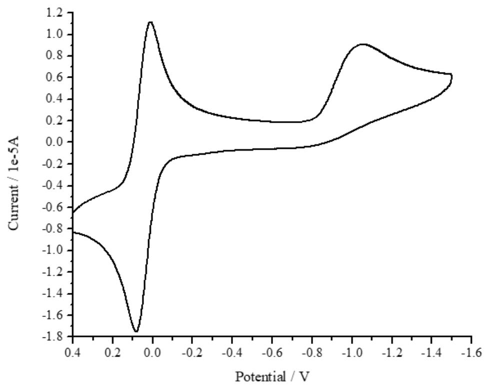

Complex **3b'**

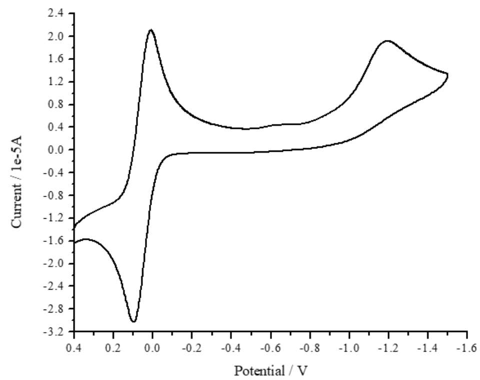

Figure S70. Cyclic voltammograms of complexes **3a**, **3b**, **3a′**, and **3b′** with ferrocene as internal reference.

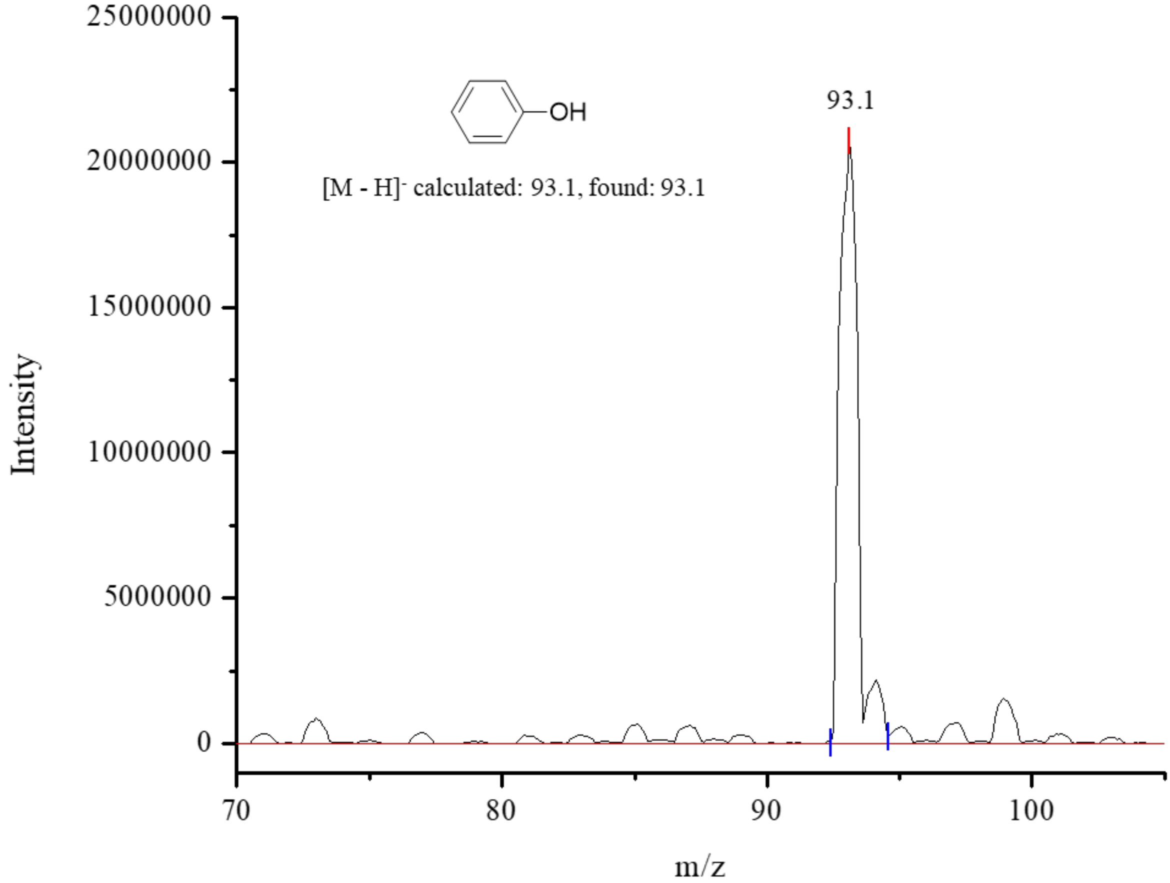

Figure S71. ESI-mass spectrum of the reduction products of **2a′** (negative ion mode).

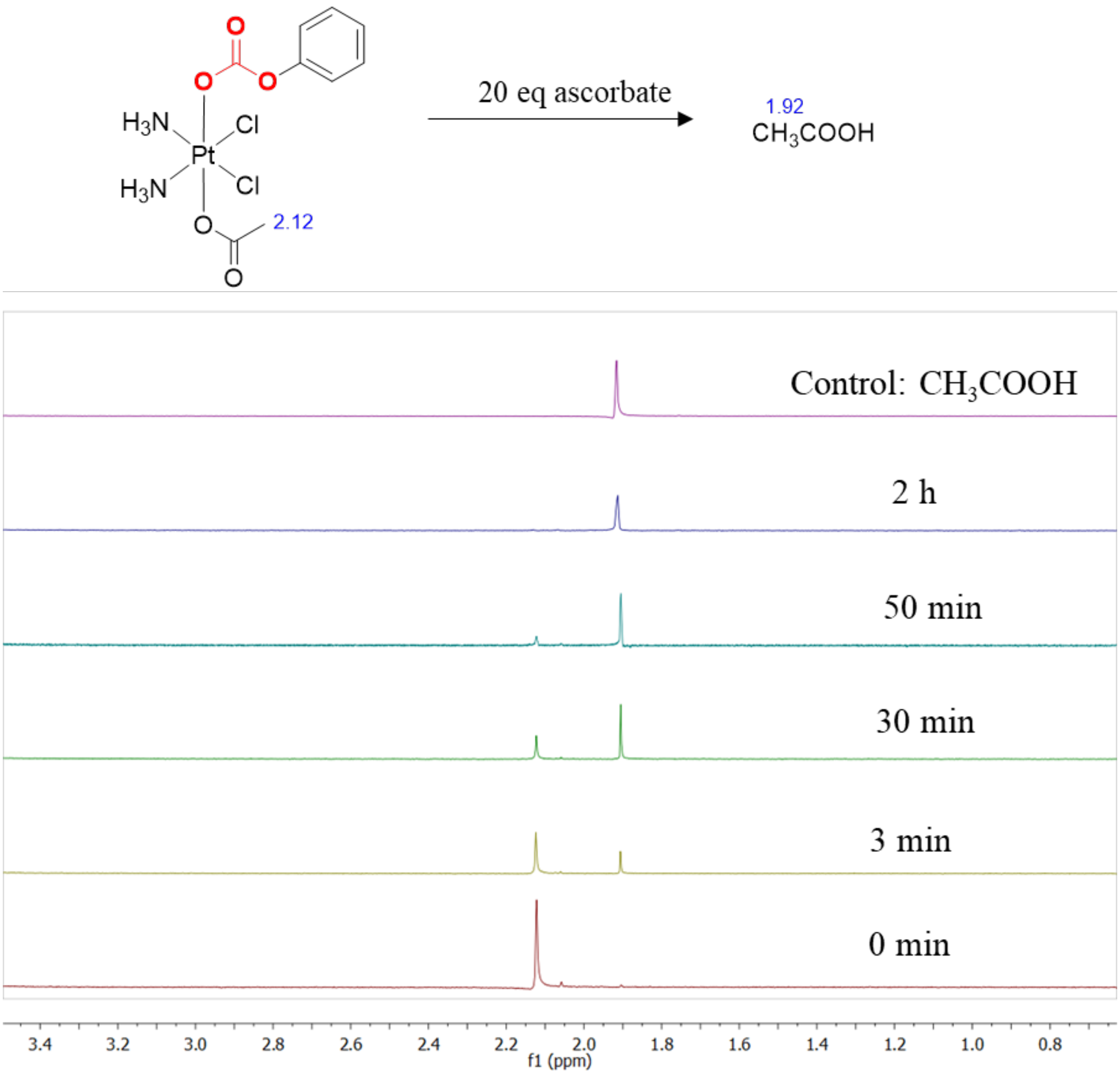

Figure S72. ^{1}H NMR spectra of the reduction of **2a'** with 20 equiv. of ascorbate.

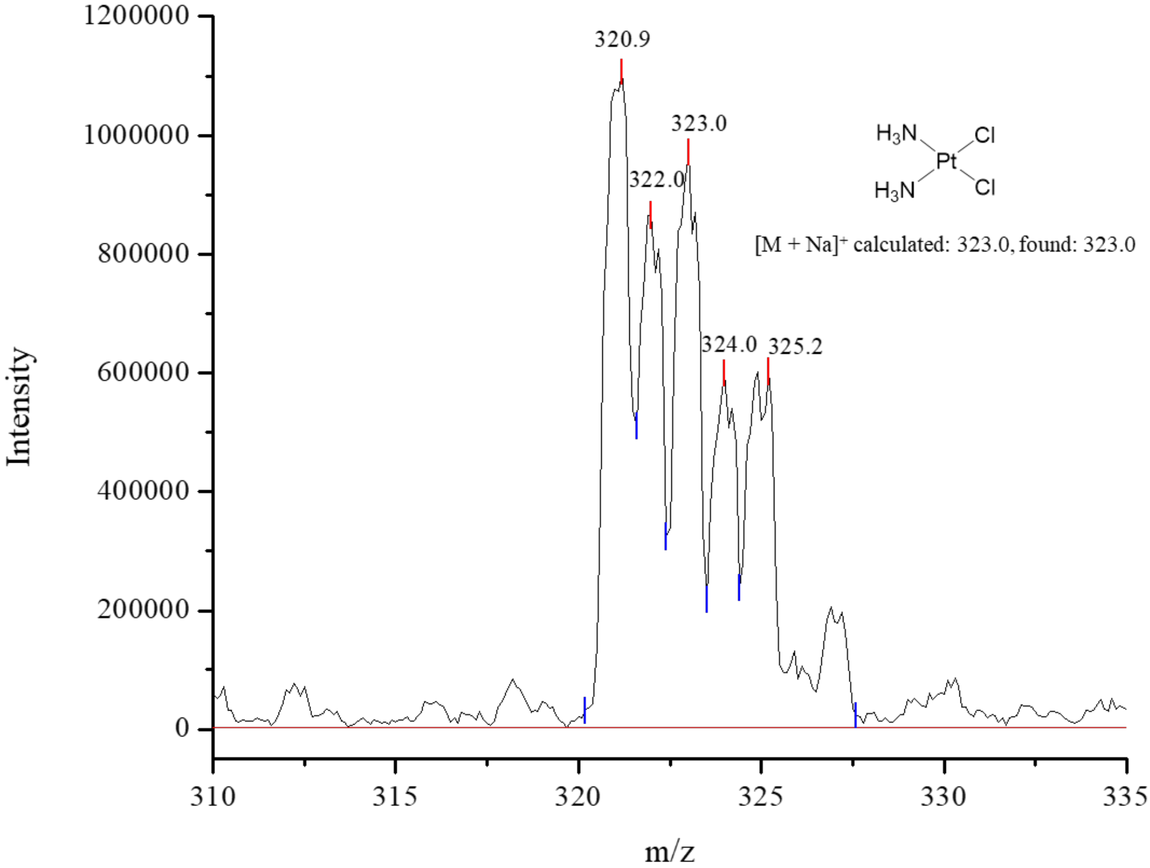

Figure S73. ESI-mass spectrum of the reduction product of **2a′** (positive ion mode).

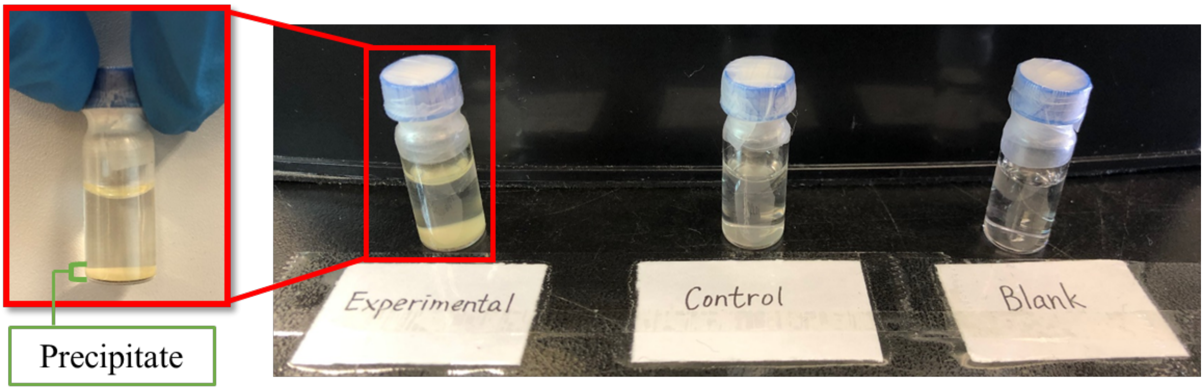

Figure S74. Detection of the presence of CO_2 with limewater. Experimemtal group: carbonate complex **2a′** (1 mM) in Milli-Q water containing 20 mM ascorbate was incubated with saturated limewater; control group: a solution containing everything but Pt(IV) complex was introduced as a control; blank: a solution containing the limewater only.

Table S1. ^{195}Pt NMR and selected ^{1}H, ^{13}C NMR chemical shifts of the carbonated and carboxylated Pt(IV) complexes in DMSO-d_6 (values in ppm).

Complex	R_1[a]	R_2[a]	δ ^{1}H, -NH_3	δ ^{13}C, -OCO-R	δ ^{195}Pt
1a	OH	$OCOO(CH_2)_5CH_3$	6.04 – 5.82	160.3	1069.7
1b	OH	$OCO(CH_2)_5CH_3$	6.05 – 5.88	181.2	1051.6
1a′	$OCOCH_3$	$OCOO(CH_2)_5CH_3$	6.53	159.7	1242.1
1b′	$OCOCH_3$	$OCO(CH_2)_5CH_3$	6.58 – 6.46	180.9	1232.8
2a	OH	OCOOPh	6.14 – 5.81	157.4	1070.1
2b	OH	OCOPh	6.27 – 5.85	173.5	1038.4
2a′	$OCOCH_3$	OCOOPh	6.57	157.0	1248.5
2b′	$OCOCH_3$	OCOPh	6.65	173.3	1214.8
3a	OH	$OCOOPhCF_3$	6.20 – 5.81	156.2	1069.5
3b	OH	$OCOPhCF_3$	6.20 – 5.89	171.9	1033.9
3a′	$OCOCH_3$	$OCOOPhCF_3$	6.59	155.8	1249.0
3b′	$OCOCH_3$	$OCOPhCF_3$	6.64	171.8	1213.0

[a] R_1 and R_2 are the axial ligands of Pt(IV) complexes based on cisplatin.

Table S2. The equation for pseudo first order reaction and half-life of cisplatin-based Pt(IV) complexes.

Compound (100 µM)	Reducing agent (2 mM)	Linear equation	k^a	$T_{1/2}$ (min)[b]
1a	ascorbate	y = -0.0064x - 0.0324 R^2 = 0.9928	0.0064	108
1b	ascorbate	y = -0.0041x - 0.0293 R^2 = 0.99	0.0041	169
1a′	ascorbate	y = -0.0224x - 0.0682 R^2 = 0.997	0.0224	31
1b′	ascorbate	y = -0.0052x - 0.0181 R^2 = 0.9907	0.0052	135
2a	ascorbate	y = -0.0254x - 0.0206 R^2 = 0.998	0.0254	27
2b	ascorbate	y = -0.0072x + 0.0423 R^2 = 0.9819	0.0072	96
2a′	ascorbate	y = -0.0533x - 0.1246 R^2 = 0.9925	0.0533	13
2b′	ascorbate	y = -0.0065x + 0.0145 R^2 = 0.9834	0.0065	107
3a	ascorbate	y = -0.0685x - 0.174 R^2 = 0.959	0.0685	10
3b	ascorbate	y = -0.0095x - 0.0297 R^2 = 0.9915	0.0095	73
3a′	ascorbate	y = -0.1155x - 0.0145 R^2 = 0.9414	0.1155	6
3b′	ascorbate	y = -0.0136x - 0.0129 R^2 = 0.9991	0.0136	51

[a]k (slope) is the rate constant determined by a linear plot of $\ln(A_t/A_0)$ to incubation time t according to an equation of pseudo first-order rate: $[A] = [A_0]e^{-kt}$. A_0 and A_t are the peak areas of Pt(IV) complexes normalized with the corresponding internal standard at 0 h, and t h. [b] The half-life of the pseudo first-order reaction $T_{1/2} = \ln2 / k$ (where 'k' denotes the rate constant). 100 µM of Pt(IV) complexes were incubated in a PBS buffer (pH = 7.4) with 2 mM ascorbate at 37 °C.